ISSN 0252-1075
Contribution from IITM
Research Report No. RR-149
ESSO/IITM/CVP/SR/02(2026)/207

Comprehensive assessment of tropical cyclones over the Indian Ocean

Vineet Kumar Singh, Rushikesh Adsul, Ganadhi Mano Kranthi, Madhu Kaundal, Biswajit Jena, Anant Parekh, C. Gnanaseelan

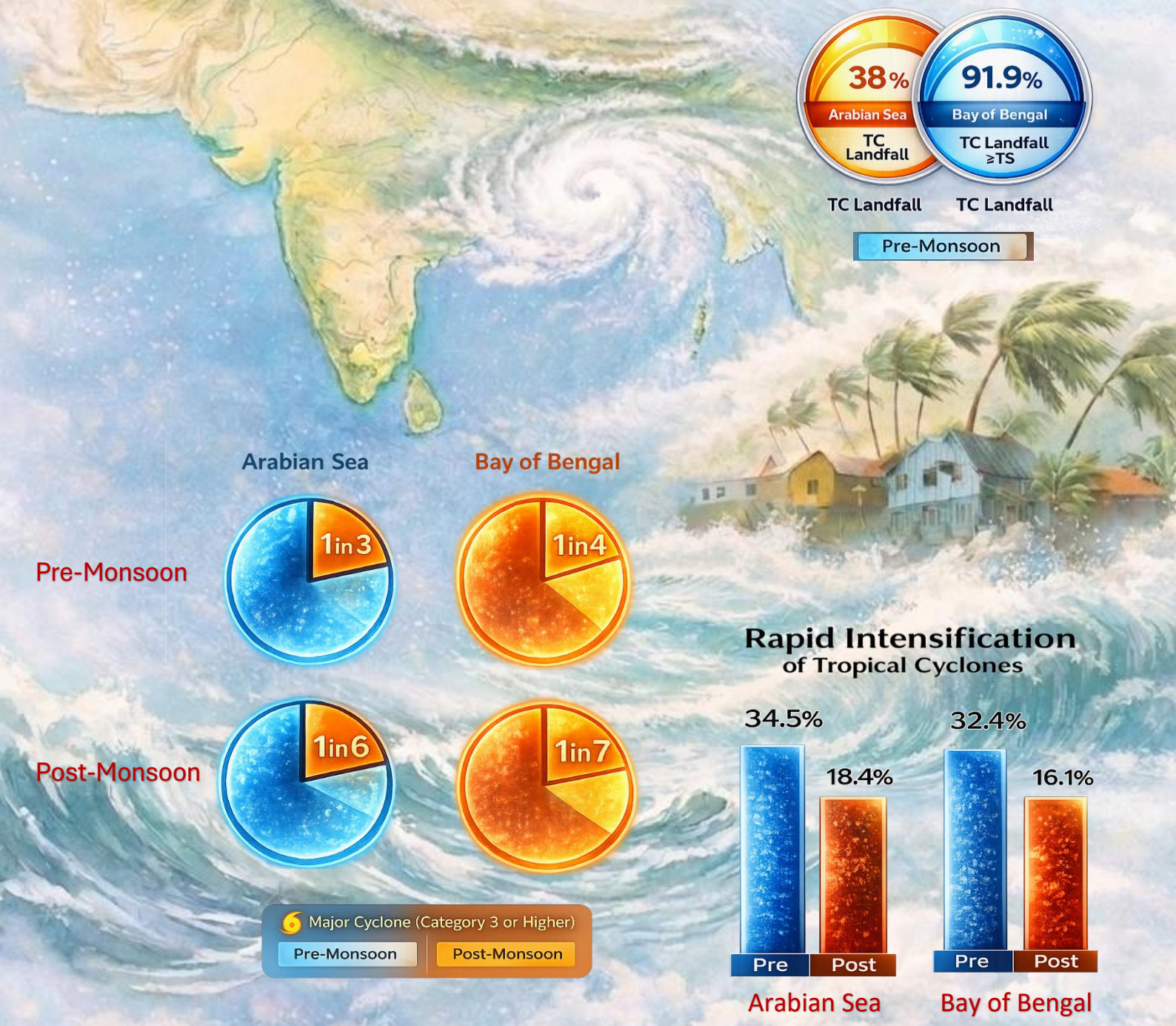

Indian Institute of Tropical Meteorology (IITM)
Ministry of Earth Sciences (MoES)
PUNE-411008, INDIA
https://www.tropmet.res.in/

ISSN 0252-1075
Contribution from IITM
Research Report No. RR-149
ESSO/IITM/CVP /SR/02(2026)/207

Comprehensive assessment of tropical cyclones over the Indian Ocean

Vineet Kumar Singh, Rushikesh Adsul, Ganadhi Mano Kranthi, Madhu Kaundal, Biswajit Jena, Anant Parekh, C. Gnanaseelan*

Climate Variability and Prediction, Indian Institute of Tropical Meteorology, Ministry of Earth Sciences, Pune 411 008 India

***Corresponding Author:**
Dr. C. Gnanaseelan
Scientist G and Project Director
Climate Variability and Prediction (CVP)
Indian Institute of Tropical Meteorology,
Dr. Homi Bhabha Road, Pashan, Pune-411 008, India.
E-mail: seelan@tropmet.res.in
Phone: +91 -(0)20-259 04 271

Indian Institute of Tropical Meteorology (IITM)
Ministry of Earth Sciences (MoES)
PUNE, INDIA
https://www.tropmet.res.in/

DOCUMENT CONTROL SHEET

Ministry of Earth Sciences (MoES)
Indian Institute of Tropical Meteorology (IITM)

ESSO Document Number
ESSO/IITM/CVP/SR/02(2026)/207

Title of the Report
Comprehensive assessment of tropical cyclones over the Indian Ocean

Authors
Vineet Kumar Singh, Rushikesh Adsul, Ganadhi Mano Kranthi, Madhu Kaundal, Biswajit Jena, Anant Parekh, C. Gnanaseelan

Reviewers
Dr. Monica Sharma
[India Meteorology Department, Delhi]
Dr. R.H.Kriplani
[Indian Institute of Tropical Meteorology, Pune]

Type of Document
Scientific Report

Number of pages and figures
82, 47

Number of references
125

Keywords
Tropical Cyclones, North Indian Ocean, Southern Tropical Indian Ocean, observed changes, future projections.

Security classification
Open

Distribution
Unrestricted

Date of Publication
March 2026

Abstract

The report presents a comprehensive assessment of observed changes in tropical cyclone (TC) characteristics over the Indian Ocean, including the Arabian Sea, Bay of Bengal, and Southern Tropical Indian Ocean. Using high-resolution simulations from CMIP6 HighResMIP models, the study examines the seasonal and basin-specific variations in TC behavior and investigates how key TC characteristics are likely to evolve during the near-future period (2015–2050) under a warming climate. On average, about five TCs form in the North Indian Ocean in a year. TCs are generally more intense during the pre-monsoon season, 9.1% stronger in the Arabian Sea and 18.7% stronger in the Bay of Bengal compared to the post-monsoon TCs. The study reports stronger intensification efficiency in the pre-monsoon season with 41.4% of TCs in the Arabian Sea and 51.4% in the Bay of Bengal reaching Category 1 or higher, compared to 36.8% and 35.6% in the post-monsoon season. Nearly one in three Arabian Sea TCs and one in four Bay of Bengal TCs become major cyclones (Category ≥ 3) in the pre-monsoon season, with one in six and one in seven, respectively, in the post-monsoon season. The higher percentage of TCs undergoing rapid intensification and larger TC size are found during the pre-monsoon season as compared to the post-monsoon season in both the basins. Landfall analysis shows that 38% (31.5%) of Arabian Sea TCs, and 91.9% (65.5%) of Bay of Bengal TCs make landfall with at least tropical-storm intensity (≥ 34 knots) during the pre-monsoon (post-monsoon) seasons. TCs last longer at tropical-storm intensity in the pre-monsoon season for about 87.7 hours in the Arabian Sea and 78.7 hours in the Bay of Bengal, which are about 15 hours and 13.5 hours longer than the post-monsoon TCs in the respective basins. Arabian Sea post-monsoon TCs reveal increasing trends in frequency (~0.2 TC/decade) and intensity (7.1 knots/decade), whereas significant increase in intensity (12.2 knots/decade) is observed during the pre-monsoon without any significant trends in frequency. The intensification rate has increased by 0.7 knots/6 hours/decade in the pre-monsoon and 2.4 knots/6 hours/decade during the post-monsoon season, with corresponding increase in rapid intensification frequency. The life cycle of Arabian Sea TC stretched at 14.4 hours/decade in the pre-monsoon season, contributing to increase in accumulated cyclone energy at 2.8–2.9 $(\text{knots})^2$ /decade. Equatorward shift in the TC genesis latitude is seen in both the basins, which is in contrast to global trends. Increasing trends in pre-monsoon TC size is observed in both the basins with Bay of Bengal displaying 29.4 n mi/decade and the Arabian Sea displaying 15.3 n mi/decade. In the Southern Tropical Indian Ocean, about 71% of annual TC activity occurs between November–April, with peak in February. Although total TC frequency remains stable, the

frequency of Category ≥ 3 TCs has increased at 0.4 TC/decade, accompanied by rising TC intensity at 3.4 knots/decade and maximum intensity at 6 knots/decade. The rapid intensification frequency also increased at 0.7 TC/decade, from ~4 to ~6 TCs per season over the last 40 years.

Near-future (2015–2050) projections indicate an overall decline in the Bay of Bengal TC frequency during both the seasons and a ~53% reduction in intense TCs during the pre-monsoon season. In the Arabian Sea, TC frequency is projected to decrease in the post-monsoon season whereas no noticeable change in the pre-monsoon season. Models project a marginal increase in the Arabian Sea TC intensity and a decrease in the Bay of Bengal during the pre-monsoon season, with no significant changes in the post-monsoon season. TC duration is projected to reduce in both the basins, while the intensification rate is projected to increase in the Arabian Sea especially during the pre-monsoon season. Moreover, the TC tracks are projected to shift poleward in the Bay of Bengal during the post-monsoon season and a basin wide decline in TC tracks during the pre-monsoon season. The report provides a comprehensive analysis of basin- and season-specific differences in TC trends, and highlights a pronounced increase in the intensity and destructive potential of cyclones over the Arabian Sea and Southern Tropical Indian Ocean.

Summary

- We have reported the TC characteristics and their changes in the North Indian Ocean and Southern Tropical Indian Ocean in this manuscript. In the North Indian Ocean (including the Arabian Sea and the Bay of Bengal), on the average ~5 TCs form per year. In a calendar year, in the Bay of Bengal, the highest probability of TC occurrence is in November, whereas in the Arabian Sea, the highest probability of TC occurrence is in June.
- On the average, TCs in the Arabian Sea and the Bay of Bengal are 9.1% and 18.7% more intense during the pre-monsoon season as compared to the post-monsoon season.
- During the pre-monsoon season, most TC activity in the Arabian Sea occurs between 16 May and 15 June, whereas in the Bay of Bengal, it occurs earlier, mainly between 26 April and 21 May.
- During the post-monsoon season, the major TC threat is between 21 October-15 November in the Arabian Sea. Whereas in the Bay of Bengal TC threat is there throughout the season, with three distinct peaks in the TC activity.

- During the pre-monsoon season, about 41.4% of TCs in the Arabian Sea and 51.4% in the Bay of Bengal intensify to Category 1 or higher, compared to 36.8% and 35.6%, respectively, in the post-monsoon season. This suggests higher TC intensification efficiency in both the basins during the pre-monsoon season.
- Nearly one in three TCs in the Arabian Sea and one in four in the Bay of Bengal become major TCs (Category 3 or higher) in the pre-monsoon season, whereas the ratio decreases to one in six and one in seven, respectively, during the post-monsoon season.
- It is observed that during the pre-monsoon season, 34.5% of TCs in the Arabian Sea and 32.4% in the Bay of Bengal undergo rapid intensification. In contrast, during the post-monsoon season, 18.4% of TCs in the Arabian Sea and 16.1% in the Bay of Bengal experience rapid intensification. Thus, in both the basins, pre-monsoon TCs have a higher probability to intensify rapidly as compared to the post-monsoon season.
- In the Arabian Sea, approximately 38% and 31.5% of TCs make landfall with at least tropical storm strength (wind speed ≥ 34 knots) during the pre-monsoon and post-monsoon seasons respectively,. In contrast, in the Bay of Bengal, about 91.9% of TCs during the pre-monsoon season and 65.5% during the post-monsoon season make landfall with at least tropical storm intensity. Thus, the probability of TCs making landfall with at least tropical storm intensity is significantly higher in the Bay of Bengal than in the Arabian Sea in both the TC seasons.
- The TC size in both the basins is larger during the pre-monsoon than the post-monsoon season.
- During the pre-monsoon season, TCs last longer at tropical storm or higher intensity, averaging 87.7 (78.7) hours in the Arabian Sea (Bay of Bengal) which is about 15 (13.5) hours longer than the post-monsoon season. However, when all TC stages (including depression and deep depression (wind speed ≥17 knots) are considered, Arabian Sea TCs persist slightly longer in the post-monsoon season (by 10.7 hours), suggesting their weaker stages dominate. In contrast, Bay of Bengal TCs remain longer-lived during the pre-monsoon season across both intensity thresholds, indicating greater overall persistence compared to post-monsoon systems.
- The land duration of TC (tropical storm strength) in the Arabian Sea is 16.2 (9.0) hours during the pre-monsoon (post-monsoon) seasons. In contrast, over the Bay of Bengal, the corresponding averages are 11.7 hours and 18.2 hours, respectively. Thus, during the pre-monsoon season, Arabian Sea TCs spend longer time over land at tropical storm

or higher intensity than those in the Bay of Bengal, whereas during the post-monsoon season, Bay of Bengal TCs persist over land for longer durations than those in the Arabian Sea. However, when all intensity stages up to dissipation are considered, Arabian Sea TCs have longer durations over land compared to Bay of Bengal TCs in both seasons.

- Further, during the pre-monsoon season, the total track length over land is greater in the Arabian Sea than in the Bay of Bengal when all TC stages are included. However, when considering only tropical storm or higher intensity stages, Bay of Bengal TCs travel farther over land than Arabian Sea TCs in this season. Whereas, for the post-monsoon season, regardless of whether all TC stages or only tropical storm or higher intensity stages are considered, Bay of Bengal TCs consistently travel longer distances over land than the Arabian Sea TCs.
- In the Arabian Sea, pre-monsoon TCs move 0.68 m s^{-1} slower than those in the post-monsoon season, whereas in the Bay of Bengal, post-monsoon TCs move 0.14 m s^{-1} slower than pre-monsoon TCs. Slower translation speeds imply a longer duration of influence over a given region, thereby increasing the potential for prolonged impacts from heavy rainfall, storm surges, and strong winds. Further, in both basins, TCs move faster over land compared to over the ocean.
- TC frequency in the Arabian Sea is increasing at the rate of ~0.2 TCs/decade during the post-monsoon season.
- The intensity (LMI) of TCs in the Arabian Sea during the pre-monsoon season has been increasing at a rate of 12.2 knots (22.6 km/hr) per decade. Similarly, during the post-monsoon season, TC intensity shows an increasing trend of 7.1 knots (13.1 km/hr) per decade. In the Bay of Bengal, there is no significant increasing trend in TC intensity.
- Not only the intensity of TC, but also the intensification rate of TCs in the Arabian Sea is increasing at the rate of 0.7 knots and 2.4 knots per 6 hour per decade during the pre-monsoon season and the post-monsoon season respectively. In line with it there is an increase in the frequency of TCs undergoing rapid intensification in both seasons.
- TC duration in the Arabian Sea is increasing at the rate of 14.4 hours per decade during the pre-monsoon season. During the post-monsoon season, TC duration shows only a marginal increase. Interestingly, in both seasons, TC land duration exhibits a decreasing trend. This indicates that although there is an overall increase in TC duration, the TC duration over land is declining.

- Due to the increase in intensity and duration of TCs in the Arabian Sea, there is a significant increase in the accumulated cyclone energy in the basin. It is increasing at the rate of 2.8 knots^2 and 2.9 knots^2 per decade during the pre-monsoon season and post-monsoon season respectively.
- The translation speed of TCs is declining in both basins during the post-monsoon season. However, over land, the rate of slowing down of TCs in less than that over the ocean.
- TC genesis latitude is shifting equatorward in both the basins and seasons, which is sharp contrast to the global basins.
- TC maximum intensity latitude in the Bay of Bengal is also shifting equatorward. This is again in contrast to the global basins. However, in the Arabian Sea, during the pre-monsoon season, it is shifting poleward, whereas during the post-monsoon season, it is shifting equatorward.
- TC size during the pre-monsoon season is increasing at the rate of 15.3 n mi (28.3 km) per decade and 29.4 n mi (54.4 km) per decade in the Arabian Sea and the Bay of Bengal respectively. On the contrary, during the post-monsoon season, TC size exhibits a non-significant declining trend.
- In the Southern Tropical Indian Ocean, 71% of the annual TC frequency occurs between November to April. The most active TC month in this basin is February. Also, it is noted that the intensity of TCs is generally more in the later part of the active season i.e. from February-April, as compared to November-January.
- Similar to the Bay of Bengal, in the Southern Tropical Indian Ocean too, there is no significant change in the TC frequency in the basin during the season (November-April). However, the frequency of category ≥ 3 TCs is increasing at the rate of 0.4 TC per decade.
- This increase in the frequency of intense TCs is reflected by the changes in TC intensity which is increasing at the rate of 3.4 knots (6.3 km/hr) per decade. Also, the upper limit of TC intensity (i.e. the maximum intensity of TC in a given season) is increasing at the rate of 6 knots (11.1 km/hr) per decade. This indicates that in recent decades the TCs in the Southern Tropical Indian Ocean are becoming more and more intense.
- Similar to the Arabian Sea, TCs intensification rate in the Southern Tropical Indian Ocean is increasing rapidly. It is increasing at the rate of 0.3 knots per 6 hours per decade. Also, the frequency of TCs undergoing rapid intensification is increasing at the

rate of 0.7 TC per decade. The number of TCs undergoing rapid intensification has increased from 4 TCs per season in the earlier part of the study period to ~6 TCs per season in recent years.

- Lastly, along with the increase in TC intensity in Southern Tropical Indian Ocean there is also a marginal increase in their duration, leading to an increase in the accumulated cyclone energy in the basin.
- To assess the impact of global warming on TC characteristics, we analyzed the multi-model mean from the best-performing CMIP6-HighResMIP models for the near-future period (2015–2050). The projections indicate a decrease in overall TC frequency in the Bay of Bengal during both the pre- and post-monsoon seasons. Furthermore, the frequency of intense TCs (Category ≥ 3) is projected to decline by approximately 53% during the pre-monsoon season. In contrast, during the post-monsoon season, the frequency of intense TCs is expected to marginally increase, from about one TC every six years in the historical period to one TC every 4.5 years in the near-future projections.
- In the Arabian Sea, multi-model mean is projecting a decrease in TC frequency during the post-monsoon season and no significant change during the pre-monsoon season.
- The multi-model mean projects a decrease in TC intensity in the Bay of Bengal during the pre-monsoon season and no significant change during the post-monsoon season. On the other hand, in the Arabian Sea, TC intensity is projected to increase marginally during the pre-monsoon season and no significant change during the post-monsoon season.
- The TC duration is projected to decrease in both basins and seasons.
- The TC intensification rate is projected to increase in the Arabian Sea during the pre-monsoon season. No significant change during the post-monsoon season. Whereas, in the Bay of Bengal, there is no significant change in the TC intensification rate in pre-monsoon season and marginal increase in the post-monsoon season.
- TC tracks are projected to shift poleward in the Bay of Bengal during the post-monsoon season. In the Arabian Sea, there is a slight northwest shift in TC tracks in pre-monsoon season. While, there is no concrete signal in the post-monsoon season.
- Observations indicate an equatorward shift in the latitude of TC genesis, whereas the multi-model mean projects a slight poleward shift in TC genesis latitude. In contrast, the multi-model mean shows almost no change in the latitude of TC maximum intensity.

Table of Contents

1. Introduction

Tropical cyclones (TCs) are intense, rapidly rotating low-pressure systems which cause the greatest environmental harm in coastal areas, economic losses, and human casualties, because of their strong winds, excessive precipitation and storm surges (Bhardwaj & Singh, 2020; Gori et al., 2020; Kim et al., 2012; Li & Zhou, 2015). The primary energy source for these TCs is the heat and moisture from warm ocean waters, typically above 26.5°C. Sufficiently warm sea surface temperature (SST, > 26 °C), Coriolis force, positive low-level relative vorticity, high mid-tropospheric relative humidity, low vertical wind shear, and pre-existing disturbance are the necessary conditions for TC genesis (Gray, 1968). The ocean plays a dominant role in providing energy to TC through the exchange of latent and sensible heat fluxes between the ocean and the atmosphere (Emanuel, 1986; Vinod et al., 2014). Increased latent heat flux from the ocean to the atmosphere moistens the boundary layer and provides conducive conditions for cyclogenesis (Gao et al., 2019) and also plays an important role in its intensification (Gao et al., 2016; Gao & Chiu, 2010; Jaimes et al., 2015; Lin et al., 2014).

The structure of TC is very complex, at the centre of intense TC, there is an eye, a nearly circular region typically 20 to 50 km wide (Teshiba et al., 2005). The eye is the region of calm to light winds, relatively clear skies, with a remarkable inversion level in the lower troposphere (Willoughby, 1998) and even sunlight is seen in some cases. Surrounding the eye is the eyewall, the most intense and dangerous part of the TC. The eyewall consists of a dense ring of towering cumulonimbus clouds that reach a height of 15-18 Km. In the eyewall, the strongest winds and heaviest rainfall occur. The rapid upward motion of warm, moist air in this region releases latent heat, which further fuels the TC. This release of latent heat within the TC makes them a warm core system, with the temperatures in the TC especially in mid to upper levels warmer than the surroundings. Extending outward from the eyewall are spiral rainbands separated with moat regions, which can stretch hundreds of kilometres. These curved bands contain clusters of thunderstorms and heavy rain. Although less intense than the eyewall, rainbands can still produce gusty winds and flash floods.

TCs primarily develop in six ocean basins: the Western North Pacific, North Atlantic, Eastern North Pacific, North Indian Ocean, South Indian Ocean, and South Pacific Ocean as shown in Figure 1.1. In general, no TCs form in the southern Atlantic Ocean (south of equator) and southeast Pacific Ocean. On an average, approximately 85 TCs form globally each year, with a standard deviation of ±10 (Sobel et al., 2021, Figure 1.2). Among the active TC basins,

the Western North Pacific accounts for about 29% of the total annual global TC frequency. Whereas, the north Indian Ocean contributes around 6%, and the Bay of Bengal and the Arabian Sea contribute approximately 4% and 2%, respectively (Figure 1.2).

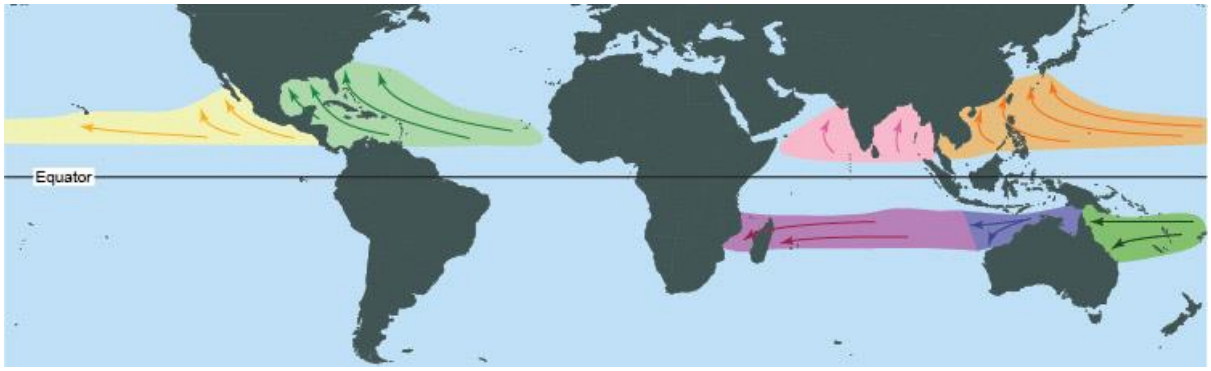

Figure 1.1. *Global Tropical Cyclone (TC) formation basins. Adapted from NOAA (https://www.noaa.gov). The arrows denote the in general TC movement in different basins.*

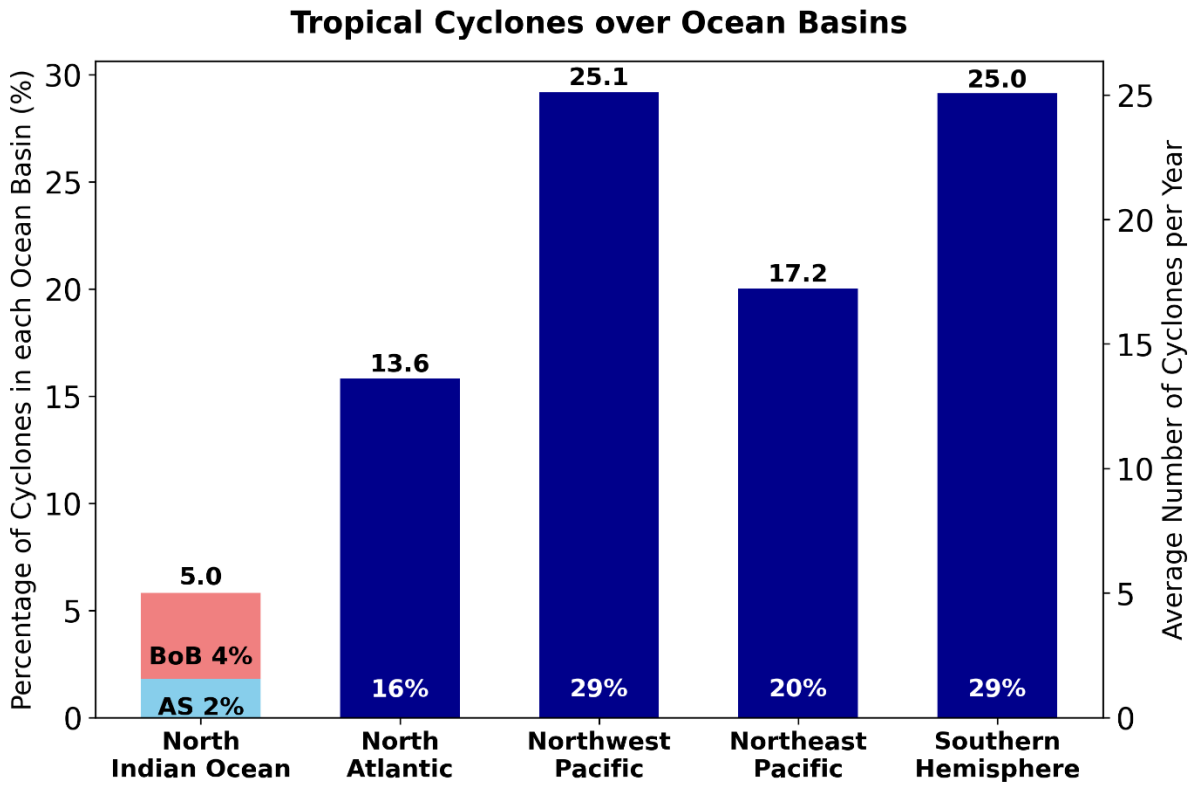

Figure 1.2. *Percentage and the average number of cyclones per year in each ocean basins, during the period 1980–2024. 4% of total cyclones occur in the Bay of Bengal and ~2% occur in the Arabian Sea. The numbers above each bar denotes the average number of cyclones per year in different ocean basins.*

The Bay of Bengal experiences a higher frequency of TCs than the Arabian Sea, primarily due to its higher SST, greater atmospheric moisture content, and the propagation of disturbances from the western North Pacific into this basin (Saha et al., 1981; Sahoo & Bhaskaran, 2016). Although the total number of TCs in this region is comparatively lower, it accounts for over 80% of cyclone-related fatalities worldwide, primarily due to coastal inundation (Beal et al., 2020). Some of the deadliest TCs have originated in the Bay of Bengal, resulting in significant loss of life across countries along its rim—especially India, Bangladesh, and Myanmar (Kikuchi et al., 2009; Madsen & Jakobsen, 2004; McPhaden et al., 2009; Mohapatra & Sharma, 2019). The region's vulnerability to TCs is significantly heightened by a combination of physical and demographic factors. The shallow coastal bathymetry and low-lying, flat terrain make the area highly susceptible to strong storm surges. When these conditions coincide with intense TCs, the impact is further amplified. Additionally, the high population density along the coastline greatly increases the risk to human life and infrastructure, often resulting in devastating loss of lives and extensive damage to property.

Along with the local ocean–atmosphere interactions, the characteristics of TCs over the north Indian Ocean are strongly modulated by large-scale climate phenomena at the subseasonal scale by the Madden–Julian Oscillation (MJO) (Krishnamohan et al., 2012; Singh et al., 2020), and at the interannual to decadal scale by the El Niño Southern Oscillation (ENSO) (Sreenivas et al., 2012; Felton et al., 2013; Girishkumar et al., 2015; Mahala et al., 2015; Bhardwaj et al., 2019), Indian Ocean Dipole (IOD) (Sreenivas et al., 2012; Yuan et al., 2013; Li et al., 2016; Wahiduzzaman et al., 2022) and Pacific Decadal Oscillation (Girishkumar et al., 2015; Roose et al., 2023).

It is reported that in the recent decades (1982–2019), SSTs in the region of TC formation in the Arabian Sea has increased by 1.4°C during the pre-monsoon season and 1.2°C during the post-monsoon season. Similarly, in the Bay of Bengal, the observed change in SST is 0.8°C during the pre-monsoon season and 0.5°C during the post-monsoon season (Singh & Roxy, 2022). This rapid warming of ocean has significantly changed some of the characteristics over the basin (Deshpande et al., 2021). In the recent years there is an increase in the intensity of TCs in the Arabian Sea, along with the increase in the frequency of rapid intensification of TCs (Kranthi et al., 2023; Nadimpalli et al., 2021; Vinodhkumar et al., 2021). Further, the TCs in this basin undergo rapid intensification in its initial stage of formation (Kranthi et al., 2023; Vinodhkumar et al., 2021). Also, the translation speed of TC is declining over the Arabian Sea

(Priya et al., 2022). Further, it is observed that the frequency of Category 1 or higher intensity TCs (wind speed > 64 knots) has increased in the Arabian Sea (Deshpande et al., 2021). Also, in the recent epoch (2001-2019) there is an 80% increase in the TC duration as compared to the earlier epoch (1982-2000) (Deshpande et al., 2021).

Although numerous studies have investigated recent changes in various TC characteristics over the north Indian Ocean, a comprehensive understanding of how global warming influences both the seasonal variability and basin-specific changes in TC behaviour remains limited. In particular, the seasonal differences in TC characteristics over the land and the way these systems have evolved after landfall in recent decades have received less attention. As the ocean continues to warm, it is crucial to examine how TC characteristics in different cyclone seasons, and across the Arabian Sea and the Bay of Bengal, will evolve under a changing climate, especially using high-resolution climate models such as the CMIP6 suite HighResMIP.

In addition, the tropical South Indian Ocean (SIO) has undergone unprecedented warming in the recent years, which likely plays a critical role in modulating TC behaviour. This region exhibits strong seasonal variations in warming patterns and significant long-term warming trends, both of which can profoundly affect TC characteristics. The SIO has also witnessed some of the most intense and destructive TCs in the recent history, including Batsirai (2022), Freddy (2023), and Chido (2024)—with Freddy notably holding the record as the longest-lived cyclone globally (Wang et al., 2025). Despite these developments, lack of comprehensive understanding of how TC characteristics are evolving in this basin under warming climate remains.

Therefore, the present report aims to address these critical gaps by:

1. Providing an improved understanding of the recent observed changes in TC characteristics across the Arabian Sea, Bay of Bengal, and tropical South Indian Ocean; and
2. Presenting a detailed assessment of future TC activity in the north Indian Ocean using CMIP6 HighResMIP high-resolution climate models.

2. Data and Methodology

2.1 Observed Data

TC data for the north Indian Ocean and tropical South Indian Ocean for the period 1982–2023 is obtained from the Joint Typhoon Warning Centre (JTWC) as archived in the International Best Track Archive for Climate Stewardship (IBTrACS) dataset (Knapp et al., 2010). The JTWC provides six-hourly TC data, including TC location, intensity (maximum sustained wind speed), mean sea level pressure and the TC size metrics such as the radius of maximum wind (R_{max}) and the radius of 34 knots wind in four quadrants of TC. As in Singh et al. (2025), we considered only those TCs that attained maximum sustained wind speeds exceeding 34 knots for analysis. Tropical depressions (with maximum wind speeds less than 34 knots) are excluded from the study.

North Indian Ocean TCs which have their genesis between 0–22°N and east of 78°E are taken as the Bay of the Bengal TCs and the TCs which have their genesis between 0–22°N and west of 78°E are considered as the Arabian Sea TCs. If a TC having its genesis in the Bay of Bengal region and it crosses into the Arabian Sea, then that is considered as Bay of Bengal TC. Whereas, for the Southern Tropical Indian Ocean the systems having their genesis between 0-30°S, 30°E-120°E are considered.

2.2 CMIP6 HighResMIP Simulations

In this study, we employ climate model simulations from HighResMIP, a component of CMIP6, which is part of the World Climate Research Programme's latest coordinated effort to produce high-resolution simulations of past and future climates (Eyring et al., 2016). The HighResMIP experiment is chosen as previous studies have shown that the high-resolution models perform better in the realistic simulation of TC as compared to the low-resolution models (Camargo, 2013; Liu et al., 2023; Roberts et al., 2020). Also, the high-resolution models could simulate high intensity TCs. The spatial grid spacing of most HighResMIP models ranges between 25 and 100 km, which is significantly higher than that of standard CMIP6 models. Details of all the HighResMIP models used, including their spatial and temporal resolutions, are summarized in Table 2.1.

Table 2.1. *CMIP6 HighResMIP models which are used in our study, their spatial and temporal resolution and modeling centers information.*

CMIP6-HighResMIP Models	Spatial and Temporal Resolution	Institution
CMCC-CM2-VHR4	25 km, 6 hourly	Euro-Mediterranean Center on Climate Change, Italy
ECMWF-IFS-HR	25 km, 6 hourly	European center for Medium-Range Weather Forecasts, UK
FGOALS-f3-H	25 km, 6 hourly	Chinese Academy of Sciences, China
HadGEM3-GC31-HM	50 km, 3 hourly	Met Office Hadley Center, UK
CNRM-CM6-1_HR	50 km, 6 hourly	National Center for Meteorological Research, France
EC-Earth3P-HR	50 km, 6hourly	EC-Earth Consortium, Europe
ECMWF-IFS-LR	50 km, 6hourly	European center for Medium-Range Weather Forecasts, UK
MPI -ESM1-2-XR	50 km, 6 hourly	Max Plank Institute for Meteorology, Germany
BCC-CSM2-HR	50 km, daily	Beijing Climate Center, China
ECMWF-IFS-MR	50 km, daily	European center for Medium-Range Weather Forecasts, UK
HadGEM3-GC31-HH	50 km, daily	Met Office Hadley Center, UK
EC-Earth3P	100 km, 6 hourly	EC-Earth Consortium, Europe
MPI -ESM1-2-HR	100 km, 6 hourly	Max Plank Institute for Meteorology, Germany
HadGEM3-GC31-MM	100 km, daily	Met Office Hadley Center, UK
CMCC-CM2-HR4	100 km, 6 hourly	Euro-Mediterranean Center on Climate Change, Italy

We selected HighResMIP Tier 2 experiment, which is ocean-atmosphere coupled simulations, covering a period from 1950–2050 (Haarsma et al., 2016). The ocean-atmosphere coupling is crucial for a realistic representation of various TC characteristics in the model (Bell et al., 2013; Scoccimarro et al., 2017; Vincent et al., 2014). For the historical period, we utilize the Hist-1950 experiment, which is initialized using the ERA-20C reanalysis. For future projections, we use the HighResMIP future experiment covering 2015–2050, which follows the SSP5–8.5 high fossil fuel usage scenario (O'Neill et al., 2016). The SSP5-8.5 scenario combines a shared socioeconomic pathway driven by fossil fuel development with

Representative Concentration Pathway 8.5, which has a radiative forcing of 8.5 W m^{-2}. To maintain consistency with the number of years available for future projections, we restricted the analysis of historical simulation in the CMIP6-HighResMIP for the period 1979–2014.

2.3 Methodology

TC monthly frequency distribution is based on the month in which the TC genesis occurs. TC categories are defined based on the Saffir-Simpson scale (Webster et al., 2005). The TC categories are as follows: tropical depression (Vmax ≤ 33 knots), tropical storm (34 knots ≤ Vmax < 64 knots), Category 1 (64 knots ≤ Vmax < 83 knots), Category 2 (83 knots ≤ Vmax < 96 knots), Category 3 (96 knots ≤ Vmax < 113 knots), Category 4 (113 knots ≤ Vmax < 137 knots) and Category 5 (Vmax ≥ 137 knots). Here, Vmax is the maximum wind speed of the TC obtained from the JTWC dataset. As per IMD classification the TCs categories are defined as follows: depression (17 ≤ Vmax < 28 knot), deep-depression (28 ≤ Vmax < 34 knots), cyclonic storm (34 knots ≤ Vmax < 48 knots), severe cyclonic storm (48 knots ≤ Vmax < 64 knots), very severe cyclonic storm (64 knots ≤ Vmax < 90 knots), extremely severe cyclonic storm (90 knots ≤ Vmax < 120 knots) and super cyclonic storm (Vmax ≥ 120 knots). A comparison of the wind speed thresholds to define TC category is mentioned in Table 2.2. Since our analysis includes both the North Indian Ocean and the Southern Tropical Indian Ocean, we adopt the Saffir–Simpson scale methodology to define TC categories, ensuring consistency across the two basins.

In observational datasets, the initial wind speed of developing systems varies; some start at 20 knots, while others begin at 25 or 30 knots, resulting in inconsistencies in identifying the TC genesis location based on the first recorded point. To ensure uniformity, similar to the methodology of Singh et al. (2024), we define the TC genesis in the observation as well as the model, as the first time when the maximum surface wind speed of a system reaches 34 knots. We show the TC tracks only for the timespan when TCs have a maximum wind speed of ≥ 34 knots. This threshold is chosen to emphasize TC tracks corresponding to systems that have reached at least tropical storm intensity, which has a threshold of 34 knots (Deng et al., 2025). TC points corresponding to the genesis and dissipation stages with wind speeds below 34 knots were excluded from the analysis.

The lifetime maximum intensity (LMI) of a TC is defined as the maximum sustained wind speed that a TC achieves during its lifetime. TC duration is counted only for the time

when the TC has its wind speed ≥ 34 knots that is the tropical storm category. TC intensification rate is defined as the rate at which a TC's maximum sustained wind speed increases from the time of its genesis (when the wind speed first reaches 34 knots) to its LMI. It is calculated as the difference between the wind speed at LMI and at genesis, divided by the time (in multiples of 6-hour) taken to reach LMI, and then multiplied by 6 to express the rate in knots/6 h. Rapid intensification of TC is defined as the increase in the wind speed of the TC by at least 30 knots (≥ 55.6 km/h) in 24 h (Kaplan & DeMaria, 2003; Osuri et al., 2017).

Table 2.2. *Saffir-Simpson scale and IMD based classification of TC categories, Vmax is the maximum wind speed of TC.*

JTWC		IMD	
Category of TC	Wind speed	Category of TC	Wind speed
Tropical storm	34 knots ≤ Vmax < 64 knots	Cyclonic storm	34 knots ≤ Vmax < 48 knots
Category 1	64 knots ≤ Vmax < 83 knots	Severe Cyclonic storm	48 knots ≤ Vmax < 64 knots
Category 2	83 knots ≤ Vmax < 96 knots	Very severe cyclonic storm	64 knots ≤ Vmax < 90 knots
Category 3	96 knots ≤ Vmax < 113 knots	Extremely severe cyclonic storm	90 knots ≤ Vmax < 120 knots
Category 4	113 knots ≤ Vmax < 137 knots	Super cyclonic storm	Vmax ≥ 120 knots
Category 5	Vmax ≥ 137 knots		

In the Southern Tropical Indian Ocean, tropical cyclones (TCs) are categorized by month according to their Lifetime Maximum Intensity (LMI), defined as the time when a TC first attains its highest wind speed. For example, TCs that form in one month but reach their LMI in another month are classified according to the month in which the LMI occurs. Thus, a TC that forms in October but reaches its LMI in November is classified as a November cyclone.

Accumulated cyclone energy (ACE) is commonly used to assess the accumulated energy of the TC (Emanuel, 2005). ACE is proportional to the square of the maximum wind

speed of the cyclone. It is calculated by summing the squares of the 6-hourly maximum wind speed in knots for the duration when the TC has a wind speed of 34 knots or higher. The number is divided by 10,000 to make it more readable and easier to interpret (Camargo & Sobel, 2005) and is given by equation 1.

$$\mathrm{ACE} = 10^{-4} \sum \mathrm{V}_{\mathrm{max}}^{2} \qquad (1)$$

Where V_{max} is the maximum wind speed of the TC.

Translation speed is calculated using neighbouring positions along each TC track (these are provided in six-hourly intervals throughout the lifetime of each TC). Distances between 6 hourly TC locations are calculated along a great circle arc. TC size can be estimated through various methods, including in-situ observations, aircraft reconnaissance, and from satellite derived winds (Knaff et al., 2017). Globally, there are no uniform criteria to define TC size. Previous studies have used various wind based criteria to define TC size, this includes the radii of 5 knots wind (Knaff et al., 2014), radii of 16 knots wind (Schenkel et al., 2018), radii of 24 knots wind (Chavas et al., 2016), radii of 30 knots wind (Cocks & Gray, 2002; Lin & Chou, 2018), radii of 34 knots wind (Chan & Chan, 2014) and the radius of the maximum wind (Hill & Lackmann, 2009). Other than winds, some studies also defined the size of TC using the low-level relative vorticity criteria (K. S. Liu & Chan, 1999) and the radius of the outermost closed isobar criteria (Brand 1972; Merrill 1984).

In the past decade, the radius of 34 knots winds (R34) representing gale-force winds has become a key parameter for characterizing TC size due to its strong relevance in assessing TC impact potential (Chan & Chan, 2014, 2015; Knaff & Sampson, 2015). The growing emphasis on R34 is also supported by the improved reliability of operational datasets (Knaff & Sampson, 2015; Landsea & Franklin, 2013). Since the JTWC reports R34 wind radii for four quadrants, we estimated TC size by averaging the R34 values across these quadrants. TC records with missing R34 data in all four quadrants were excluded, while cases with at least one available quadrant value were retained for analysis. The TC size was calculated at 6-hour intervals, considering only the standard synoptic observation times (00, 06, 12, and 18 UTC), and only for those time steps when the maximum sustained wind speed exceeds 34 knots.

2.4 Tropical cyclones in the CMIP6 HighResMIP models

We considered all models with a horizontal grid spacing of 100 km or finer and a temporal resolution of at least 24 hours (Table 1). Most selected models provide the necessary variables at 6-hourly intervals; however, a few models—namely BCC-CSM2-HR, ECMWF-IFS-MR, HadGEM3-GC31-MM, and HadGEM3-GC31-HH provide data only at 24-hour intervals. To ensure consistency across the dataset, only the first ensemble member of each model is included in the analysis, even when multiple members are available. It is important to note that the ECMWF-IFS-HR, ECMWF-IFS-LR, and ECMWF-IFS-MR models contain only historical simulations and lack future projection data. Therefore, these models are used exclusively for evaluating historical simulations against observations and are excluded from the analysis of the future TC projections.

TCs in the model datasets are identified using the Centre National de Recherches Météorologiques (CNRM) TC tracking and detection algorithm (Chauvin et al., 2006) and the justification for the same is provided by Adsul et al. (2026b). The CNRM algorithm was chosen because of its demonstrated superiority in realistically representing TC characteristics over the North Indian Ocean compared to other widely used detection methods, such as the University of Zaragoza (UZ) and Okubo-Weiss-Zeta (OWZ) algorithms (Tory et al., 2013). The CNRM algorithm shows the highest probability of TC frequency detection (Adsul et al. 2026b). In addition, evaluation of TC track accuracy shows that about 65% of TC locations identified by the CNRM algorithm have track errors smaller than 50 km, indicating the lowest positional error among all algorithms examined. This is consistent with Bell et al. (2018), who reported that although the OWZ algorithm performs well in several ocean basins, it is less effective in accurately capturing TC tracks and durations over the North Indian Ocean.

To identify the location of TC, the CNRM algorithm utilises sea level pressure, wind, temperature and relative vorticity at different levels. TC detection in this algorithm is based on the following criteria:

1. The sea level pressure must be lower than the surrounding, the region of pressure minimum indicates the system's centre.
2. Relative vorticity (ζ_{850hPa}) $\geq 1.5 \times 10^{-4}$ s^{-1}.
3. U850 hPa ≥ 5 m s^{-1}.

4. The sum of the temperature anomalies averaged over the 700, 500, 300 hPa pressure levels ≥ 1 K.
5. Difference in temperature anomaly (850 hPa minus 300 hPa) ≤ 1 K.
6. Difference in wind speed (300 hPa minus 850 hPa) ≤ 5 m s^{-1}.

Where, ζ_{850hPa} is the relative vorticity at 850 hPa. U850 is the wind speed at 850 hPa.

In the model data, only systems with wind speeds exceeding 34 knots are selected, i.e. only tropical storms and stronger TCs are included in the analysis. During tracking, if a TC weakened below 34 knots but later re-intensified to at least 34 knots, a relaxation criterion is applied to prevent artificial breaks in the TC track. This criterion, based on a relative vorticity threshold of 2.5×10^{-4} s^{-1} at 850 hPa, allows for the reconstruction of the complete TC life cycle by reconnecting segments that may have been separated due to temporary weakening (Bourdin et al., 2022). The TC category in the CMIP6 model is defined based on the Saffir-Simpson scale, similar to the observation discussed earlier.

To evaluate the performance of the best-performing models, we compared the simulated TC genesis and tracks from the historical period (1979–2014) with the observed TC genesis and tracks. This comparison enhances confidence in the model-based projections. Model performance was assessed using the Taylor diagram approach (Taylor, 2001), a widely adopted method for quantitatively comparing model outputs with a reference dataset (Ngoma et al., 2021; Randriatsara et al., 2023). The Taylor diagram effectively summarizes key statistical measures such as correlation coefficient, centred root-mean-square difference, and standard deviation within a single plot, providing a concise visual representation of model skill.

The correlation coefficient quantifies the degree of spatial or temporal similarity between the model and observations, the root mean square difference reflects the magnitude of deviation between the two datasets (error), and the standard deviation represents the variability in each field. Taylor analysis provides together, these metrics offer a comprehensive evaluation of model fidelity (Taylor, 2001). Additionally, the Taylor skill score was employed to rank models based on their overall agreement with observations, where values closer to 1 indicate better performance. The statistical significance of the results was assessed using a two-tailed Student's *t*-test.

3. Climatology of Tropical Cyclone Characteristics in the North Indian Ocean

3.1 Seasonal climatology of TC frequency and track

In the North Indian Ocean (comprising the Arabian Sea and the Bay of Bengal), the monthly TC distribution shows that there are two peaks in the TC activity (Figure 3.1). The first peak is from April–June, called the pre-monsoon season and the second peak is from October–December and is called the post-monsoon season. The definition of the TC seasons is consistent with earlier studies (Balaji et al., 2018; Murakami et al., 2017; Priya et al., 2022; Rajeevan et al., 2013; Sahu & Pattnaik, 2024; Vidya et al., 2023). Further, Mohapatra et al. (2013) demonstrated that although June is officially part of the monsoon season, TCs forming in June exhibit characteristics similar to those of pre-monsoon systems. Therefore, June TCs are often categorized as pre-monsoon cyclones in scientific analyses. On average ~3 TCs form in the Bay of Bengal in a year, with ~0.8 TCs/year during the pre-monsoon and ~1.7 TCs/year during the post-monsoon. Whereas, in the Arabian Sea, on average ~2 TCs form in the Arabian Sea in a year with ~0.7 TCs/year during the pre-monsoon and ~0.9 TCs/year during the post-monsoon. (Figure 3.1). Further, we see that among all months in the Bay of Bengal, the highest frequency of TCs is observed in November, whereas, in the Arabian Sea, the highest frequency of TCs is observed in June. It is important to note that in the peak monsoon months (July–September), the TC frequency is very low due to very high vertical wind shear in this season (Li et al., 2013). Among all the TC active basins, the North Indian Ocean is the only basin with such a bimodal distribution of TC activity in a calendar year.

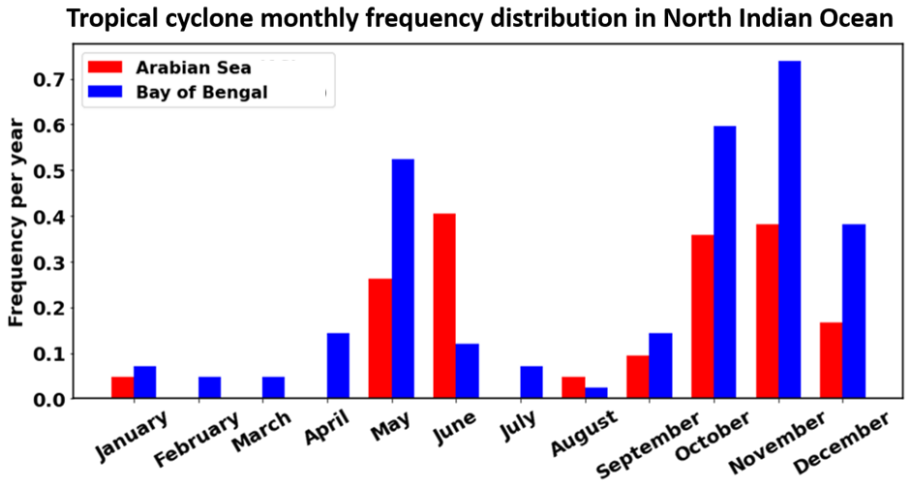

Figure 3.1. *Tropical Cyclone frequency per year in the Arabian Sea (red) and Bay of Bengal (blue) in different months during the period 1982-2023.*

The TCs forming in the Arabian Sea and Bay of Bengal affect the vastly populated coastline of the Indian Ocean rim countries (Adsul et al., 2026a). The pre-monsoon TCs form at an average latitude of 13.8°N in the Bay of Bengal, whereas the genesis of TCs shifts equatorward in the post-monsoon season (Figure 3.2) with an average TC genesis latitude of 12.7°N (Table 3.1). Similarly, in the Arabian Sea, the TC genesis location is ~2.8°N poleward in the pre-monsoon season than in the post-monsoon season (Table 3.1). Thus, in both basins, there is an equatorward shift in the TC genesis location in the post-monsoon season compared to the pre-monsoon season.

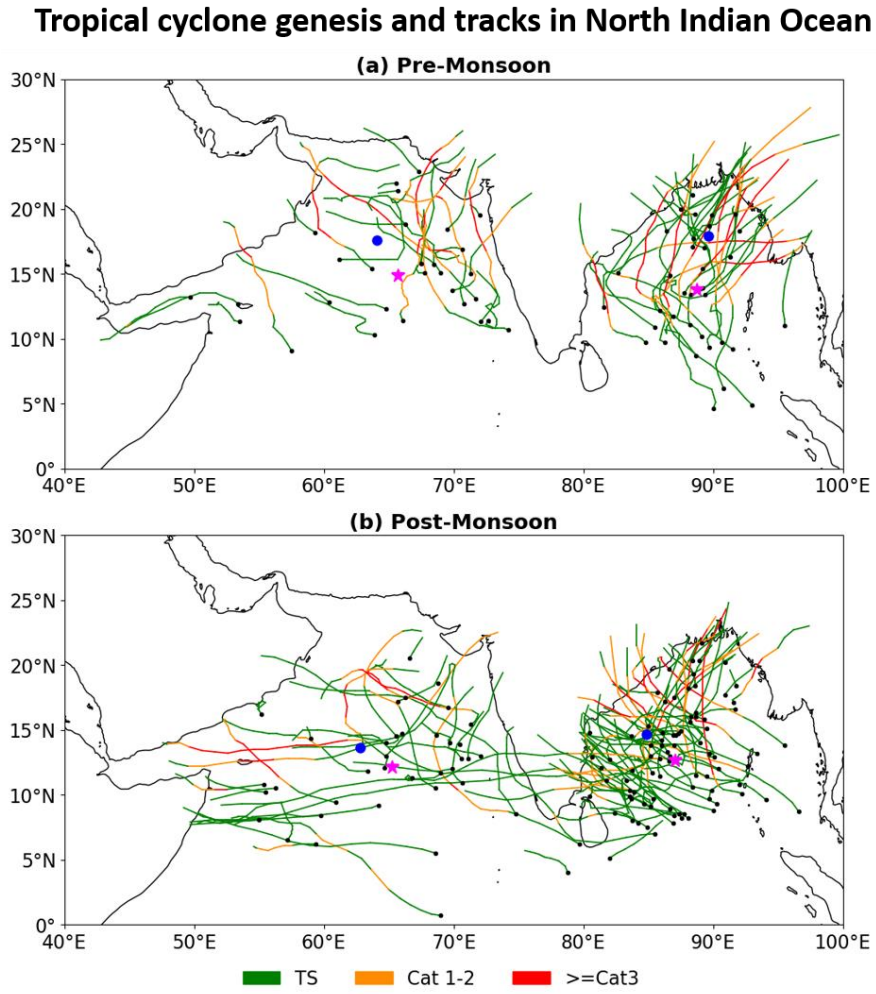

Figure 3.2. *Tropical cyclone tracks (when wind speed of TC ≥ 34 knots) in the Arabian Sea and Bay of Bengal during the (a) Pre-monsoon (April–June) and (b) Post-monsoon (October–December) seasons for the period 1982–2023. Pink star denotes mean TC genesis location and blue circle denotes TC lifetime maximum intensity (LMI) mean location. The genesis points of each TC (location where the first time TC attained winds ≥ 34 knots) are marked with solid black circle. The color along the TC track denotes the category of TC as tropical storm (green), Category 1-2 (orange) and Category ≥3 (red).*

***Table 3.1**. Tropical cyclone (TC) average genesis latitude and longitude in the Bay of Bengal and Arabian Sea during the pre-monsoon (April–June) and post-monsoon (October–December) seasons for the period 1982–2023.*

	Average Genesis latitude (°N)		Average Genesis longitude (°E)	
	Pre-Monsoon	Post-Monsoon	Pre-Monsoon	Post-Monsoon
Bay of Bengal	13.79 ± 4.5	12.66 ± 3.84	88.72 ± 2.67	87.08 ± 3.52
Arabian Sea	14.91 ± 3.66	12.14 ± 3.91	65.73 ± 6.28	65.22 ± 5.48

Along with the seasonal differences in the TC genesis location, there is a marked difference in the TC tracks between the two seasons. During the pre-monsoon season, in the Bay of Bengal, TCs travel more north-northeastward direction and make landfall at the West Bengal coast of India or Bangladesh, or Myanmar coast (Figure 3.2a). Whereas, during the post-monsoon season, TCs travel more west-northwestward direction, as a result, TCs make landfall over the east coast of India or the Sri Lanka coast (Figure 3.2a). At the east coast of India during the post-monsoon season, TCs often strike the Odisha and West Bengal coast in October, Andhra Pradesh coast in November and Tamil Nadu coast in December (Mohapatra & Sharma, 2019). Also, a few TCs after making landfall at the east coast of India do not weaken completely and re-emerge in the Arabian Sea, where due to favourable ocean conditions, they intensify into a TC (Figure 3.2). As in the Bay of Bengal, in the Arabian Sea too, TCs travel more in a north-northeastward direction and make landfall at the west coast of India in the pre-monsoon season (especially Gujarat coast) or Pakistan coast. Whereas, during the post-monsoon season, TCs in this basin travel west-northwestward direction, as a result, very few TCs make landfall over the west coast of India (Figure 3.2b). Thus, the east coast of India is more prone to post-monsoon TCs. Whereas the west coast of India (especially Gujarat) is more prone to pre-monsoon TCs. The coastline of Karnataka and Kerala rarely experience direct TC landfall, mainly due to the lack of recurving TCs in the Arabian Sea at low latitudes.

3.2 Seasonal variations in TC intensity and its rapid intensification

Previously, it was observed that the frequency of TCs is higher during the post-monsoon season compared to the pre-monsoon season. However, despite the lower frequency, some of the most intense TCs tend to occur during the pre-monsoon season and often make landfall along the east coast of India. For instance, TC Fani (2019), with a maximum wind speed of 150 knots

(278 km/h), was the most intense pre-monsoon TC recorded in the Bay of Bengal. As shown in Figure 3.3b, the average LMI of TCs in the Bay of Bengal during the pre-monsoon season is 139.6 km/h, which is 23.9 km/h higher than in the post-monsoon season. Similarly, in the Arabian Sea, the average LMI of TCs during the pre-monsoon season is approximately 11 km/h higher than in the post-monsoon season (Figure 3.3b). Overall, TCs in the Bay of Bengal are approximately 18.7% stronger during the pre-monsoon season compared to the post-monsoon season, while those in the Arabian Sea are about 9.1% stronger. If we compare the two basins, then during the pre-monsoon season, the average LMI of TCs is higher in the Bay of Bengal as compared to the Arabian Sea. However, during the post-monsoon season, the average LMI of TCs in the two basins is nearly the same (Figure 3.3b). Moreover, not only the LMI but also the mean TC intensity (averaged from genesis to dissipation) is higher during the pre-monsoon season by about 11.0% in the Bay of Bengal and 8.8% in the Arabian Sea relative to the post-monsoon season (Figure 3.3a).

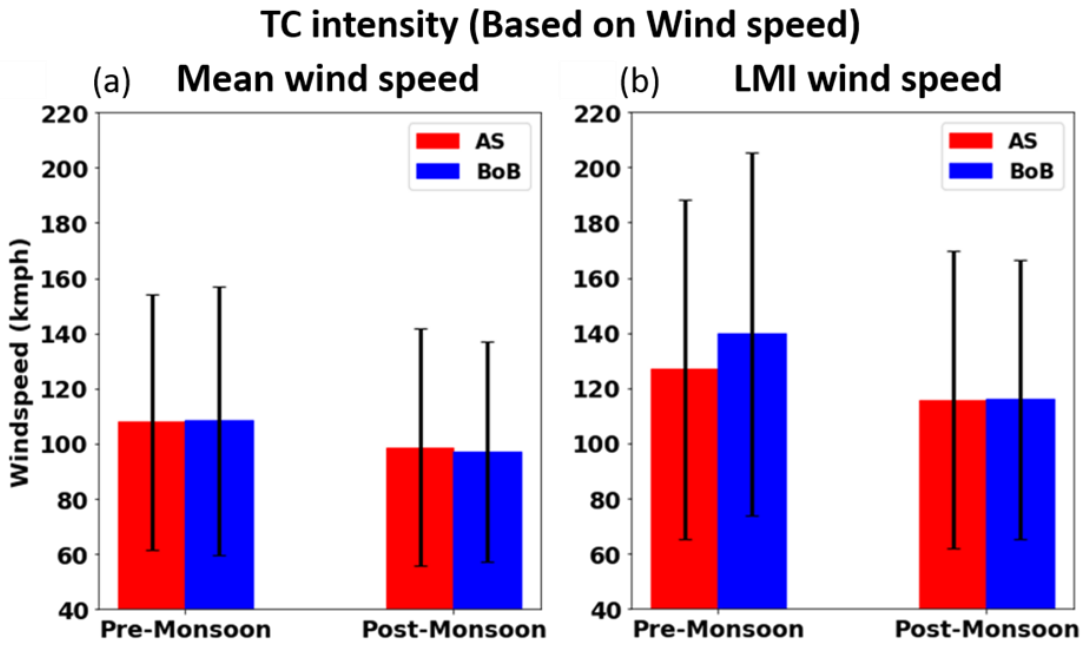

Figure 3.3. *(a) TC mean intensity (averaged from genesis till dissipation, km/h) and (b) TC mean lifetime maximum intensity (LMI, km/h) in the Arabian Sea (red) and the Bay of Bengal (blue) during the pre-monsoon (April–June) and post-monsoon (October–December) seasons for the period 1982–2023. The black vertical line along the bar denotes one standard deviation.*

Further, to increase confidence in our results, we also analyzed the MSLP during TCs. Since the MSLP data is available only from 2002 onwards, the TC intensity analysis based on MSLP is restricted to the period 2002–2023. The TC wind–pressure relationship depends on a

number of factors such as regional environmental climatology, TC latitude, size and its intensity (Knaff & Zehr, 2007; Kossin & Velden, 2004).

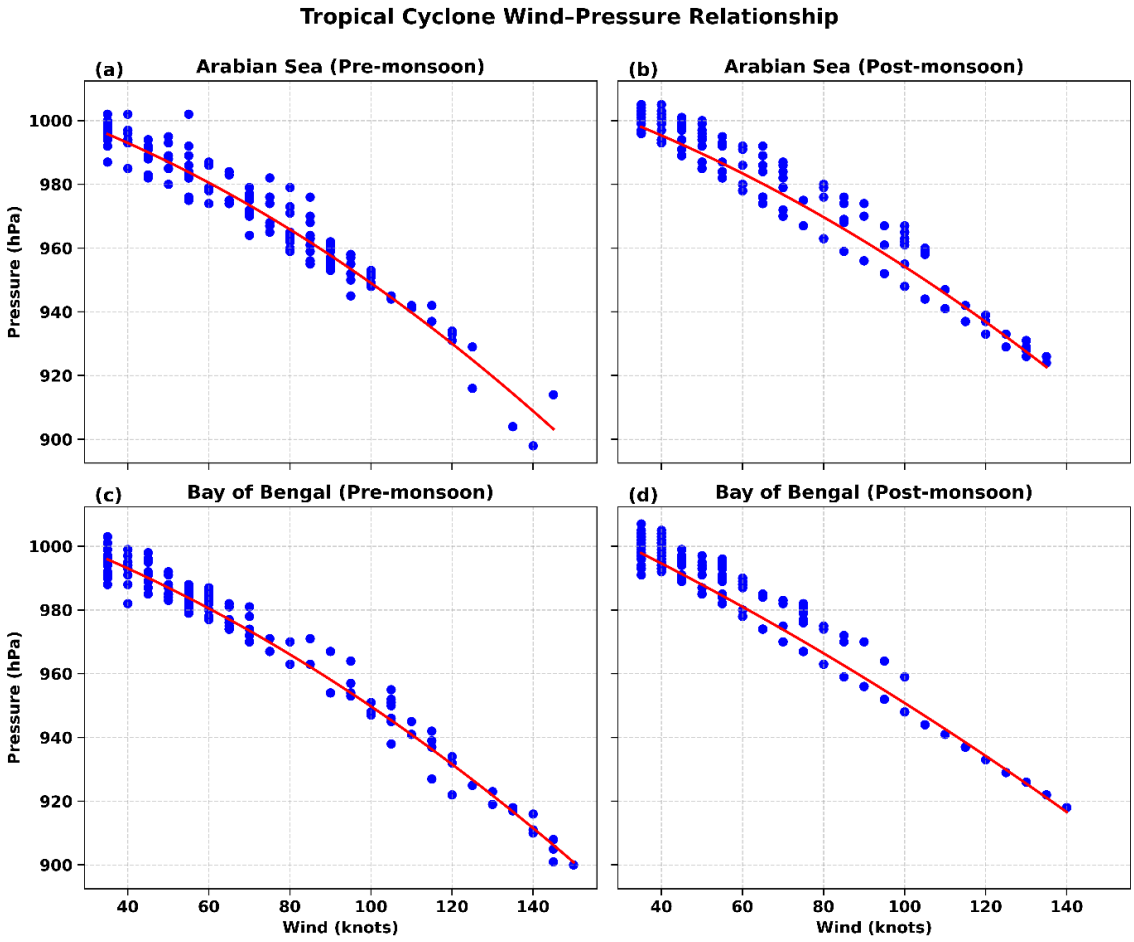

Figure 3.4. *Scatter plot of Mean Sea Level Pressure (MSLP, hPa) at TC center vs maximum wind speed of TC (knots) for the (a) Arabian Sea pre-monsoon season (b) Arabian Sea post-monsoon season (c) Bay of Bengal pre-monsoon season and (d) Bay of Bengal post-monsoon season.*

From the scatter plot, it is evident that during the pre-monsoon season, the lowest central pressure of TCs can reach up to 900 hPa, and the pressure decreases more steeply with increasing TC intensity, exhibiting a parabolic relationship between wind speed and pressure (Figure 3.4 a, c). The correlation between pressure and maximum sustained wind speed is 0.98 for both the Arabian Sea and the Bay of Bengal. In contrast, during the post-monsoon season, the wind–pressure relationship appears nearly linear, with a correlation of 0.97 in both basins (Figure 3.4 b, d). The stronger curvature of the relationship in the pre-monsoon season can be attributed to the relatively higher average latitudes of TCs during this season in both the basins (Figure 3.2). At higher latitudes, the Coriolis force is stronger, which reduces the tangential

wind required to balance the pressure gradient force. Consequently, TCs forming at higher latitudes tend to exhibit lower central pressures for the same wind speed, resulting in a steeper pressure decline with increasing TC category during the pre-monsoon season.

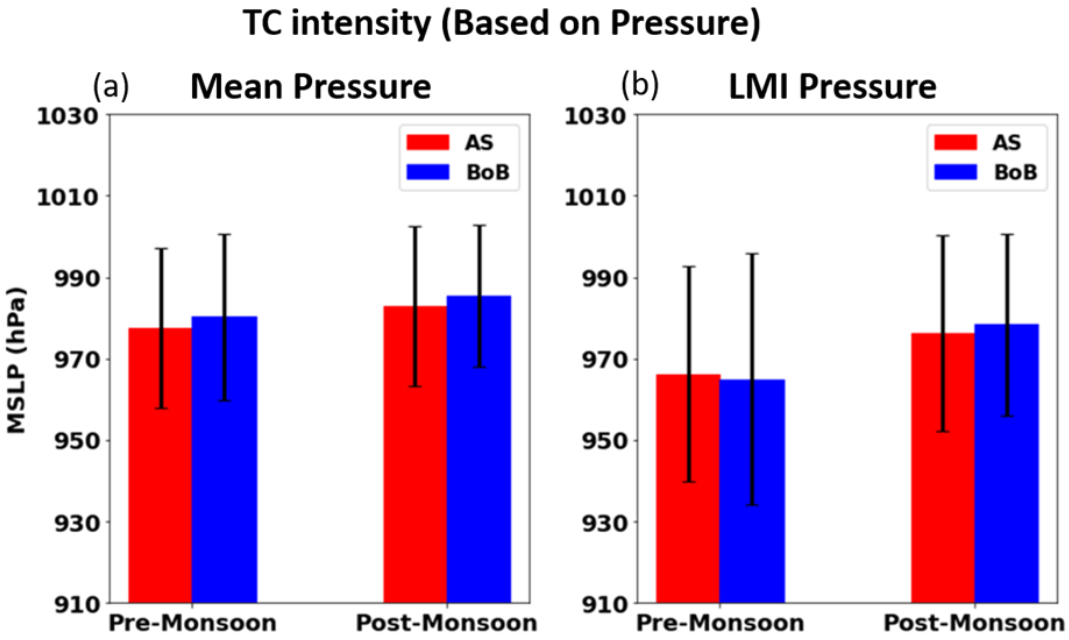

Figure 3.5. *(a) TC mean sea level pressure (MSLP, averaged from genesis till dissipation, hPa) and (b) MSLP at LMI (hPa) in the Arabian Sea (red) and the Bay of Bengal (blue) during the pre-monsoon (April–June) and post-monsoon (October–December) seasons for the period 2002–2023. The vertical black line denotes one standard deviation.*

During the pre-monsoon season, the MSLP at the LMI of TCs in the Arabian Sea is 966.19 hPa, which is approximately 9.9 hPa lower than that observed during the post-monsoon season. Similarly, in the Bay of Bengal, the average MSLP at LMI during the pre-monsoon season is 964.95 hPa, about 13.4 hPa lower than in the post-monsoon season (Figure 3.5b). In addition, the average intensity of TCs based on MSLP in the Bay of Bengal and the Arabian Sea is approximately 5 hPa and 4.5 hPa lower, respectively, during the pre-monsoon season compared to the post-monsoon season (Figure 3.5a). These results indicate that, consistent with the intensity inferred from maximum wind speed, the pressure-based analysis also confirms that TCs in both basins are generally more intense during the pre-monsoon season than during the post-monsoon season.

Furthermore, in agreement with the wind speed–based results for both the shorter and longer analysis periods, the pressure-based analysis reveals that during the pre-monsoon

season, TCs in the Bay of Bengal (average LMI MSLP: 964.95 hPa) tend to be more intense than those in the Arabian Sea (average LMI MSLP: 966.19 hPa). In contrast, during the post-monsoon season for the longer period (1982–2023), no significant difference is found in the mean LMI of TCs based on wind speed analysis. However, for the shorter and more recent period (2002–2023), the average LMI of TCs, based on both wind speed and MSLP analyses, is found to be higher in the Arabian Sea compared to the Bay of Bengal (Table 3.2). Overall, these findings highlight a distinct seasonal contrast: during the pre-monsoon season, TCs in the Bay of Bengal are generally more intense, whereas during the post-monsoon season, TCs in the Arabian Sea exhibit greater intensity, particularly in the recent period (2002–2023).

Table 3.2. *Tropical cyclone (TC) average LMI (in terms of wind speed (km/h) and MSLP (hPa) in the Bay of Bengal and Arabian Sea during the pre-monsoon (April–June) and post-monsoon (October–December) seasons for the period 2002–2023.*

	TC average LMI based on wind speed (km/h)		TC average LMI based on pressure (hPa)	
	Pre-Monsoon	Post-Monsoon	Pre-Monsoon	Post-Monsoon
Bay of Bengal	140.2 ± 66.6	116.4 ± 54.4	964.95 ± 31.02	978.3 ± 22.43
Arabian Sea	141.8 ± 64.5	125.0 ± 63.0	966.19 ± 26.41	976.08 ± 24.09

A category-wise distribution analysis of TCs over the North Indian Ocean reveals that both the Arabian Sea and the Bay of Bengal exhibit the highest frequency of storms in the tropical storm (TS) category (Figure 3.6 a–b). During the analysis period, only one Category 5 TC was observed in the Arabian Sea, occurring during the pre-monsoon season, with none recorded in the post-monsoon season. In contrast, the Bay of Bengal experienced a total of seven Category 5 TCs—four during the pre-monsoon season and three during the post-monsoon season (Figure 3.6 a–b). This highlights that a higher number of category 5 TCs form in the Bay of Bengal as compared to the Arabian Sea.

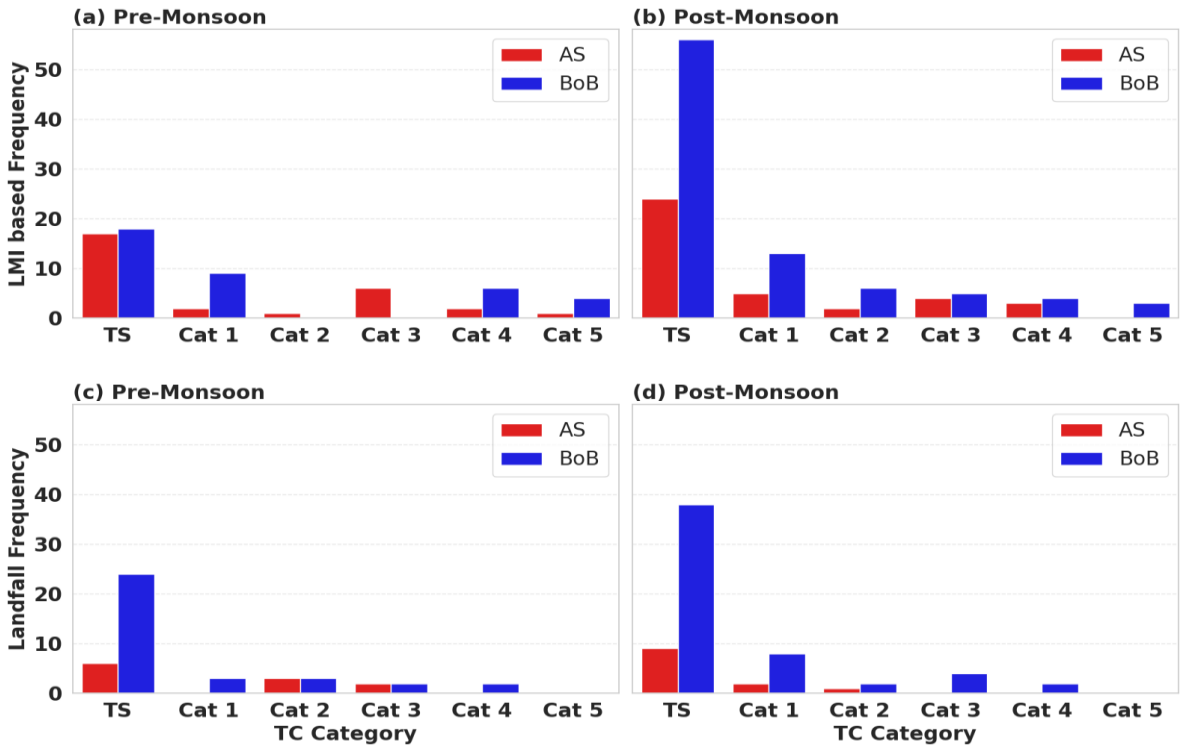

Figure 3.6. *Frequency of tropical cyclones (TCs) across different categories for the Arabian Sea (red) and Bay of Bengal (blue) during the pre-monsoon (April–June) and post-monsoon (October–December) seasons for the period 1982–2023. Panels (a–b) show the overall TC frequency, while panels (c–d) depict the frequency of TCs at the time of landfall.*

In terms of percentage distribution of TCs in different categories, during the pre-monsoon season, approximately 41.4% of TCs in the Arabian Sea and 51.4% in the Bay of Bengal intensify to Category 1 or higher intensity (maximum wind speed > 64 knots). In contrast, during the post-monsoon season, only 36.8% and 35.6% of TCs in the Arabian Sea and Bay of Bengal, respectively, reach Category 1 or higher intensity (Table 3.3). This indicates that, in both basins, a larger proportion of TCs attain at least typhoon strength (Category 1 or higher) during the pre-monsoon season compared to the post-monsoon season and the TC intensification efficiency in both basins is higher in the former season than in the latter season. Furthermore, in the Arabian Sea, nearly one in every three TCs intensifies into a major TC (Category 3 or higher, winds ≥ 100 knots) during the pre-monsoon season, whereas only one in every six TCs achieves such intensity during the post-monsoon season. Similarly, in the Bay of Bengal, about one in every four TCs reaches major TC intensity during the pre-monsoon season, while only one in every seven TCs does so during the post-monsoon season (Table 3.3).

Table 3.3. *Percentage of TCs intensifying to at least Category 1 or higher intensity TC (wind speed > 64 knots) and Category 3 or higher intensity TC (wind speed ≥ 100 knots) in the Arabian Sea and the Bay of Bengal during the pre-monsoon (April–June) and the post-monsoon (October–December) seasons for the period 1982–2023.*

	TC Category ≥ 1		TC Category ≥ 3	
	Pre-Monsoon	Post-Monsoon	Pre-Monsoon	Post-Monsoon
Arabian Sea	41.4%	36.8%	31.0%	18.4%
Bay of Bengal	51.4%	35.6%	27.0%	13.8%

Table 3.4. *Number of Tropical Cyclones (TCs) and the percentage of total number of TCs undergoing rapid intensification (in bracket) in the Arabian Sea and the Bay of Bengal during the pre-monsoon (April–June) and the post-monsoon (October–December) season for the period 1982–2023.*

	Pre-Monsoon	Post-Monsoon
Arabian Sea	10 (34.5%)	7 (18.4%)
Bay of Bengal	12 (32.4%)	14 (16.1%)

The rapid intensification of TCs poses a severe challenge for forecasters as it involves the understanding of internal dynamics, interplay of environmental parameters, and nonlinear processes (Neetu et al., 2020; Zhang & Oey, 2019) and has large forecast errors across the globe (Bhatia et al., 2022; Trabing & Bell, 2020). Such rapidly intensifying TCs also possess significant challenge for disaster preparedness, especially if a TC intensifies rapidly closer to the coast (Lok et al., 2021). It is observed that during the pre-monsoon season, 34.5% of TCs in the Arabian Sea and 32.4% in the Bay of Bengal undergo rapid intensification. In contrast, during the post-monsoon season, 18.4% of TCs in the Arabian Sea and 16.1% in the Bay of Bengal experience rapid intensification (Table 3.4). Although the absolute number of rapidly intensifying TCs is higher in the Bay of Bengal during the post-monsoon season—owing to the greater overall number of TCs in that period, the likelihood of a TC undergoing rapid intensification is notably higher during the pre-monsoon season (Table 3.4). Thus, in both the basins, during the pre-monsoon season TCs have a higher probability to intensify rapidly as compared to the post-monsoon season. Also, we found that during the pre-monsoon season, most TC rapid intensification events occur near the west coast of India (Figure 3.7). In contrast, during the post-monsoon season, the rapid intensification locations shift westward, away from

the Indian mainland. However, over the Bay of Bengal, no pronounced seasonal differences in TC rapid intensification locations are observed.

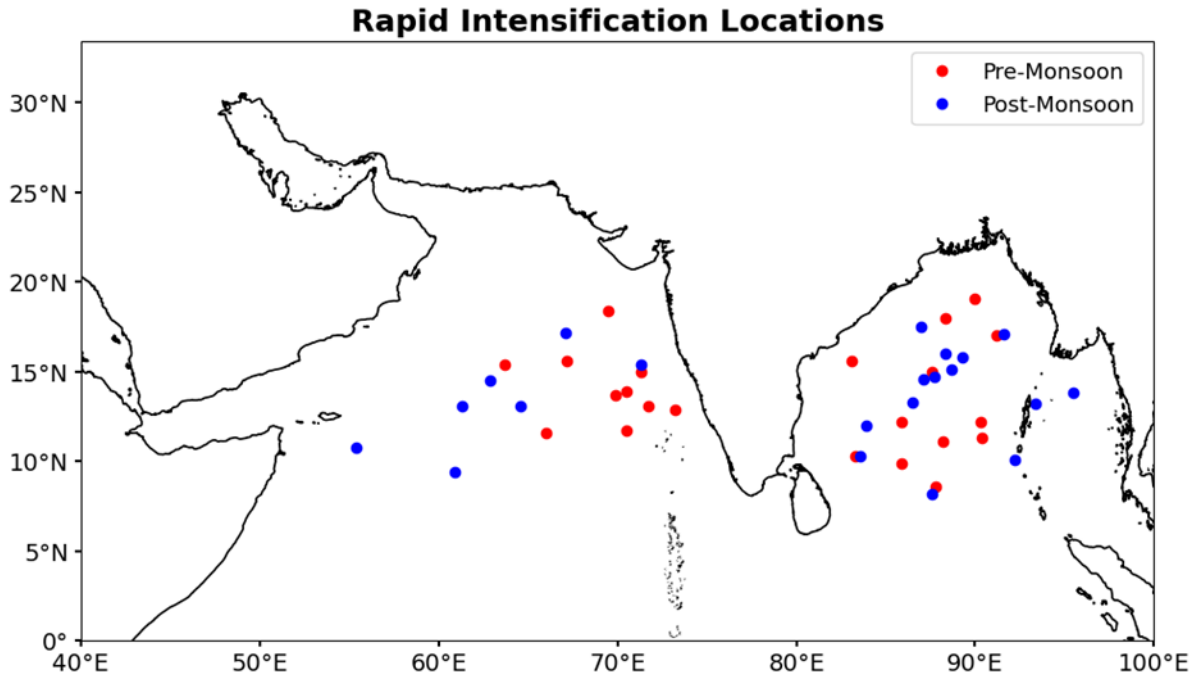

Figure 3.7. *TC rapid intensification location in the North Indian Ocean during the Pre-Monsoon season (April–June, red filled circle) and Post-Monsoon season (October–December, blue filled circle) for the period 1982–2023.*

In the North Indian Ocean, TCs generally attain their peak intensity over the open ocean before weakening slightly as they approach the coast and make landfall due to increased surface friction (Figure 3.2). In the Arabian Sea, approximately 38% and 31.5% of TCs during the pre-monsoon and post-monsoon seasons, respectively, make landfall with at least tropical storm strength (wind speed ≥ 34 knots). In contrast, in the Bay of Bengal, about 91.9% of TCs during the pre-monsoon season and 65.5% during the post-monsoon season make landfall with at least tropical storm intensity (Figure 3.6 c-d). Thus, the probability of TCs making landfall with at least tropical storm intensity is significantly higher in the Bay of Bengal than in the Arabian Sea during both seasons, with a notably greater likelihood during the pre-monsoon season. This highlights a sharp contrast between the two basins.

Further, it is observed that during the period1982–2023, no TC in the North Indian Ocean has made landfall with Category 5 intensity (wind speed ≥ 140 knots) (Figure 3.6 c-d). In the Arabian Sea, only two TCs during the pre-monsoon season have made landfall with

major intensity (Category 3 or higher, wind speed ≥ 100 knots), whereas no such landfall has occurred during the post-monsoon season. In the Bay of Bengal, TCs have made landfall with intensities up to Category 4, with two Category 4 landfalls recorded in both the pre-monsoon and post-monsoon seasons (Figure 3.6 c-d).

Not only the LMI of TC but also the location where the TC attains its LMI is crucial, as it helps to understand how far away from the coast the TC is attaining its maximum intensity. A closer proximity of LMI to the coast possess greater threat to the coastline. TCs in the Bay of Bengal reach their LMI at approximately 17.9°N during the pre-monsoon season and around 14.7°N during the post-monsoon season (Figure 3.2, Table 3.5). In the Arabian Sea, TCs attain their LMI about 4° farther poleward in the pre-monsoon season compared to the post-monsoon season (Figure 3.2, Table 3.5). This latitudinal difference in LMI location primarily arises from variations in TC genesis regions and track characteristics between the two seasons. During the pre-monsoon season, TCs tend to form at higher latitudes and follow more northward trajectories, leading to higher-latitude LMIs. In contrast, during the post-monsoon season, TC genesis shifts equatorward, and the systems generally move west-northwestward, resulting in LMIs occurring at lower latitudes. Consequently, due to these differences in TC tracks, the LMI location in the Bay of Bengal tends to be closer to the east coast of India during the post-monsoon season compared to the pre-monsoon season.

Table 3.5. *Tropical cyclone (TC) average lifetime maximum intensity (LMI) latitude and longitude in the Bay of Bengal and Arabian Sea during the pre-monsoon (April–June) and post-monsoon (October–December) seasons for the period 1982–2023.*

	Average LMI latitude (°N)		**Average LMI longitude (°E)**	
	Pre-Monsoon	Post-Monsoon	Pre-Monsoon	Post-Monsoon
Bay of Bengal	17.89 ± 3.69	14.65 ± 4.06	89.62 ± 3.27	84.86 ± 3.98
Arabian Sea	17.57 ± 3.57	13.63 ± 4.32	64.11 ± 7.03	62.78 ± 6.33

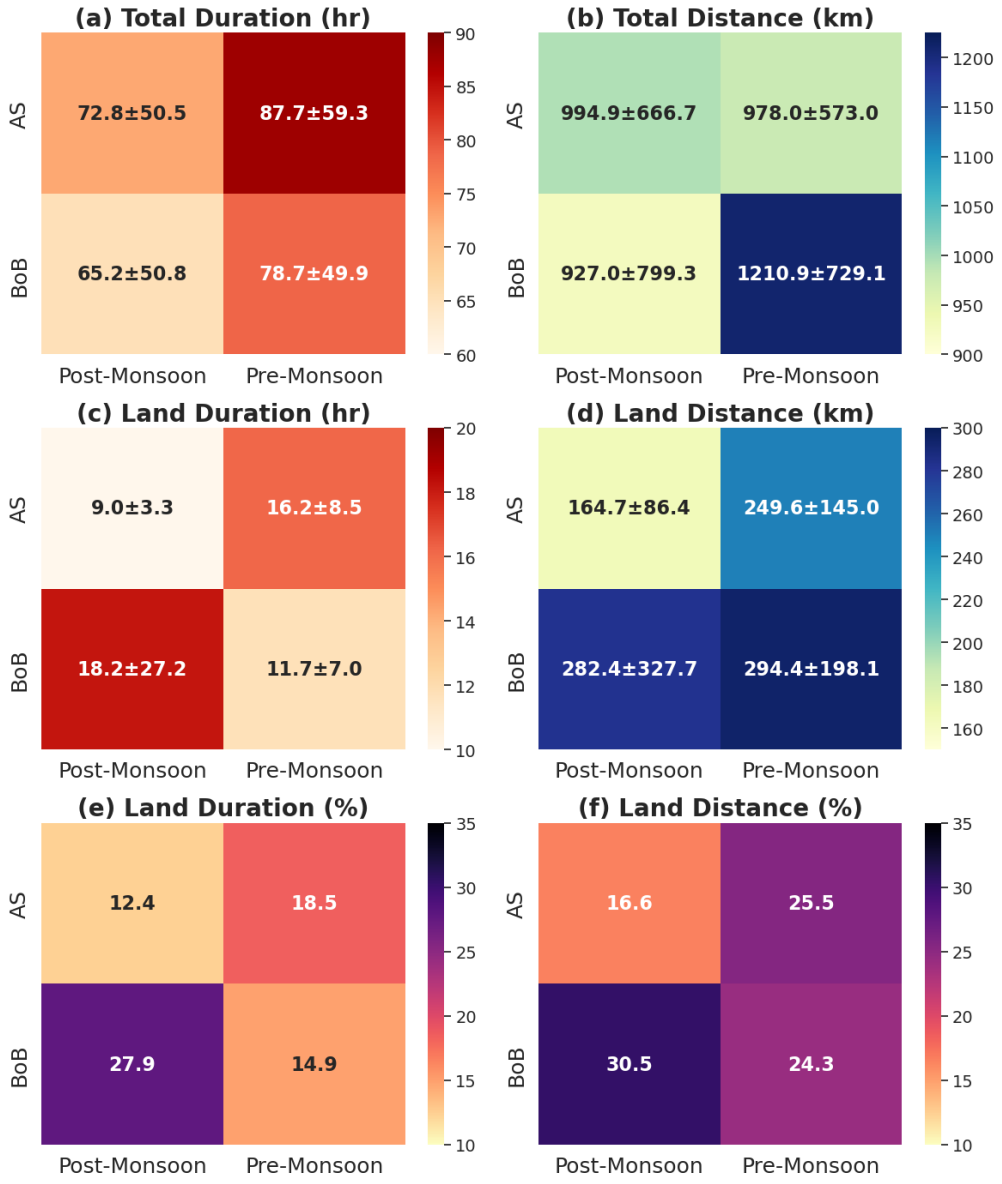

Figure 3.8. *(a) TC total average duration (hours) (b) TC total distance (km) (c) TC duration over land (hours) (d) TC distance over land (km). (e) Percentage of TC duration over land (f) Percentage of TC distance over land in the Arabian Sea and the Bay of Bengal during the pre-monsoon (April–June) and the post-monsoon (October–December) seasons for the period 1982–2023. Here, the TC duration and distance are computed when the system has a wind speed ≥ 34 knots.*

3.3 Seasonal characteristics of TC duration

As in the seasonal contrast observed in TC frequency and intensity, the TC duration over both the Arabian Sea and the Bay of Bengal displays distinct seasonal variations (Figure 3.8). During the pre-monsoon season, TCs over the Arabian Sea have an average duration of 87.7 hours, which is 14.9 hours longer than in the post-monsoon season. In the Bay of Bengal,

the mean TC duration during the pre-monsoon season is 78.7 hours, about 13.5 hours longer than in the post-monsoon season (Figure 3.8a). Hence, in both basins, TCs tend to persist longer during the pre-monsoon season when considering only the tropical storm or higher intensity stage (wind speed ≥ 34 knots).

Interestingly, when all TC stages—including the weaker phases with wind speeds down to 17 knots are considered, a different pattern emerges. In the Arabian Sea, during the pre-monsoon season, the average TC duration increases to 138.8 hours (~5.75 days), which is 10.7 hours shorter than in the post-monsoon season (Figure 3.9a). This suggests that although TCs in the Arabian Sea during the post-monsoon season persist longer overall, their tropical storm or higher intensity phase (wind speed ≥ 34 knots) is comparatively shorter than that of pre-monsoon TCs. In contrast, over the Bay of Bengal, even after including the weaker stages, TCs during the pre-monsoon season remain slightly longer lived than those in the post-monsoon season (Figure 3.9a). This consistency across intensity thresholds indicates that Bay of Bengal TCs generally sustain longer durations during the pre-monsoon season compared to the post-monsoon season.

When comparing the two basins, during the pre-monsoon season, TCs in the Bay of Bengal during the tropical storm or higher intensity stage have a mean duration of 78.7 hours (~3.5 days), which is approximately 9 hours shorter than those in the Arabian Sea (Figure 3.8a). Similarly, during the post-monsoon season, Bay of Bengal TCs last for an average of 65.2 hours (~2.75 days), which is about 7.6 hours shorter than TCs in the Arabian Sea (Figure 3.8a). Thus, in both seasons, TCs in the Arabian Sea generally exhibit longer lifetimes compared to those in the Bay of Bengal. This is consistent even after including wind speed up to 17 knots. Overall, we found that TCs forming over the North Indian Ocean are relatively short-lived compared to the western North Pacific where on average TC duration (wind speed ≥ 34 knots) is roughly 5 days (Kushwaha et al., 2025).

TC duration over land has pronounced socio-economic implications, as longer-lasting landfalling TCs tend to cause more extensive damage and disruption. To assess this, we examined TC duration over land for two intensity thresholds: (i) only the tropical storm stage and above (wind speed ≥ 34 knots), and (ii) the complete duration until dissipation (wind speed down to 17 knots).

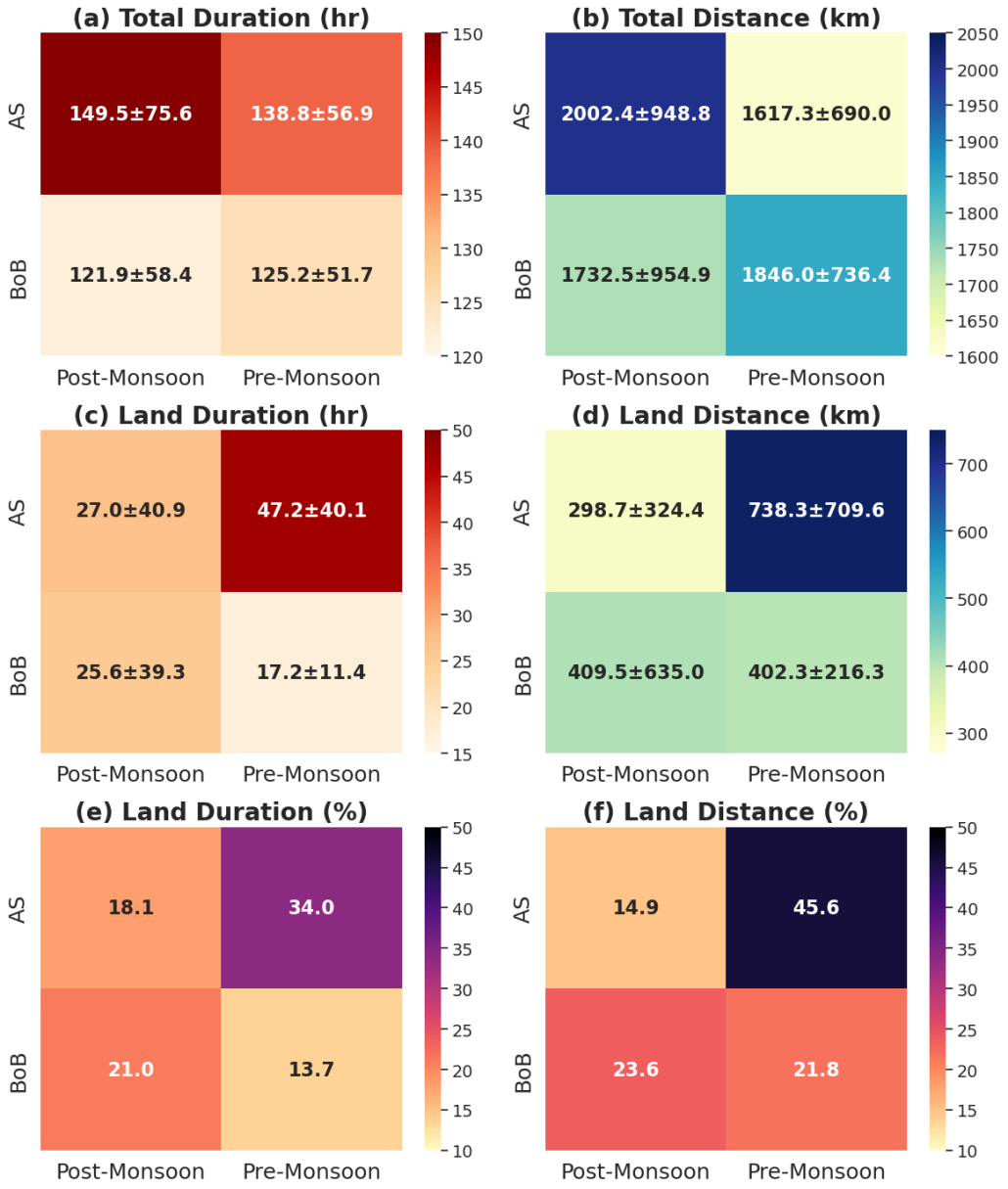

Figure 3.9. *(a) TC total average duration (hours) (b) TC total distance (km) (c) TC duration over land (hours) (d) TC distance over land (km). (e) Percentage of TC duration over land (f) Percentage of TC distance over land in the Arabian Sea and the Bay of Bengal during the pre-monsoon (April–June) and the post-monsoon (October–December) seasons for the period 1982–2023. Here, the duration and distance are computed when the system has a wind speed ≥ 17 knots.*

In the Arabian Sea, the average TC land duration at tropical storm intensity is 16.2 hours during the pre-monsoon season and 9.0 hours during the post-monsoon season (Figure 3.8c). In contrast, over the Bay of Bengal, the corresponding averages are 11.7 hours and 18.2 hours, respectively. Expressed as a fraction of total TC lifetime, Bay of Bengal TCs spend 14.9% of their duration over land during the pre-monsoon season and 27.9% during the post-monsoon season (Figure 3.8e). These results indicate that during the pre-monsoon season, Arabian Sea

TCs spend a longer time over land at tropical storm or higher intensity than those in the Bay of Bengal, whereas during the post-monsoon season, Bay of Bengal TCs persist over land for longer durations than those in the Arabian Sea.

When the full TC lifetime (including weaker stages up to 17 knots) is considered, the Arabian Sea shows markedly longer land interaction. The average TC land duration is 47.2 hours (~2 days) in the pre-monsoon season and 27 hours (~1 day) in the post-monsoon season (Figure 3.9c). These correspond to 34% and 18.1% of the total TC duration, respectively (Figure 3.9e). In the Bay of Bengal, the average TC land duration is 17.2 hours (~0.75 days) during the pre-monsoon season, accounting for 13.7% of the total duration, and 25.6 hours (~1 day) during the post-monsoon season, representing 21% of the total duration (Figure 3.9c, e).

Overall, these results reveal distinct seasonal and regional contrasts. At tropical storm or higher intensities, Arabian Sea TCs during the pre-monsoon season spend the longest time over land, while Bay of Bengal TCs during the post-monsoon season exhibit greater land persistence. However, when all intensity stages up to dissipation are considered, Arabian Sea TCs consistently spend longer durations over land compared to Bay of Bengal TCs in both seasons. This finding underscores the importance of these aspects while assessing the regional disaster risks and preparedness.

3.4 Seasonal characteristics of TC track length

The total distance travelled by TCs exhibits notable seasonal and basin-specific differences. Considering only the period when TCs are at tropical storm intensity or higher (wind speed ≥ 34 knots), the average track length in the Arabian Sea is 978.0 km during the pre-monsoon season and 994.9 km during the post-monsoon season (Figure 3.8b). Of this, the distance travelled over land is 249.6 km in the pre-monsoon season and 164.7 km in the post-monsoon season (Figure 3.8d), corresponding to 25.5% and 16.6% of the total track length, respectively (Figure 3.8f). The longer track overland during the pre-monsoon season contributes to the higher TC duration observed in this season compared to the post-monsoon season.

In the Bay of Bengal, the average TC track length is 1210.9 km during the pre-monsoon season and 927.0 km during the post-monsoon season (Figure 3.8b). The distance travelled over land is 294.4 km (24.3% of total distance) in the pre-monsoon season and 282.4 km

(30.5% of total distance) in the post-monsoon season (Figures 3.8d, f). When all TC stages are considered (wind speeds down to 17 knots), the Arabian Sea TCs during the pre-monsoon season travel an average total distance of 1617.3 km, compared to 2002.4 km during the post-monsoon season (Figure 3.9b). Analysis of the distance over land shows that pre-monsoon TCs travel 738.3 km (~45.6% of total track length) over land, whereas post-monsoon TCs travel 298.7 km (~14.9% of total track length) over land (Figures 3.9d, f). Although post-monsoon TCs cover a slightly longer total distance, pre-monsoon TCs cover larger distance over land, indicating that landfalling pre-monsoon storms in the Arabian Sea have the potential to impact a wider area. This pattern is consistent with the analysis restricted to tropical storm or higher intensity stages (wind speed ≥ 34 knots). In contrast, in the Bay of Bengal, the total TC track length is longer during the pre-monsoon season than in the post-monsoon season. The distance travelled over land is 402.3 km (~21.8% of the total distance) in the pre-monsoon season and 409.5 km (~23.6%) in the post-monsoon season (Figures 3.9d, f).

A basin-wise comparison further highlights clear contrasts. During the pre-monsoon season, the total track length over land is greater in the Arabian Sea than Bay of Bengal when all TC stages are included. However, when considering only tropical storms or higher intensity stages, Bay of Bengal TCs travel farther over land than Arabian Sea TCs in this season (Figures 3.8, 3.9). For the post-monsoon season, regardless of whether all TC stages or only tropical storm or higher intensity stages are considered, Bay of Bengal TCs consistently travel longer distances over land than the Arabian Sea TCs.

3.5 Seasonal characteristics of accumulated cyclone energy (ACE)

The ACE is commonly used to assess the accumulated energy of TC. It is an integrated metric of TC intensity and its duration (Emanuel, 2005). During the pre-monsoon season, the average ACE of TCs in the Arabian Sea and the Bay of Bengal is higher than the post-monsoon season (Figure 3.10). This higher ACE in the pre-monsoon season is due to the higher intensity of TCs as well as longer duration of TCs (Figure 3.8a) in both the basins.

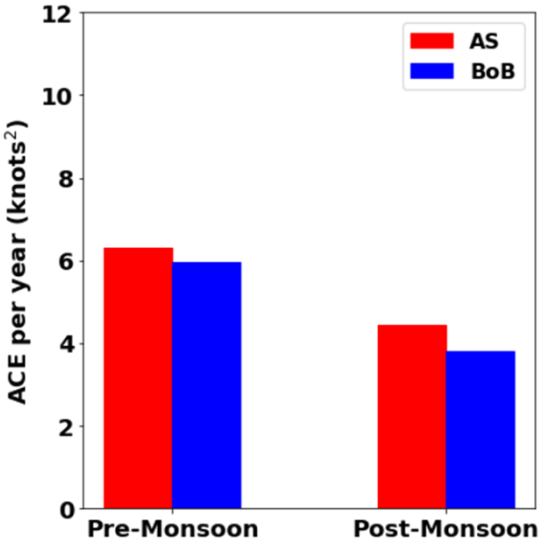

Figure 3.10. *Accumulated cyclone energy per cyclone (×10⁴ knots²) in the Arabian Sea (red) and the Bay of Bengal (blue) during the pre-monsoon and the post-monsoon season for the period 1982–2023.*

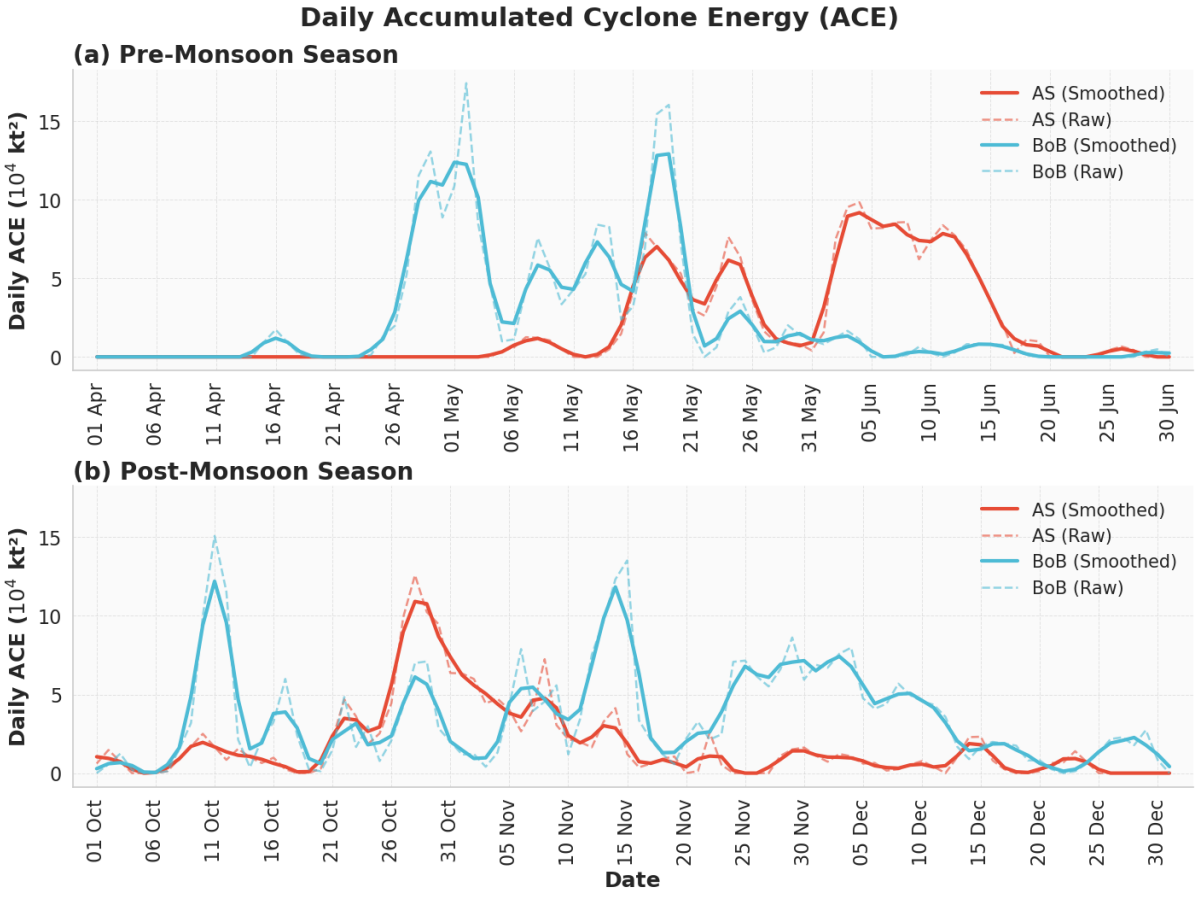

Figure 3.11. *Daily climatology of Accumulated cyclone energy (ACE ×10⁴, knots²) in the Arabian Sea (red) and the Bay of Bengal (blue) during (a) pre-monsoon season (April–June) and (b) post-monsoon season (October–December) for the period 1982–2023. The dash line indicates the raw value of ACE, whereas the thick continuous line denotes the 3-day running mean of ACE.*

We also computed the daily climatology of the ACE, which helps identify the periods of peak TC activity within a season. As shown in Figure 3.11a, in the Arabian Sea during the pre-monsoon season, TC activity begins after 15 May and reaches its peak during the first two weeks of June. After 15 June, a sharp decline in activity (indicated by a steep drop in ACE) is observed, primarily due to the full establishment of the southwest monsoon. In contrast, in the Bay of Bengal, the daily ACE climatology reveals two distinct peaks in TC activity—the first between 28 April and 4 May, and the second during the third week of May (Figure 3.11a). Unlike the Arabian Sea, TC activity in the Bay of Bengal decreases sharply after the third week of May. Overall, these results highlight that during the pre-monsoon season, most TC activity in the Arabian Sea occurs between 16 May and 15 June, whereas in the Bay of Bengal, it occurs earlier, mainly between 26 April and 21 May. The reason for the difference in the peak TC activity between the two seasons needs detailed investigation.

For the post-monsoon season, in the Arabian Sea, the peak in the TC activity is confined between the last week of October to first week of November, and hardly any major TC activity is seen beyond 2nd week of November. Whereas, in the Bay of Bengal, the TC activity is more spread out with three distinct peak activities in 2nd week of October, than around mid-November and lastly from 25 November to 5 December (Figure 3.11b). In short the major TC threat in the Arabian Sea during post-monsoon is between 21 October to 15 November. Whereas, in the Bay of Bengal TC threat is there throughout the season with three distinct peaks.

3.6 Seasonal characteristics of TC translation speed

Translation speed of TCs is one of the important features, as slower-moving TCs have a longer duration of influence, which can significantly enhance the impacts of associated severe weather events such as heavy rainfall, storm surges, and strong winds (Emanuel, 2017). TCs are generally steered by the atmospheric forcings and background winds (Singh et al., 2022). We have computed the translation speed for the entire duration of the system, including weaker intensity than tropical storm stage (wind speed up to 17 knots). It is observed that during the pre-monsoon season, the average translation speed of TCs in the Arabian Sea and the Bay of Bengal is 3.30 m s^{-1} and 4.20 m s^{-1}, respectively (Figure 3.12). In the Arabian Sea, the

translation speed during the pre-monsoon season is 0.68 m s^{-1} lower than that in the post-monsoon season, indicating that TCs move more slowly in the pre-monsoon season. In contrast, over the Bay of Bengal, TCs during the post-monsoon season move 0.14 m s^{-1} slower than those in the pre-monsoon season (Figure 3.12). Hence, the translation speed of TCs exhibits distinct seasonal variations in both basins.

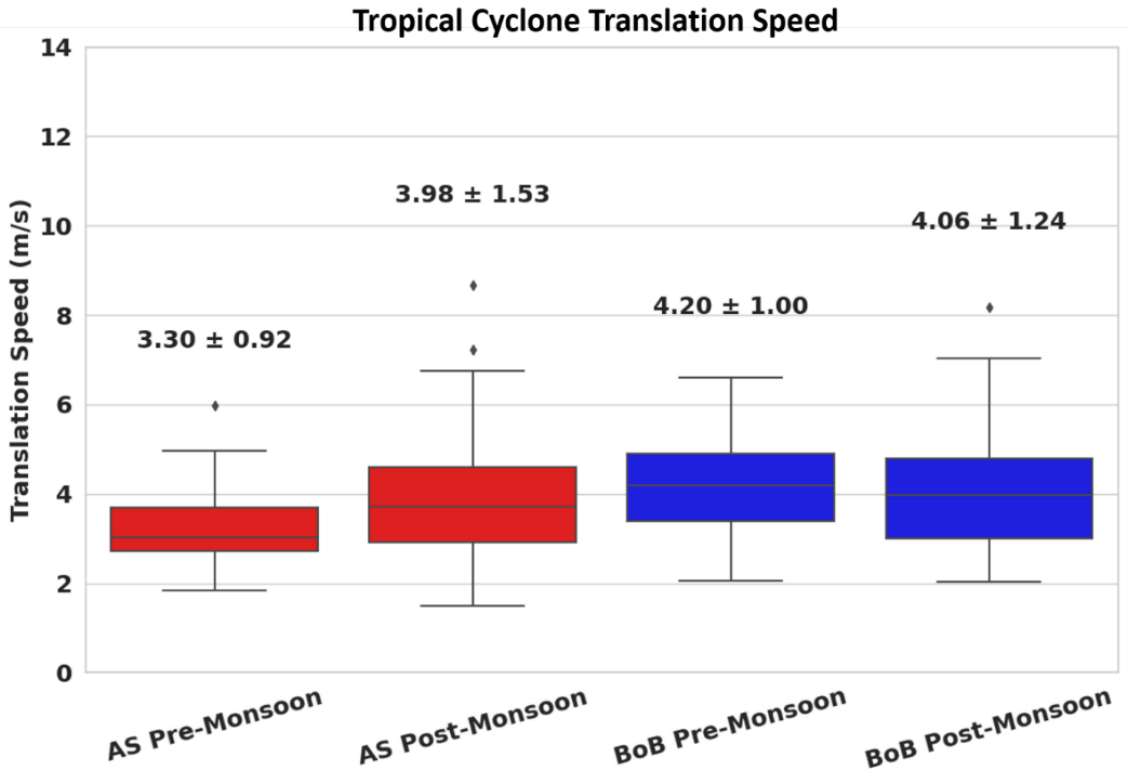

Figure 3.12. *Box plot of tropical cyclone (TC) translation speed (m/s) in the Arabian Sea and the Bay of Bengal during the pre-monsoon (April–June) and the post-monsoon (October–December) seasons for the period 1982–2023. The values over each box plot denote the mean translation speed along with the standard deviation.*

Since the TC translation speed is significantly influenced by land interaction after landfall, we computed the TC translation speed separately over the ocean and land. It is evident that in both the basins, TCs move faster over land than over the ocean (Table 3.6). In the Arabian Sea, the average translation speed over land is 4.2 m/s during the pre-monsoon season and 4.4 m/s during the post-monsoon season (Table 3.6). Thus, TCs during the pre-monsoon season move slightly slower, and combined with their longer travel distance over land, they tend to have a longer duration over land compared to post-monsoon TCs.

Table 3.6. *Mean translation speed of Tropical Cyclone (TC) and its standard deviation over ocean and over land (when the wind speed ≥ 17 knots) (m/s) in the Arabian Sea and the Bay of Bengal during the pre-monsoon (April–June) and the post-monsoon (October–December) season for the period 1982–2023.*

	TC translation speed over the ocean (m/s)		TC translation speed over land (m/s)	
	Pre-Monsoon	Post-Monsoon	Pre-Monsoon	Post-Monsoon
Arabian Sea	3.1 ± 1.6	3.7 ± 1.9	4.2 ± 2.4	4.4 ± 2.2
Bay of Bengal	3.6 ± 1.6	3.7 ± 1.8	6.5 ± 3.3	5.2 ± 2.9

In the Bay of Bengal, the average translation speed of TCs over land during the pre-monsoon season is 6.5 m/s, while during the post-monsoon season it is 5.2 m/s. Over the ocean (excluding land areas), the translation speed is 3.6 m/s in the pre-monsoon season and 3.7 m/s in the post-monsoon season (Table 3.6). This indicates that TCs move slightly faster over the ocean during the post-monsoon season than during the pre-monsoon season. However, once over land, TCs move more rapidly in the pre-monsoon season compared to the post-monsoon season. The reason for such seasonal contrast over ocean and land needs detailed research in the future. As discussed earlier, the total distance travelled by Bay of Bengal TCs over land is nearly the same in both seasons (Figure 3.9d). Nevertheless, the slower translation speed during the post-monsoon season results in a longer residence time of TCs over land. Consequently, the post-monsoon TCs in the Bay of Bengal exhibit higher land exposure duration at a given location compared to those in the pre-monsoon season.

3.7 Relationship between TC translation speed and TC intensity

During the pre-monsoon season, in both basins, there is a positive relationship between TC translation speed and intensity, indicating that stronger TCs generally move faster than weaker ones (Figure 3.13a). This pattern is consistent with earlier findings reported across global tropical basins (Mei et al., 2012). The translation speed of a TC plays a crucial role in regulating its intensity by influencing the strength of SST feedback. Faster-moving TCs produce weaker ocean surface cooling and experience shorter exposure to the cooled waters, thereby reducing the negative SST feedback that typically suppresses intensification. As a result, there exists a minimum translation speed threshold for TC intensification, and this

threshold increases with storm intensity—defining a minimum speed necessary for the maintenance of TCs within each intensity category.

In contrast, during the post-monsoon season, in both the basins, this relationship between translation speed and intensity is absent (Figure 3.13b). This suggests that the coupling between TC propagation and intensity, exhibits strong seasonal variability, highlighting the need for further research to understand the underlying mechanisms driving these differences.

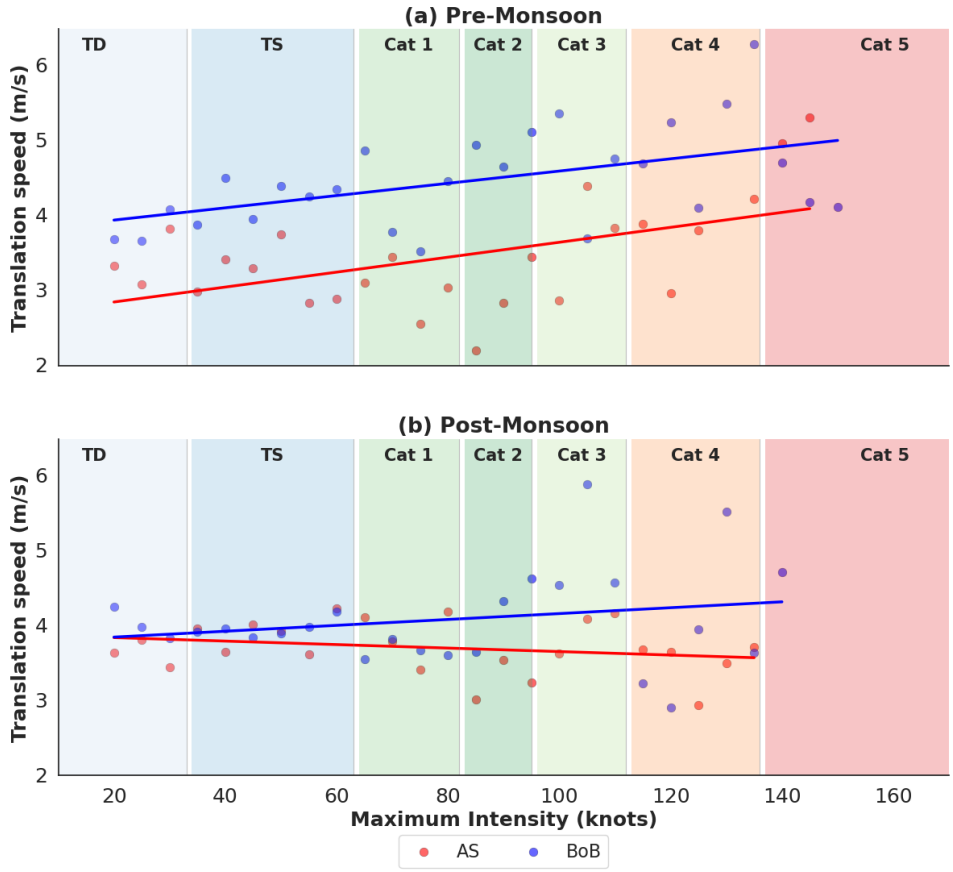

Figure 3.13. *Average translation speed (m/s) of all TCs in the Arabian Sea (red) and the Bay of Bengal (blue) as a function of TC intensity (knots) during (a) Pre-monsoon season (April-June) (b) Post-monsoon season (October-December) for the period 1982–2023.*

3.8 Seasonal characteristics of TC size

Along with intensity, the size of TC plays a crucial role in determining the areal extent of its impact. Two TCs of similar intensity can produce vastly different levels of socio-economic damage depending on their size; a larger TC with a broader extent of gale-force winds can affect a much wider area compared to a smaller one. To examine the size characteristics of TCs

over the North Indian Ocean, we computed the TC size represented by the radius of 34 kt winds (R34) for the pre-monsoon and post-monsoon seasons. The analysis period is restricted to 2002–2023, owing to the lack of TC size data prior to 2002.

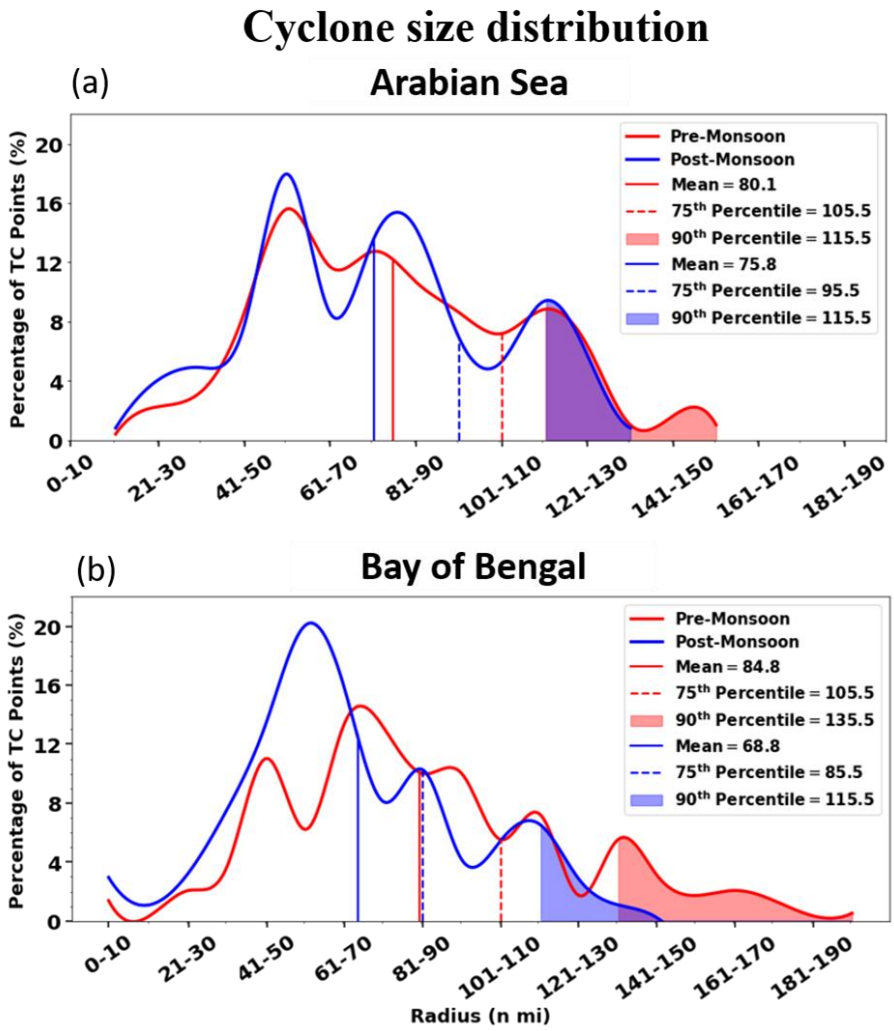

Figure 3.14. *Percentage distribution of Tropical Cyclone size (R_{34}, n mi) in the (a) Arabian Sea and the (b) Bay of Bengal during the pre-monsoon (red) and the post-monsoon season (blue) for the period 2002–2023. The thick straight line denotes the mean R_{34} (n mi) the dash line denotes the 75th percentile of R34 (n mi) and the shaded region denotes the R_{34} values ≥ 90th percentile.*

In the Arabian Sea, the mean TC size (R34) during the pre-monsoon season is 80.1 n mi (148.3 km), slightly larger than the post-monsoon mean of 75.8 n mi (140.4 km), indicating an increase of 4.3 n mi (5.7%) (Figure 3.14). In the Bay of Bengal, the contrast is more pronounced, with the mean R34 during the pre-monsoon season being 84.8 n mi (157.0 km)

compared to 68.8 n mi (127.4 km) in the post-monsoon season—an increase of 16 n mi (23.3%). Moreover, the 75th and 90th percentiles of TC size in the Arabian Sea during the pre-monsoon season exceed those of the post-monsoon season by about 10 n mi, while the difference reaches 20 n mi in the Bay of Bengal (Figure 3.14). These results emphasize the distinct seasonal contrast in TC size between the two basins. Further insight is provided by the percentage frequency distribution of R34 values (Figure 3.14). In the Arabian Sea, TC sizes during the post-monsoon season generally do not exceed 140 n mi, whereas during the pre-monsoon season they reach up to 160 n mi. Similarly, in the Bay of Bengal, no TCs during the post-monsoon season exceed 150 n mi, while approximately 9% of pre-monsoon TCs surpass 150 n mi. Collectively, these findings indicate that TCs over the North Indian Ocean are larger during the pre-monsoon season than during the post-monsoon season.

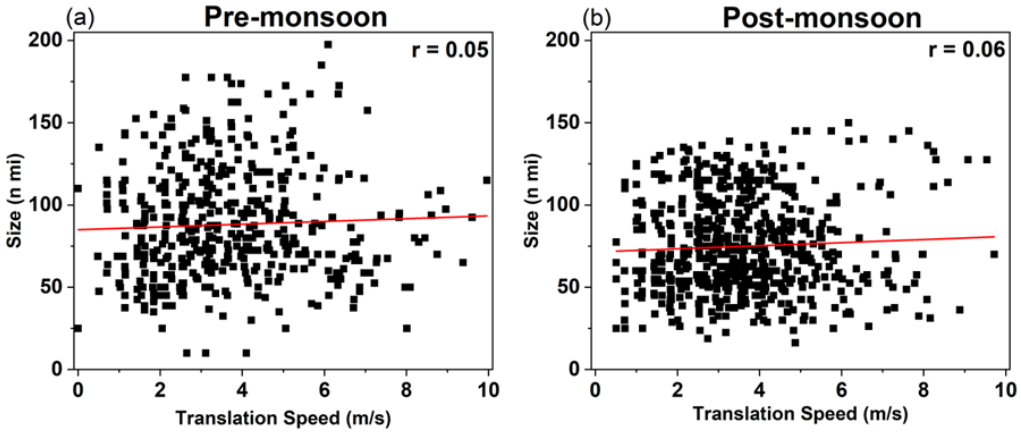

Figure 3.15. *Relationship between TC translation speed (m/s) and TC size (n mi) in the north Indian Ocean during the (a) Pre-monsoon season (April–June) and (b) Post-monsoon season (October-December) for the period 2002–2023. The r value in the top right corner denotes the correlation between the TC translation speed and TC size.*

Lastly, we computed the relationship between the TC size and TC translation speed for all the TCs for which TC size data is available for the period 2002–2023. It can be seen from Figure 3.15 that during both seasons, there is negligible correlation (r=0.05 in the pre-monsoon and r=0.06 in the post-monsoon season) between the TC size and TC translation speed in the North Indian Ocean.

4. Recent Observed Changes in Tropical Cyclone Characteristics in the North Indian Ocean

4.1 Observed changes in TC frequency and its intensity

With global warming, the North Indian Ocean continues to warm rapidly (Chand et al., 2022; Roxy et al., 2019). Also, the North Indian Ocean has a densely populated coastline. Therefore, it is important to closely monitor the observed changes in TC characteristics in this basin.

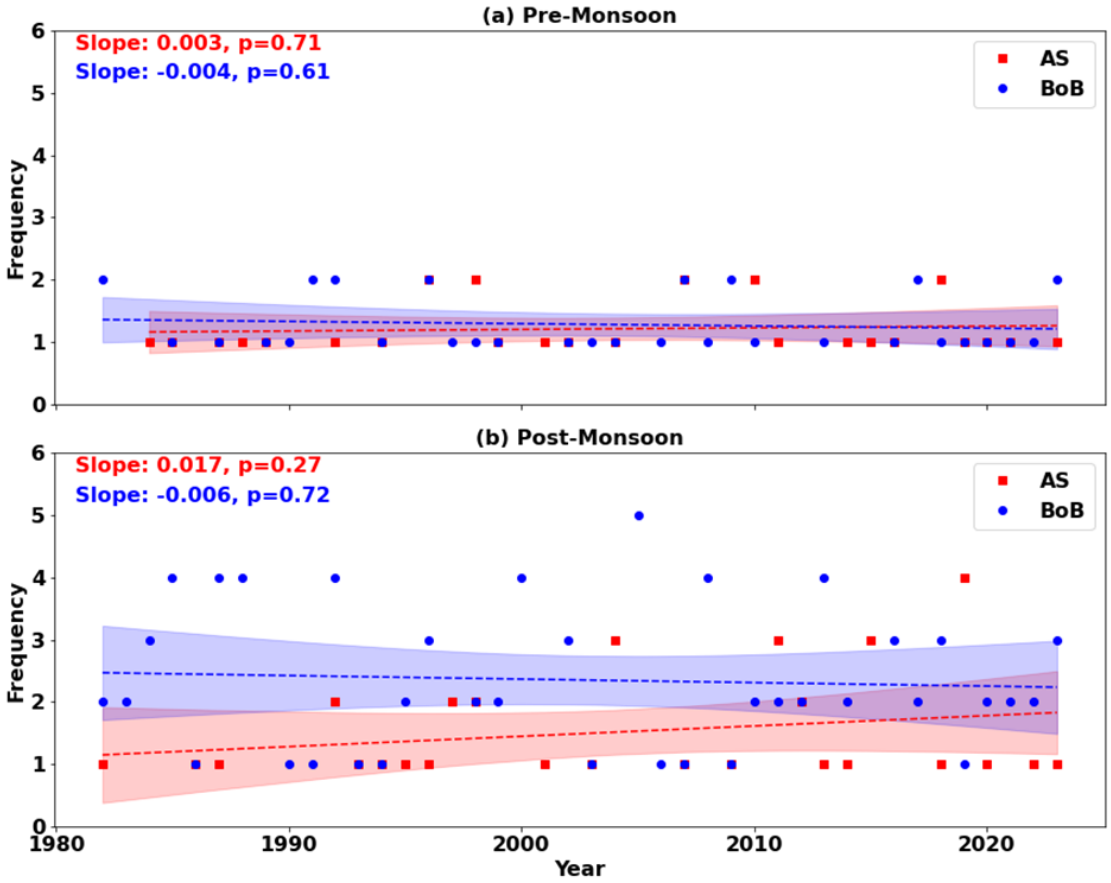

Figure 4.1. *Observed trend in Tropical Cyclone (TC) frequency in the Arabian Sea (red) and the Bay of Bengal (blue) during the (a) Pre-monsoon (April–June) and (b) Post-monsoon (October–December) seasons for the period 1982–2023. The slope values (red for Arabian Sea and blue for Bay of Bengal) indicate the trend in TC frequency/year and the p-value denotes its statistical significance using two tailed Student's t-test. The shading denotes the 95th percentage confidence interval band.*

From Figure 4.1, it is evident that during the period 1982–2023, the Bay of Bengal shows a slight decrease in TC frequency in both the seasons; however, this decline is not statistically significant. In the Arabian Sea, no significant trend is observed in TC frequency

during the pre-monsoon season. In contrast, the post-monsoon season exhibits a gradual increase in TC frequency, with a trend of approximately 0.2 TCs per decade. During the earlier decades of the analysis period, the Bay of Bengal typically experienced a higher number of TCs than the Arabian Sea during the post-monsoon season. However, in the recent years, the Arabian Sea has witnessed a notable rise in TC activity, with almost every year registering at least one TC occurrence (Figure 4.1). This is in line with a recent study by Deshpande et al. (2021), which shows that there is a gradual increase in TC activity in the Arabian Sea.

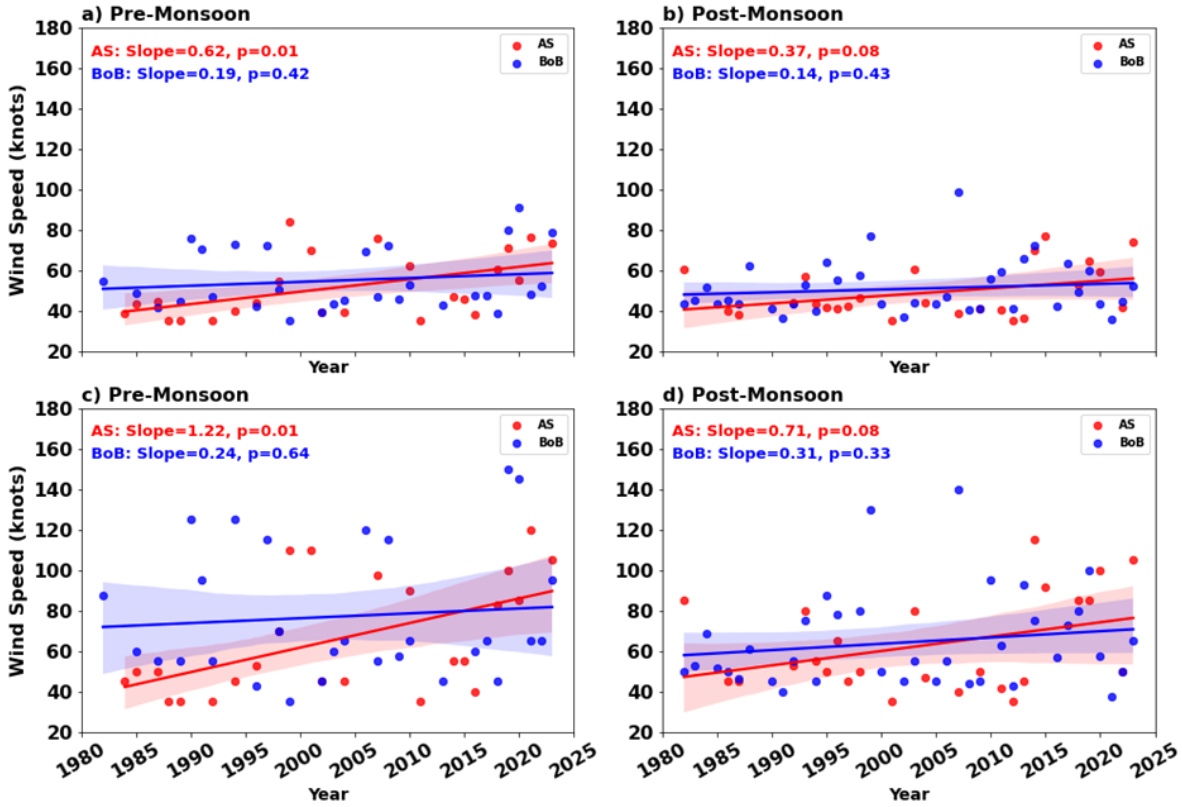

Figure 4.2. *(a-b) TC mean intensity (average from genesis till dissipation, knots) and (c-d) TC LMI (knots) during the pre-monsoon (April–June) and post-monsoon (October–December) seasons in the Arabian Sea (red) and Bay of Bengal (blue) for the period 1982–2023. The slope values (red for the Arabian Sea and blue for the Bay of Bengal) indicate the trend in TC intensity/year and the p-value denotes its statistical significance using two tailed Student's t-test. The shading along the mean trend line denotes the 95th percentage confidence interval band around the mean.*

Further analysis reveals that in the Arabian Sea, the LMI of TCs during the pre-monsoon season has been increasing at a rate of 12.2 knots (22.6 km/hr) per decade, which is statistically significant ($p < 0.01$; Figure 4.2c). Similarly, during the later season, TC intensity shows an increasing trend of 7.1 knots (13.1 k/hr) per decade, which is also statistically

significant (p = 0.08; Figure 4.2d). This intensification in the LMI is further supported by the observed rise in the mean intensity of TCs over the basin. The mean TC intensity during the pre-monsoon season has increased at a rate of 6.2 knots (11.5 km/hr) per decade, while during the later season, it has risen by 3.7 knots (6.9 km/hr) per decade (Figures 4.2a–b). The trends in the mean intensity during both the seasons are statistically significant, indicating a consistent strengthening of TCs in the Arabian Sea over the study period, and a higher increase in TC intensity during the pre-monsoon season than the post-monsoon season.

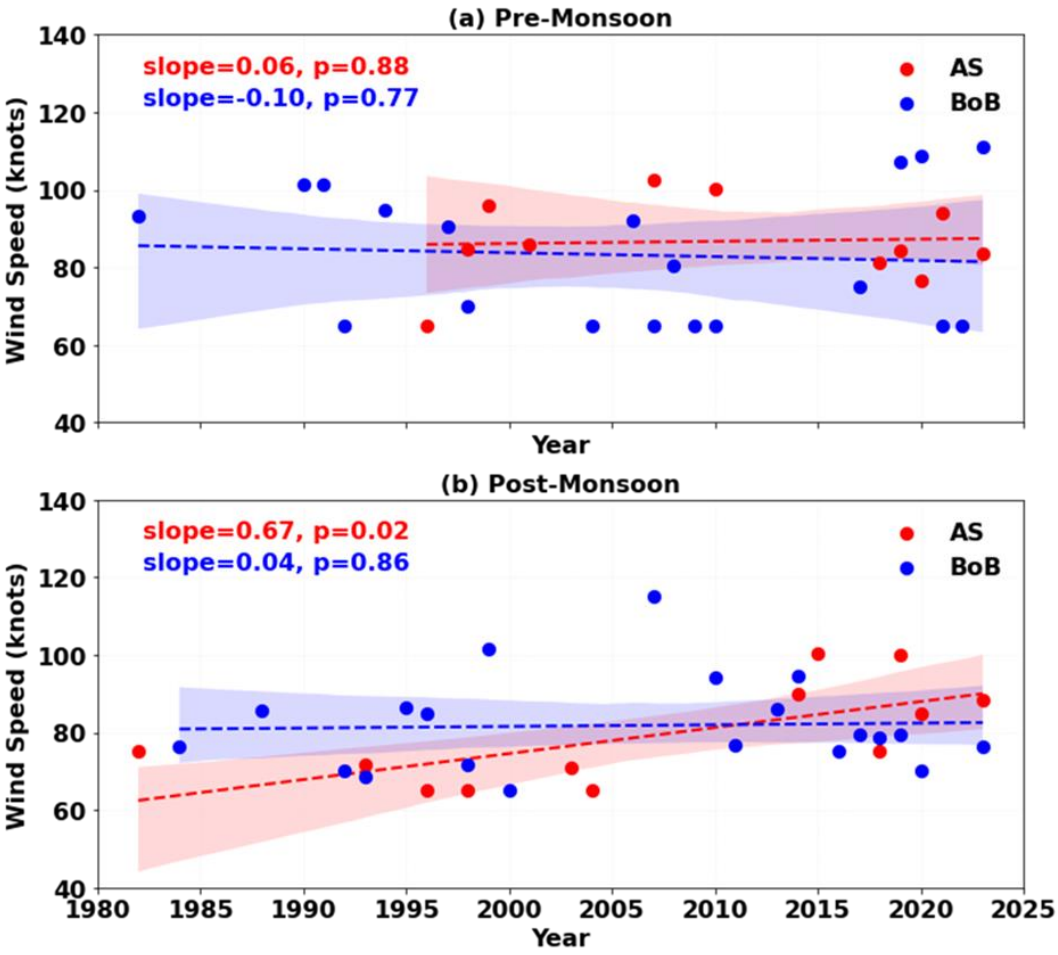

Figure 4.3. *TC intensity (knots) only for TC which are greater than category 1 (wind speed > 64 knots) in the Arabian Sea (red) and the Bay of Bengal (blue) during the (a) Pre-monsoon (April–June) and (b) Post-monsoon (October–December) seasons for the period 1982–2023. The slope values (red for the Arabian Sea and blue for the Bay of Bengal) indicate the trend in TC intensity/year and the p-value denotes its statistical significance using two tailed Student's t-test. The shading along the mean trend line denotes the 95th percentage confidence interval band.*

In contrast to the Arabian Sea, the TC intensity (LMI) in the Bay of Bengal shows only a marginal and statistically insignificant increase of 2.4 knots (4.4 km/hr) per decade during the pre-monsoon season and 3.1 knots (5.7 km/hr) per decade during the post-monsoon season (Figure 4.2c-d). The mean intensity also exhibits no significant change over the past four decades (Figure 4.2a-b). This highlights that the Arabian Sea is emerging as a new hotspot of frequent and more intense TCs.

Further analysis of intense TCs (wind speed > 64 knots) reveals contrasting trends between seasons and basins. In the Arabian Sea, during the pre-monsoon season, no significant change is observed in the intensity of intense TCs (Figure 4.3a). This indicates that the overall increase in TC intensity over the Arabian Sea during this season is primarily driven by the strengthening of weaker TCs rather than changes in the most intense ones. In contrast, during the post-monsoon season, the Arabian Sea exhibits a significant increase ($p < 0.05$) in the intensity of intense TCs, with an estimated rise of 6.7 knots (12.4 km/hr) per decade (Figure 4.3b). This trend is consistent with the recent emergence—particularly after 2010 of more frequent Category 3 and Category 4 TCs. Meanwhile, in the Bay of Bengal, no significant change in the intensity of intense TCs is detected (Figure 4.3a-b).

4.2 Observed changes in TC intensification rate and their rapid intensification

Recently, it is observed that TCs are intensifying overnight into a powerful TCs. For example, TC Gati in the Arabian Sea intensified from just tropical storm (wind speed 40 knots) to powerful Category 3 TC (wind speed 100 knots) in just 6 hours as per JTWC data. This is the most intense intensification rate ever observed by a TC in the Arabian Sea. Overall, the intensification rate of TCs in the Arabian Sea is increasing at the rate of 0.7 knots (1.3 km) per 6 hours per decade ($p = 0.14$) during the pre-monsoon season (Figure 4.4a). The increase is even more pronounced during the post-monsoon season, where the increasing rate is approximately 2.4 knots (4.4 km) per 6 hours per decade ($p = 0.02$) (Figure 4.4b).

The rise in intensification rates of TCs in the Arabian Sea is further supported by the statistically significant increase in the frequency of rapidly intensifying TCs (Figure 4.5a–b). Notably, the occurrence of rapid intensification events in the post-monsoon season has been largely confined to the recent decade (after 2010) (Figure 4.5b). These findings indicate that TCs over the Arabian Sea are not only becoming stronger but are also intensifying more rapidly

over shorter timescales, posing increasing challenges for operational forecasting and disaster preparedness. The observed enhancement in both the rate and frequency of rapid intensification over the Arabian Sea is consistent with similar trends reported in the North Atlantic, western North Pacific, and eastern North Pacific basins. (Bhatia et al., 2022; Bhatia et al., 2019; Manikanta et al., 2023).

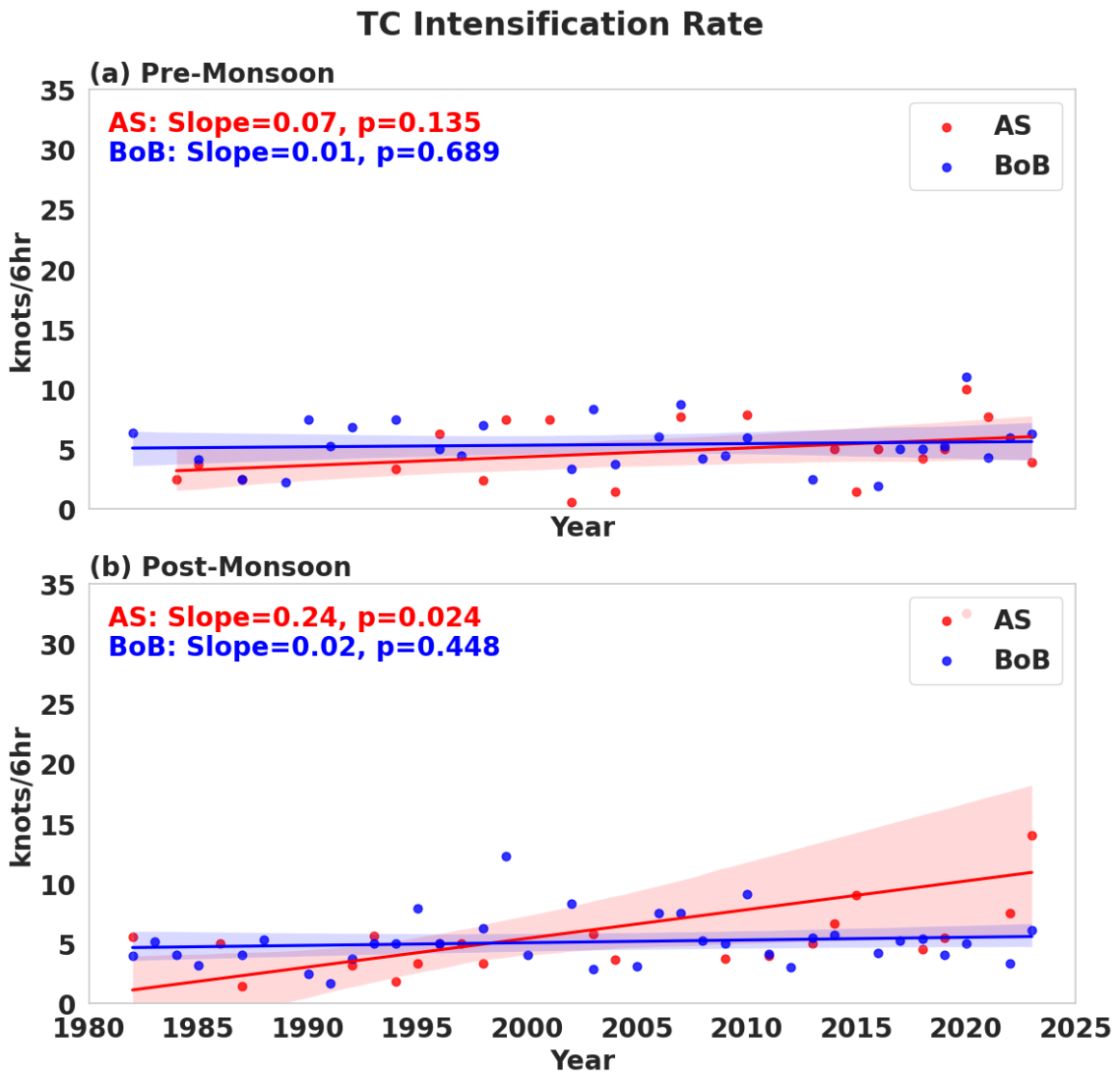

Figure 4.4. *TC intensification rate (knots/6 hr) in the Arabian Sea (red) and the Bay of Bengal (blue) during the (a) Pre-monsoon (April–June) and (b) Post-monsoon (October–December) season for the period 1982–2023. The slope values (Arabian Sea denoted by red and Bay of Bengal denoted by blue) indicate the trend in TC intensification rate/year and the p-value denotes its statistical significance using two tailed Student's t-test. The shading along the mean trend line denotes the 95th percentage confidence interval band.*

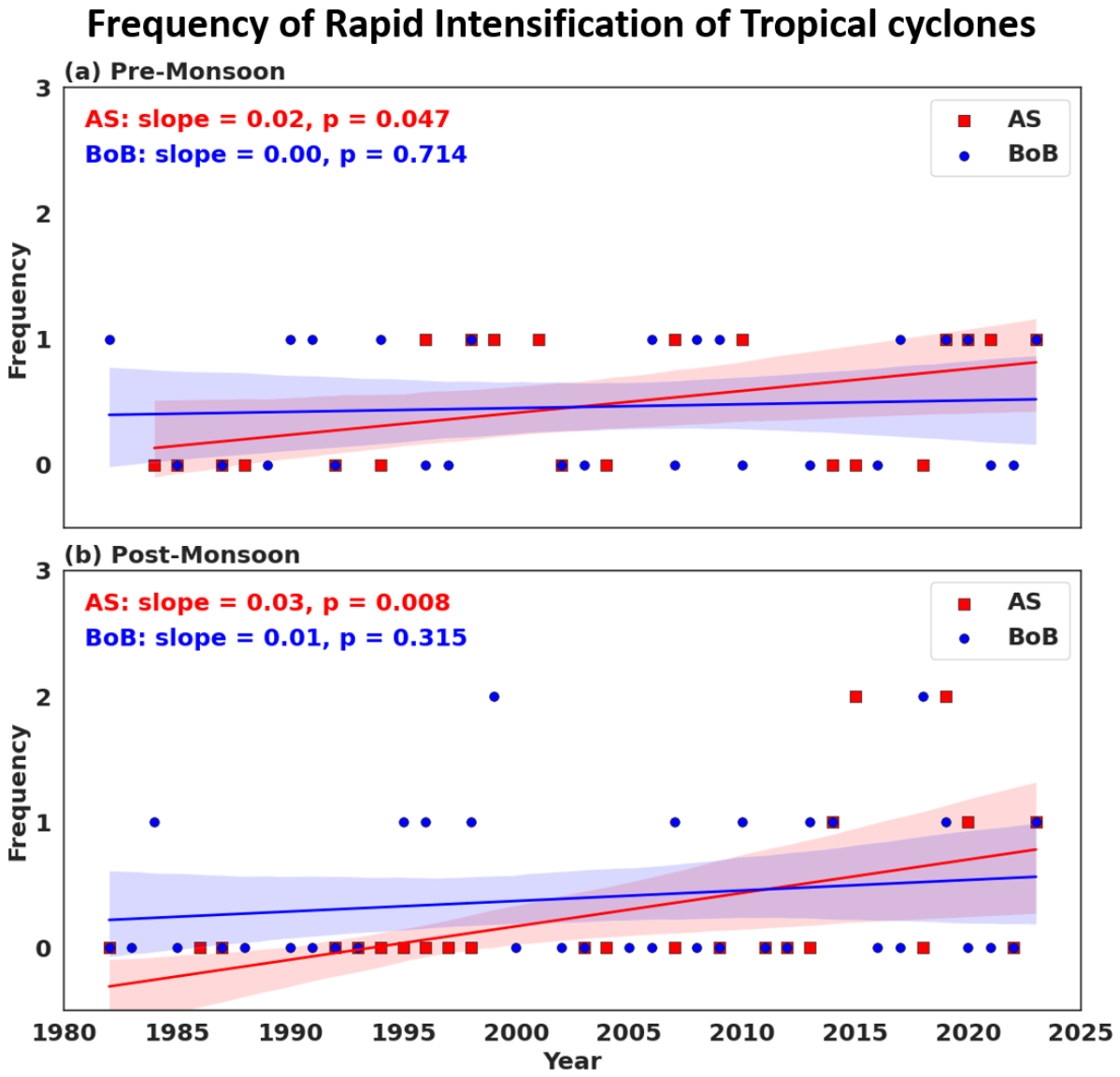

Figure 4.5. *Frequency of rapid intensification of TC in the Arabian Sea (red) and the Bay of Bengal (blue) during the (a) Pre-monsoon (April–June) and (b) Post-monsoon (October–December) seasons for the period 1982–2023. The slope values indicate the trend in the frequency of TC rapid intensification/year and the p-value (Arabian Sea denoted by red, and Bay of Bengal denoted by blue) denotes its statistical significance using two tailed Student's t-test. The shading along the mean trend line denotes the 95th percentage confidence interval band.*

In contrast to the Arabian Sea, the intensification rate of TCs in the Bay of Bengal has shown only a marginal increase during the two TC seasons which is not statistically significant (Figure 4.4a–b). Furthermore, there is no significant change in the frequency of rapidly intensifying TCs in the basin, although a slight, statistically insignificant increase ($p = 0.31$) is

observed during the post-monsoon season (Figure 4.5a–b). These results highlight a significant contrast between the Arabian Sea and the Bay of Bengal.

4.3 Observed changes in the Accumulated Cyclone Energy and TC duration

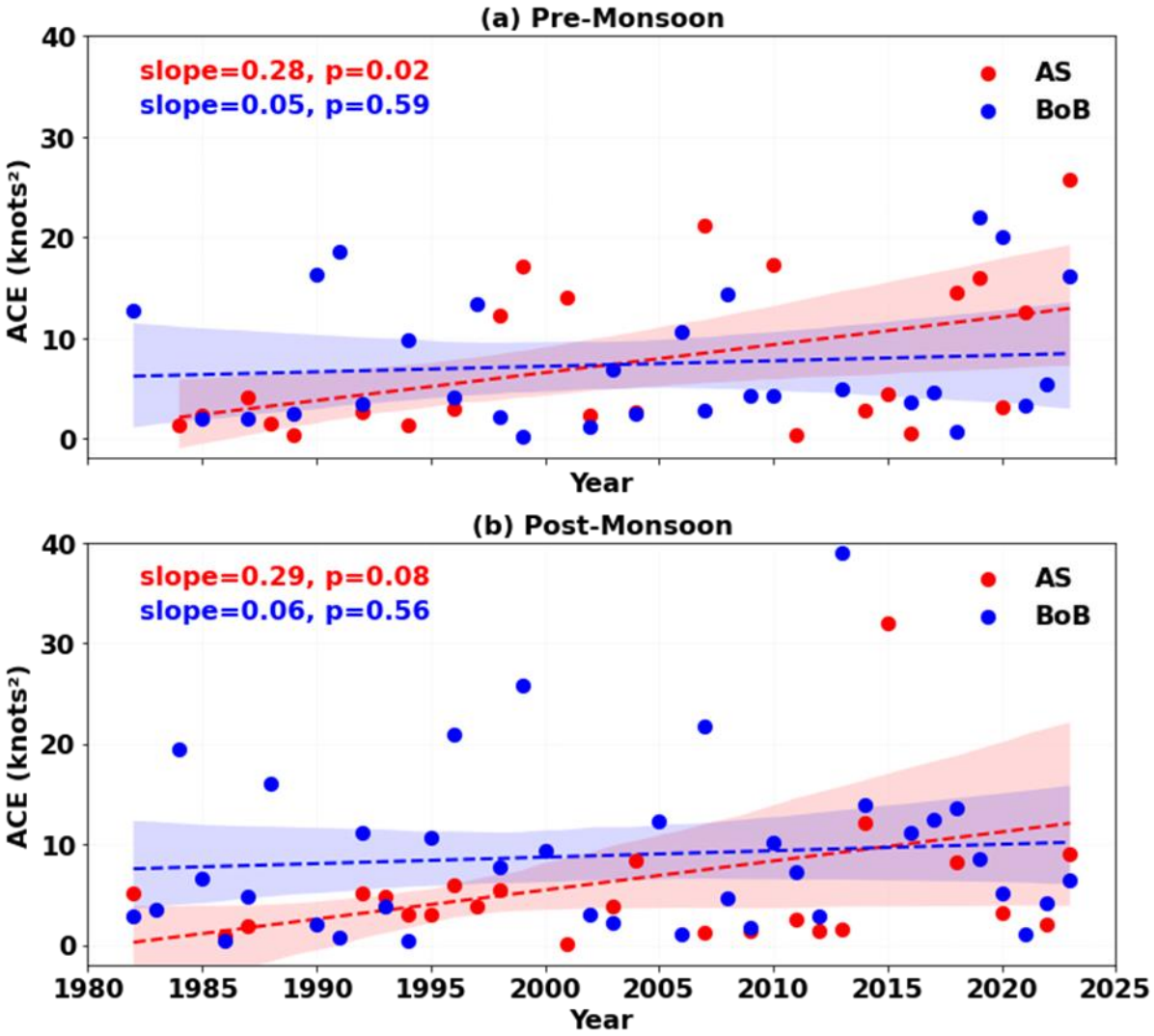

Figure 4.6. *TC Accumulated Cyclone Energy (×10^4, knots^2) in the Arabian Sea (red) and the Bay of Bengal (blue) during (a) Pre-monsoon (April–June) and (b) Post-monsoon (October–December) seasons for the period 1982–2023. The slope values (red for the Arabian Sea and blue for the Bay of Bengal) indicate the trend in TC ACE/year and the p-value denotes its statistical significance using two tailed Student's t-test. The shading along the mean trend line denotes the 95th percentage confidence interval band.*

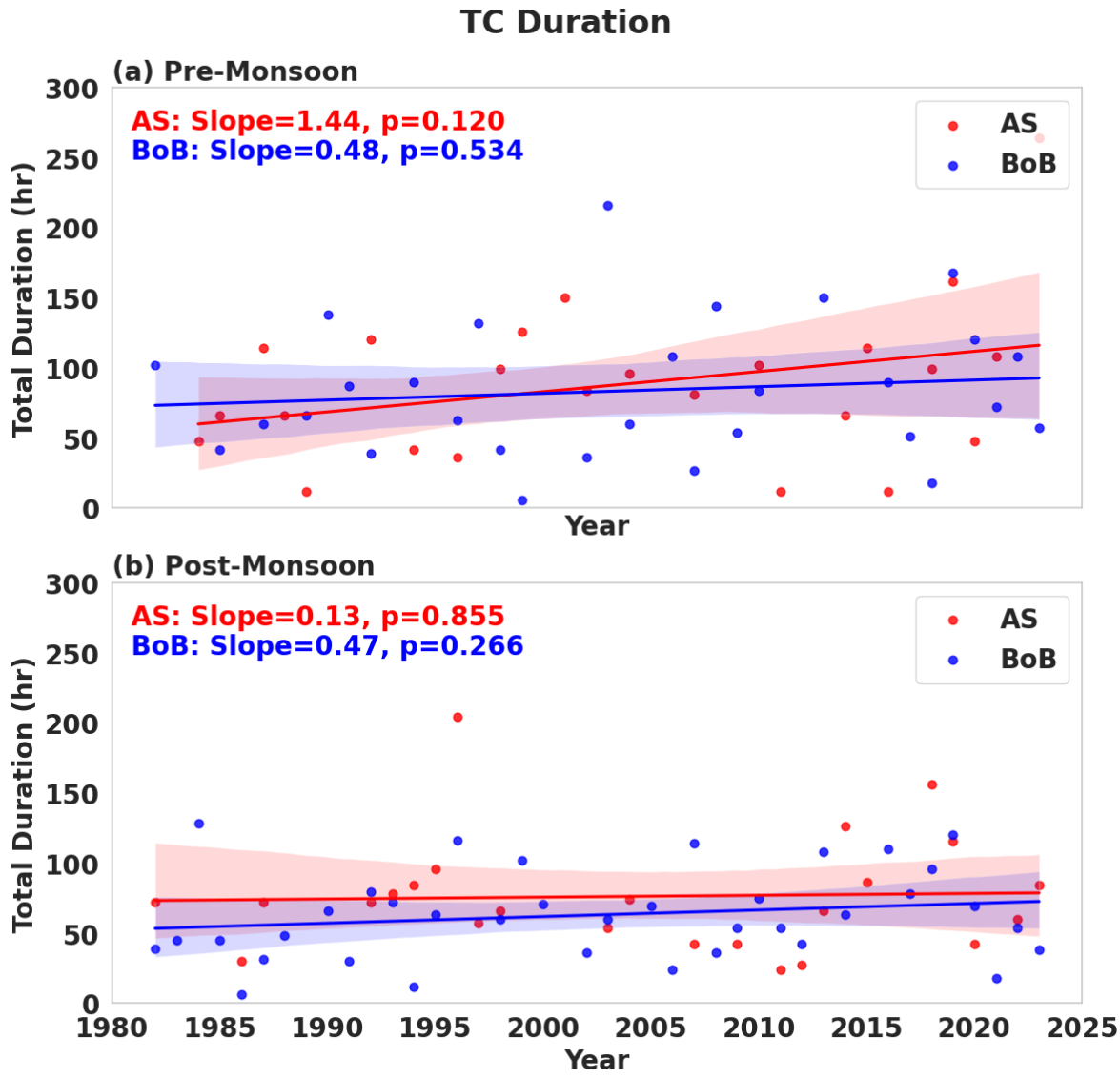

Figure 4.7. *Observed trend in TC total duration (hours, including TC points with wind speed ≥ 34 knots) in the Arabian Sea (red) and the Bay of Bengal (blue) during the (a) Pre-monsoon (April–June) and (b) Post-monsoon (October–December) seasons for the period 1982–2023. The slope values indicate the trend in TC duration/year and the p-value denotes its statistical significance using two tailed Student's t-test. The shading along the mean trend line denotes the 95th percentage confidence interval band.*

We also examined the changes in the ACE per year. As discussed earlier, ACE is a key metric that integrates both TC intensity and duration, thereby providing a comprehensive measure of the total energy generated by TCs and their potential impact. From Figure 4.6, it is evident that in the Arabian Sea, ACE has increased during both the pre-monsoon and post-monsoon seasons, at rates of 2.8 knots^2 per decade and 2.9 knots^2 per decade, respectively. This

increase in ACE is statistically significant for both seasons. During the pre-monsoon season, the rise in ACE is primarily attributed to the combined effect of increasing TC intensity (Figure 4.2c) and prolonged TC duration (Figure 4.7a). The duration of TCs has increased at a rate of approximately 14.4 hours per decade, which is marginally significant ($p = 0.12$). This indicates that TCs are persisting longer over the ocean, allowing more time for the transfer of oceanic heat and moisture fluxes into the atmosphere. Such sustained air–sea interactions not only support further intensification but also contribute to the overall enhancement of ACE. In contrast, during the post-monsoon season, the increase in ACE is primarily driven by the rise in TC intensity (Figure 4.2d), whereas the duration of TCs does not exhibit any significant trend (Figure 4.7b). Since the intensity of TCs during the post-monsoon season is increasing rapidly without any significant change in their duration, the intensification rate shows a sharp rise (Figure 4.4b), as TCs are now reaching higher peak intensities within the same timeframe.

In the Bay of Bengal, ACE shows only a marginal increase of 0.5 knots² per decade during the pre-monsoon season and 0.6 knots² per decade during the post-monsoon season (Figure 4.6a–b). However, these changes are not statistically significant, likely because neither TC intensity (Figure 4.2c–d) nor duration (Figure 4.7a–b) shows any significant changes in this basin. Overall, these results indicate that the most pronounced and statistically significant increase in ACE is observed only over the Arabian Sea during both seasons.

4.4 Observed changes in TC duration over land

We also examined the observed changes in TC duration over land, as variations in this parameter can have substantial socio-economic impacts. For this analysis, we have included weaker stages of TC (i.e. wind speed up to 17 knots). During the pre-monsoon season, the TC duration over land in the Arabian Sea shows a declining trend of 6.4 hours per decade, while in the Bay of Bengal it is decreasing at a rate of 1.2 hours per decade (Figure 4.8a). However, these declining trends in both the basins are not statistically significant. Therefore, it can be inferred that although the overall TC duration (including both land and ocean) is increasing, the duration specifically over land is slightly decreasing, indicating that TCs are spending marginally less time over land.

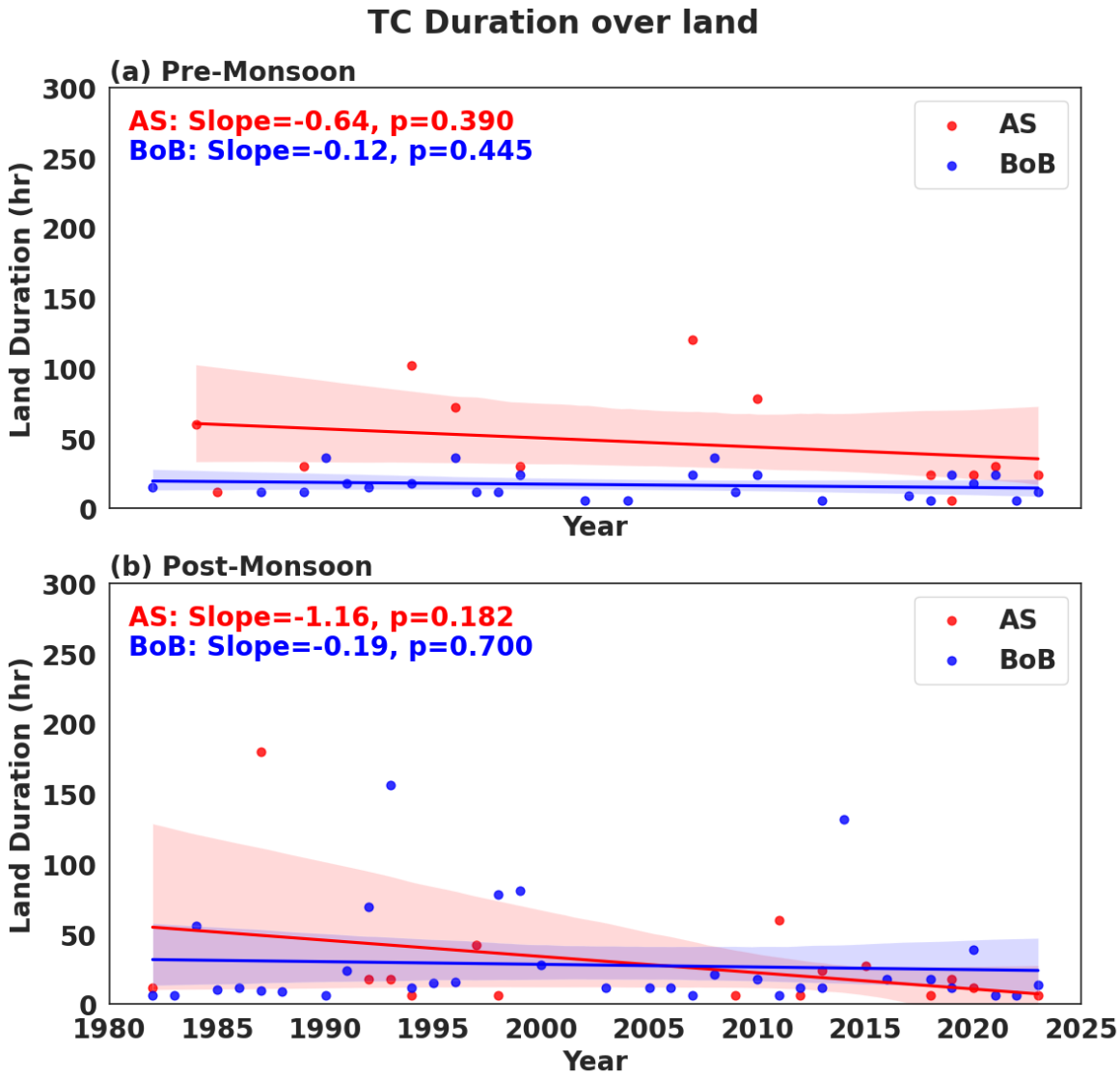

Figure 4.8. *Observed trend in TC duration over land (hours, including all TC points with wind speed ≥ 17 knots) in the Arabian Sea (red) and the Bay of Bengal (blue) during the (a) Pre-monsoon (April–June) and (b) Post-monsoon (October–December) seasons for the period 1982–2023. The slope values indicate the trend in TC duration/year and the p-value denotes its statistical significance using two tailed Student's t-test. The shading along the mean trend line denotes the 95th percentage confidence interval band around the mean.*

During the post-monsoon, TC land duration for the Arabian Sea TCs is decreasing at a much faster rate compared to the pre-monsoon TCs. Similarly, in the Bay of Bengal also TC duration over land shows a marginal declining trend, however it is not statistically significant (p = 0.7; Figure 4.8b). The reason for this contrasting trend over ocean and land in TC duration needs a detailed investigation in future.

4.5 Observed changes in TC translation speed over ocean and land

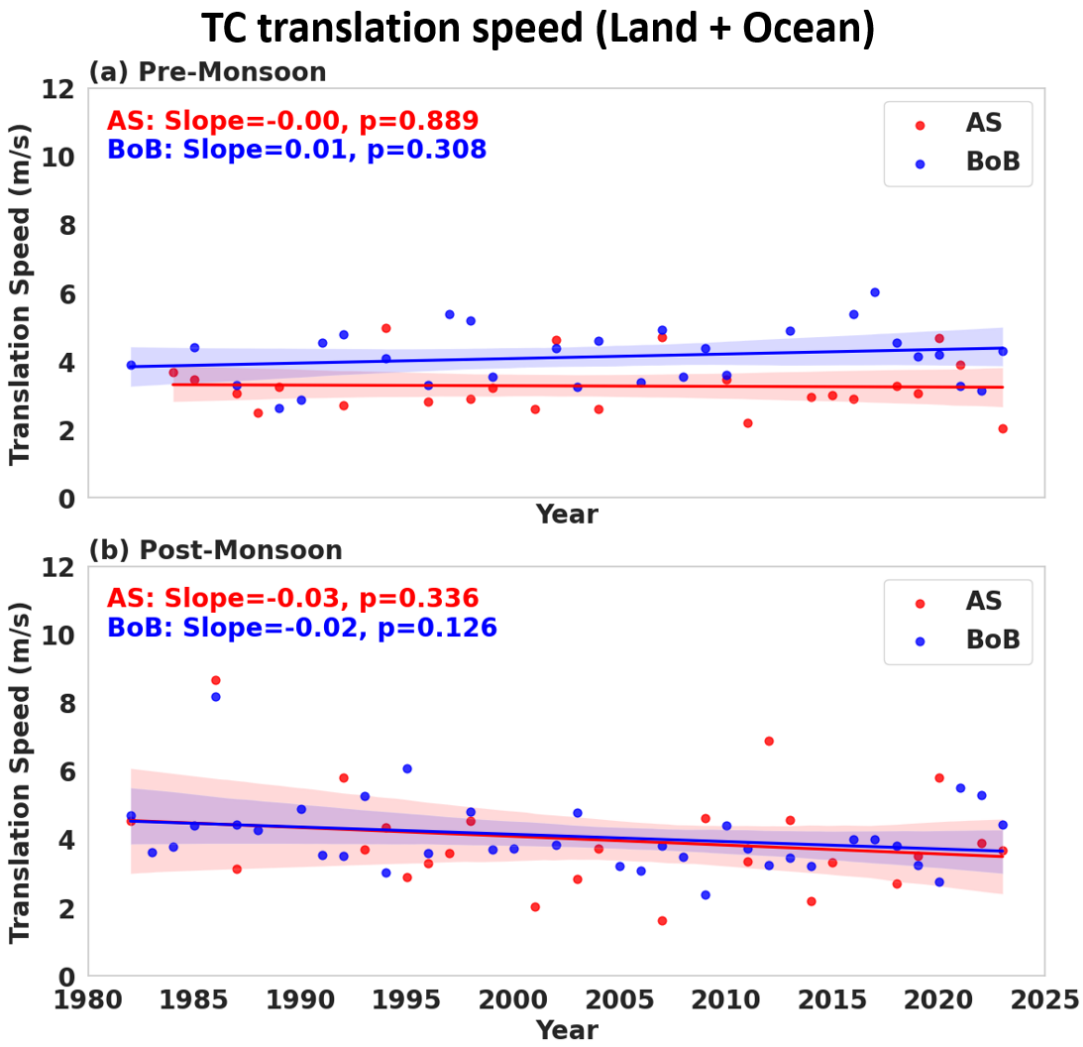

Figure 4.9. *Observed trend in TC Translation speed (m/s, land and ocean combined for all TC points (wind speed ≥ 17 knots)) in the Arabian Sea (red) and the Bay of Bengal (blue) during the (a) Pre-monsoon (April–June) and (b) Post-monsoon (October–December) seasons for the period 1982–2023. The slope values indicate the trend in TC translation speed/year and the p-value denotes its statistical significance using two tailed Student's t-test. The shading along the mean trend line denotes the 95th percentage confidence interval band.*

The observed increase in TC overall duration (land and ocean included) can be partially attributed to changes in their translation speed. A slowdown in translation speed causes a TC to move more slowly, thereby prolonging its duration. In the Arabian Sea, during the pre-monsoon season, the overall translation speed of TCs (including all TC points up to wind speed ≥ 17 knots) is decreasing marginally at a rate of 0.04 m/s per decade (Figure 4.9a). A more pronounced slowdown is observed during the post-monsoon season, when the TC translation

speed is decreasing at the rate of 0.3 m/s per decade (Figure 4.9b). However, as shown earlier, although TC duration is increasing more rapidly during the pre-monsoon season, the slowdown in translation speed is greater in the post-monsoon season. This indicates that the increase in TC duration cannot be fully explained by the observed changes in translation speed, suggesting that other contributing factors may be at play and warrant further investigation.

In the Bay of Bengal, a similar pattern is observed during the post-monsoon season, when TCs exhibit a significant slowdown, with translation speed declining at a rate of 0.2 m/s per decade, which is marginally significant ($p = 0.12$, Figure 4.9b). Conversely, a slight increase in translation speed (0.1 m/s per decade) is noted during the pre-monsoon season ($p = 0.31$, Figure 4.9a). Overall, these findings highlight a basin-wide tendency for TCs to slow down during the post-monsoon season. This slowing down of TCs especially during the post-monsoon season, is line with global slowdown of TCs in recent decades (Kossin, 2018) and is related to the weakening of the global tropical circulation forced by anthropogenic warming (Grise & Polvani, 2017; He & Soden, 2015; Mann et al., 2017).

We also analyzed the changes in TC translation speed (considering all TC points with wind speeds ≥ 17 knots) separately over the ocean and land. As shown in Figure 4.10, the changes in TC translation speed over the ocean (excluding land points) are similar to the overall changes in translation speed (including both land and ocean; Figure 9), with a slightly weaker declining trend over the Bay of Bengal during the post-monsoon season. In contrast, the analysis of TC translation speed over land reveals that during the pre-monsoon season, the translation speed of TCs in both the Arabian Sea and the Bay of Bengal shows an increasing trend of about 0.4 m/s per decade (Figure 4.11a). However, during the post-monsoon season, similar to the oceanic trend, the translation speed over land exhibits a declining trend in both basins (Figure 4.11b).

Interestingly, despite the observed slowing down of TCs over land during the post-monsoon season, the duration of TCs over land is decreasing. This suggests that factors other than translation speed—possibly related to changes in atmospheric circulation or land–atmosphere interactions may be contributing to the overall decline in TC duration over land, warranting further investigation. Conversely, the slight increase in translation speed during the

pre-monsoon season over the Bay of Bengal highlights the role of seasonal variability in modulating TC movement under a warming climate. This points to a complex and seasonally dependent response of TC behaviour to global warming in this basin, which needs detailed future research.

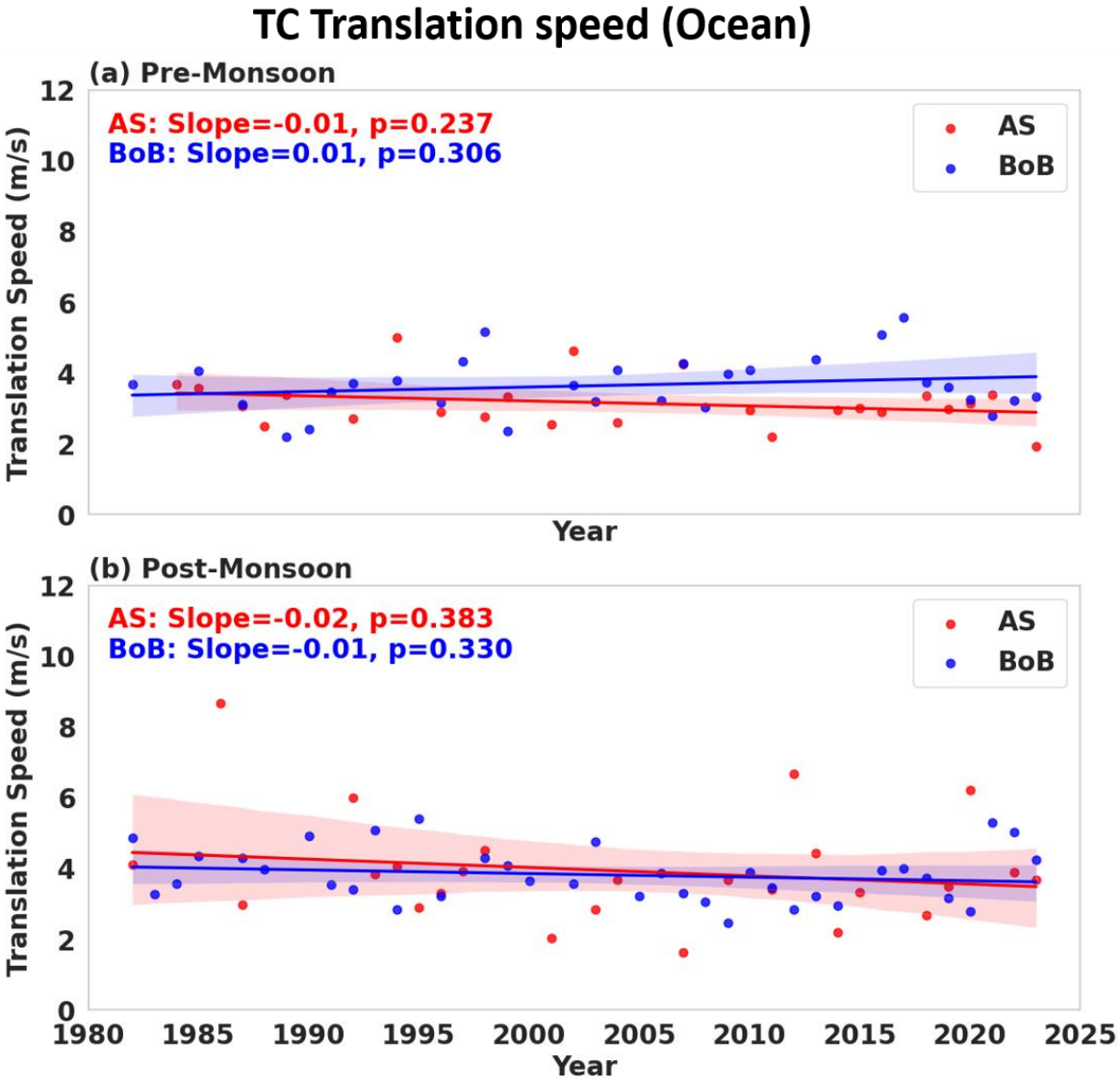

***Figure 4.10**. Observed trend in TC Translation speed (m/s) over the ocean in the Arabian Sea (red) and the Bay of Bengal (blue) during the (a) Pre-monsoon (April–June) and (b) Post-monsoon (October–December) seasons for the period 1982–2023. The slope values indicate the trend in TC translation speed/year and the p-value denotes its statistical significance using two tailed Student's t-test. The shading along the mean trend line denotes the 95th percentage confidence interval band around the mean.*

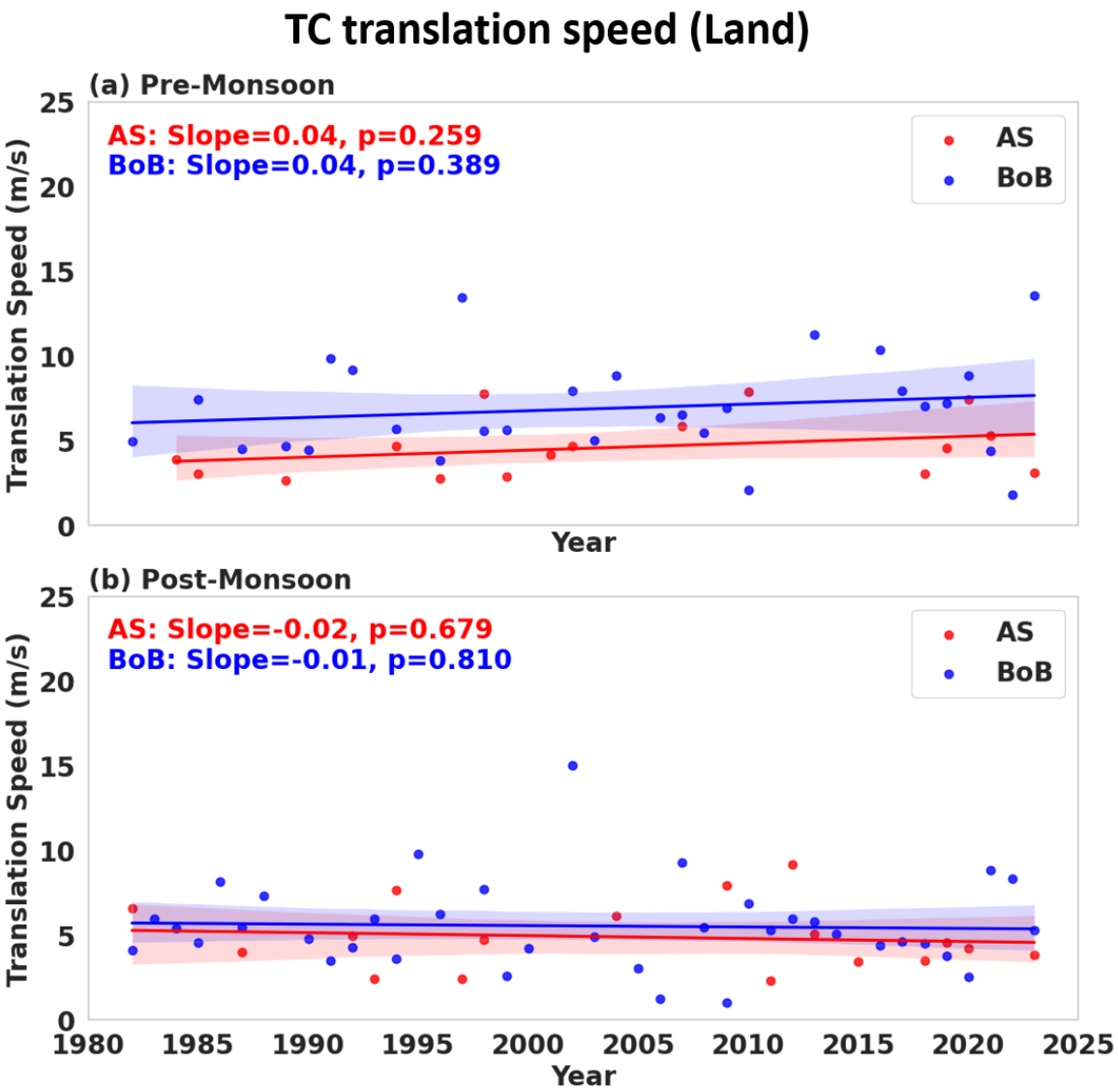

Figure 4.11. *Observed trend in TC Translation speed (m/s) over the land in the Arabian Sea (red) and the Bay of Bengal (blue) during the (a) Pre-monsoon (April–June) and (b) Post-monsoon (October–December) seasons for the period 1982–2023. The slope values indicate the trend in TC translation speed/year and the p-value denotes its statistical significance using two tailed Student's t-test. The shading along the mean trend line denotes the 95th percentage confidence interval band.*

4.6 Observed changes in TC genesis and LMI latitude

Long-term changes are not limited to TC intensity, frequency or its translation speed, the preferred regions of TC formation have also undergone a latitudinal shift in recent decades. In the Arabian Sea, the latitude of TC genesis is shifting equatorward at a rate of 0.5°N per decade during the pre-monsoon season and 0.4°N per decade during the post-monsoon season

(Figure 4.12a-b). This equatorward shift is even more pronounced in the Bay of Bengal, where TC genesis is shifting southward by 1.0°N per decade in the pre-monsoon season and 0.4°N per decade in the post-monsoon season (Figure 4.12a-b). Such an equatorward shift in TC formation over the North Indian Ocean contrasts sharply with the global trend, where TC genesis locations are generally moving poleward (Shan & Yu, 2020; Sharmila & Walsh, 2018).

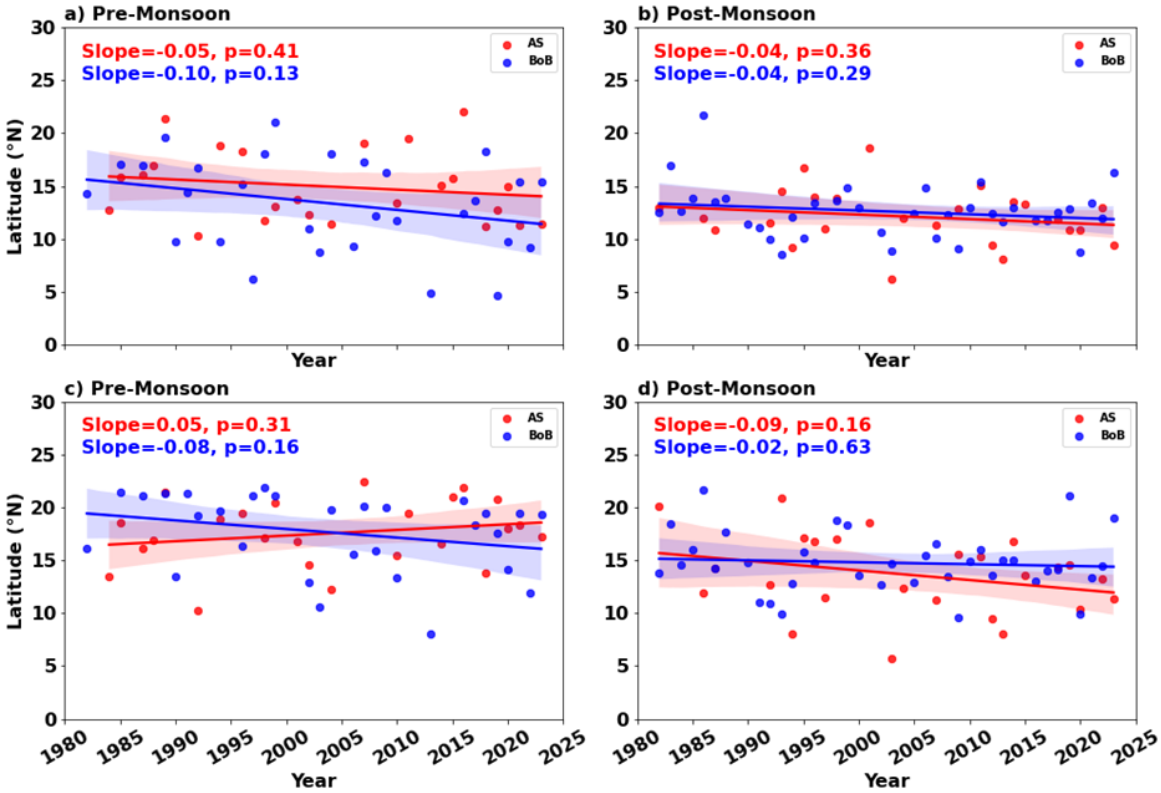

Figure 4.12. *(a-b) Observed trend in TC Genesis Latitude (°N) and (c-d) TC lifetime maximum intensity (LMI, °N) latitude in the Arabian Sea (red) and the Bengal (blue) during the Pre-monsoon (April–June, left column) and Post-monsoon seasons (October–December, right column) for the period 1982–2023. The slope values indicate the trend in TC genesis and LMI latitude/year and the p-value denotes its statistical significance using two tailed Student's t-test. The shading along the mean trend line denotes the 95th percentage confidence interval band.*

Furthermore, the latitude of the TC LMI has also shown notable variations in recent decades. In the Arabian Sea, during the pre-monsoon season, the LMI latitude is shifting poleward at a rate of 0.5° per decade, which is opposite to the equatorward shift observed in TC genesis latitude. In contrast, during the post-monsoon season, the LMI latitude is shifting equatorward at a rate of 0.9° per decade (Figure 4.12c–d). However, these shifts in both seasons

are not statistically significant. In the Bay of Bengal, the LMI latitude is shifting equatorward in both seasons—by 0.8° per decade during the pre-monsoon season and 0.2° per decade during the post-monsoon season (Figure 4.12c–d). This indicates that in the Bay of Bengal, the equatorward shift in LMI latitude is more pronounced during the pre-monsoon season. The equatorward shift in TC LMI location in the Bay of Bengal is in sharp contrast to global TCs, where it is shifting poleward (Lin et al., 2024; Moon et al., 2015; Song & Klotzbach, 2018; Wang & Wu, 2019; Zhan & Wang, 2017).

4.7 Observed changes in TC size

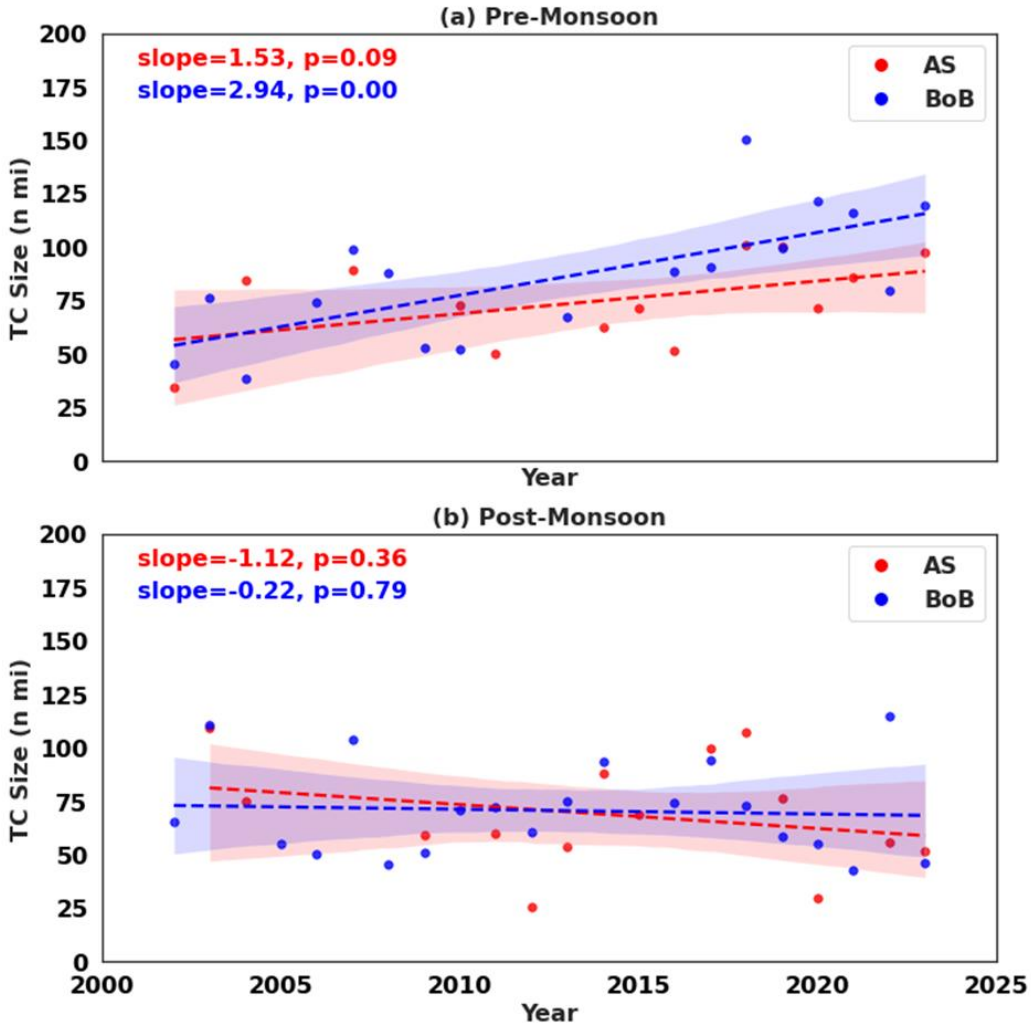

Figure 4.13. *Observed trend in the TC Size (R34, n mi) in the Arabian Sea (red) and the Bay of Bengal (blue) during the (a) Pre-monsoon (April–June) and (b) Post-monsoon (October–December) season for the period 2002–2023. The slope values indicate the trend in the TC size/year and the p-value denotes its statistical significance using two tailed Student's t-test. The shading along the mean trend line denotes the 95th percentage confidence interval.*

Additionally, our analysis reveals that during the pre-monsoon season, the size of TCs (R34) has increased significantly in both basins. In the Arabian Sea, TC size is expanding at a rate of 1.53 n mi per year, while in the Bay of Bengal, the increase is even more pronounced at 2.94 n mi per year, which is statistically significant (Figure 4.13a). This indicates that in the Arabian Sea, TCs are not only intensifying more rapidly but are also becoming larger, thereby affecting a wider area. In contrast, although the increase in TC intensity in the Bay of Bengal is less robust, the TC size has nearly doubled over the past few decades. This suggests that TCs of similar intensity now impact almost twice the area, substantially increasing the hazard potential and exposure risk for coastal populations. In sharp contrast to the pre-monsoon season, the size of TCs decreases in both basins during the post-monsoon season, with a more pronounced reduction observed in the Arabian Sea (Figure 4.13b). However, this decrease is not statistically significant. Overall, these findings highlight a distinct seasonal variation in TC size evolution over the North Indian Ocean — with increasing size during the pre-monsoon season, and a weak, non-significant reduction in size during the post-monsoon season.

5. Climatology and observed changes in Tropical Cyclone characteristics in the Southern Tropical Indian Ocean

5.1 Climatology of TC frequency, tracks and intensity in the Southern Tropical Indian Ocean

The Southern Tropical Indian Ocean (30°E–135°E) experiences tropical cyclones (TCs) primarily between November and April. Approximately 71% of the annual TCs in this basin occur during this period, which is therefore defined as the main TC season (Figure 5.1a). The highest TC frequency is observed in February, with an average of 3.4 TCs per year, followed by January (3.3 TCs per year) and March (2.9 TCs per year). On the average, about 15 TCs occur annually in the basin (Figure 5.1a). This indicates that TC activity in the Southern Tropical Indian Ocean is substantially higher than in the North Indian Ocean, and the timing of the season also differs between the two basins.

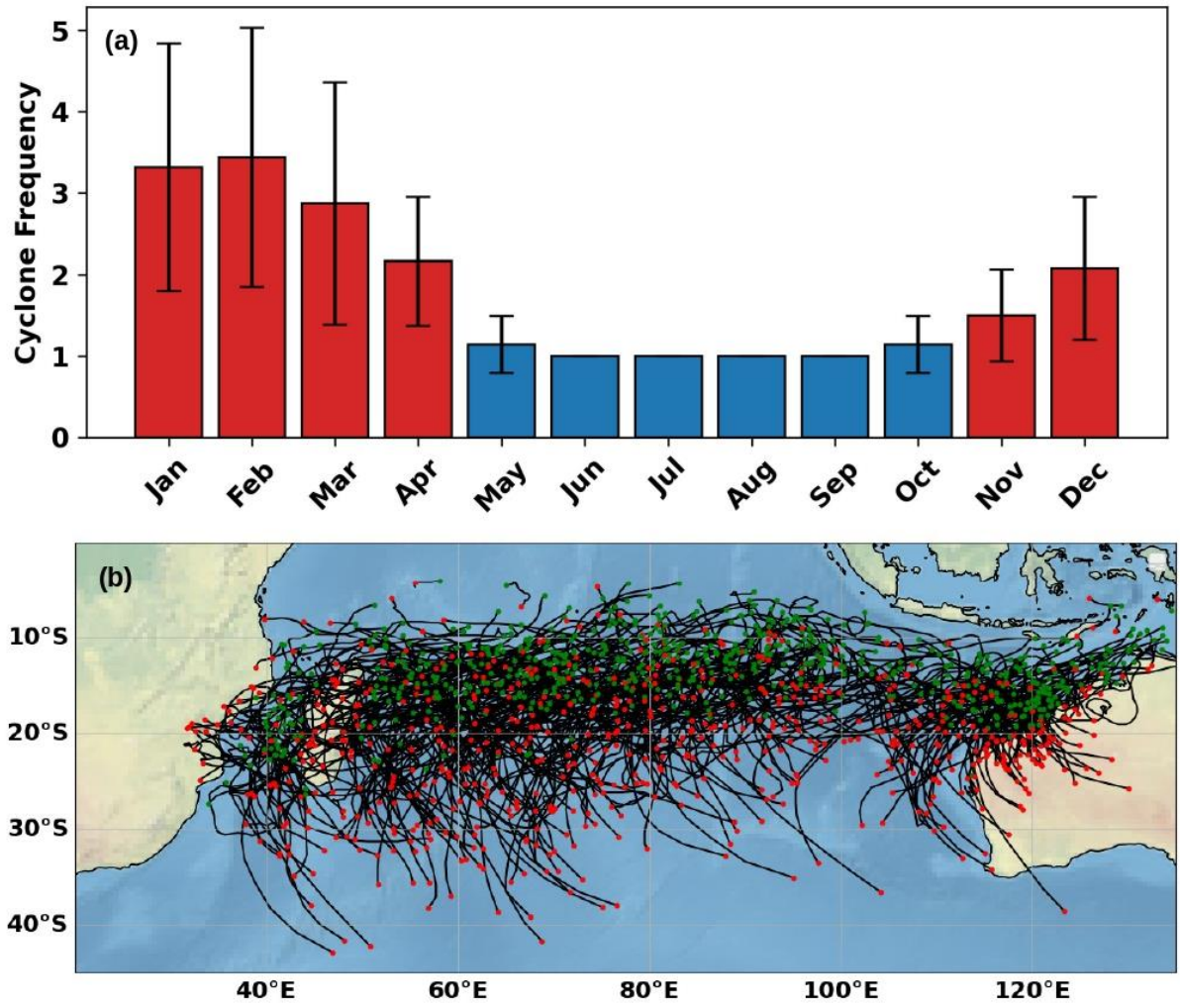

Figure 5.1. *(a) Monthly climatology of Tropical Cyclone (TC) frequency in the Southern Tropical Indian Ocean for the period 1983–2023. The vertical line along each bar denotes one standard deviation. The red color bars denote the main TC season in this basin. (b) Climatology of TC track from genesis (wind speed ≥34 knots) till dissipation (wind speed = 34 knots). The green dots indicate the TC genesis locations and the red dots indicate the TC dissipation location.*

TCs that form in this basin affects Australia, Madagascar and parts of Africa continent mainland (Figure 5.1b). Also, TCs in this basin are generally confined in a very narrow band from 9°S-25°S. TCs in the basin generally move westward after their formation, whereas few TCs recurve and move in south/south eastward direction (Figure 5.1b).

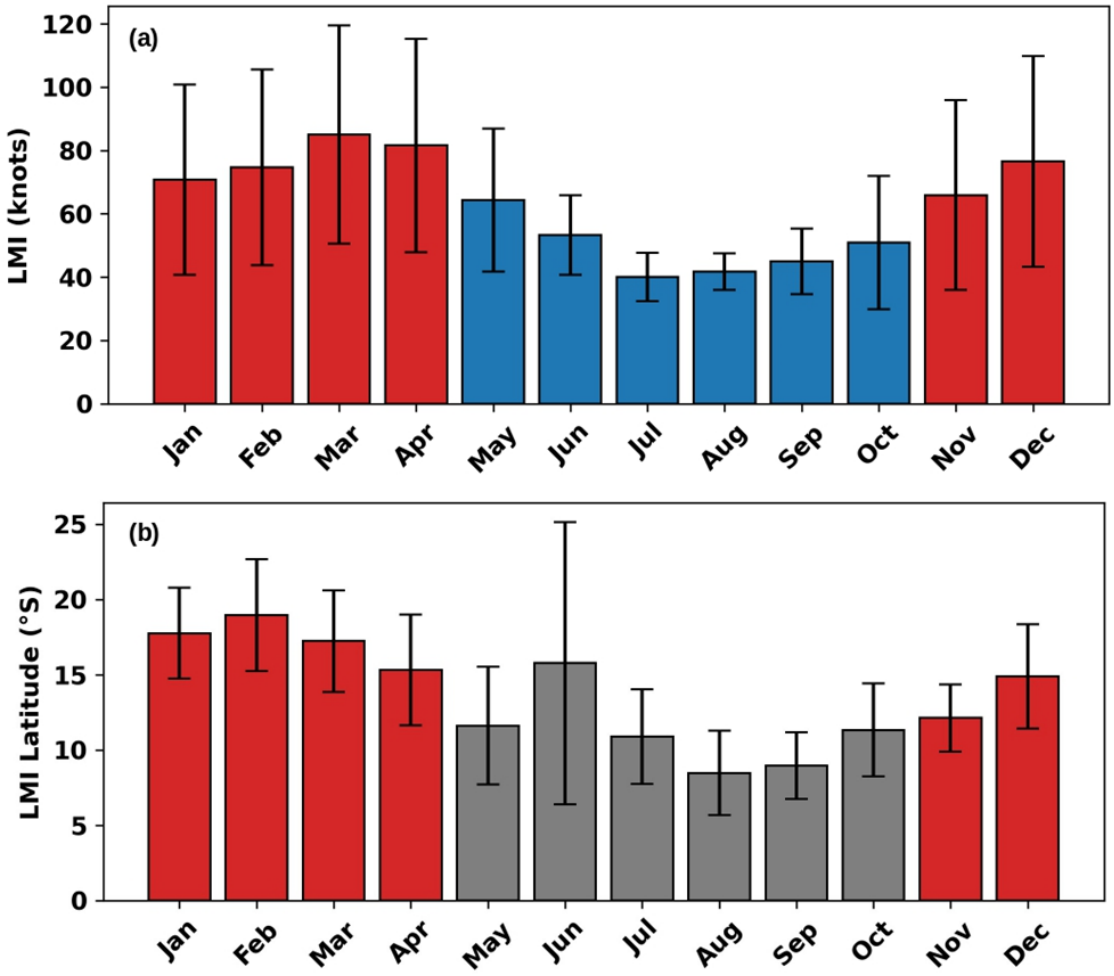

Figure 5.2. *Monthly climatology of mean (a) Lifetime maximum intensity (knots) of TCs (b) mean latitude of lifetime maximum intensity of TCs for the period 1983–2023. The vertical line along each bar denotes one standard deviation. The red color bars denote the main TC season in this basin.*

The monthly TC LMI distribution shows that the TCs in this basin achieve their maximum intensity in the later part of the season (Figure 5.2a). On average, the highest TC LMI is observed in March when the mean LMI is 85 knots (157.4 km/hr). The 2nd highest mean LMI is observed in April when the mean TC LMI is 81.6 knots (151.1 km/hr, Figure 5.2a). Whereas, the 3rd highest mean LMI is observed in December when the mean TC LMI is 76.5 knots (141.7 km/hr). In this basin, 57.2% of total TCs intensify to Category 1 or category TCs, whereas 30.5% of TCs intensify to Category 3 or higher intensity TCs. Overall, during the season, the mean LMI of TCs in this basin is higher than that in the North Indian Ocean. However, compared to the western North Pacific, TCs in the Southern Tropical Indian Ocean are relatively less intense (Singh et al., 2025).

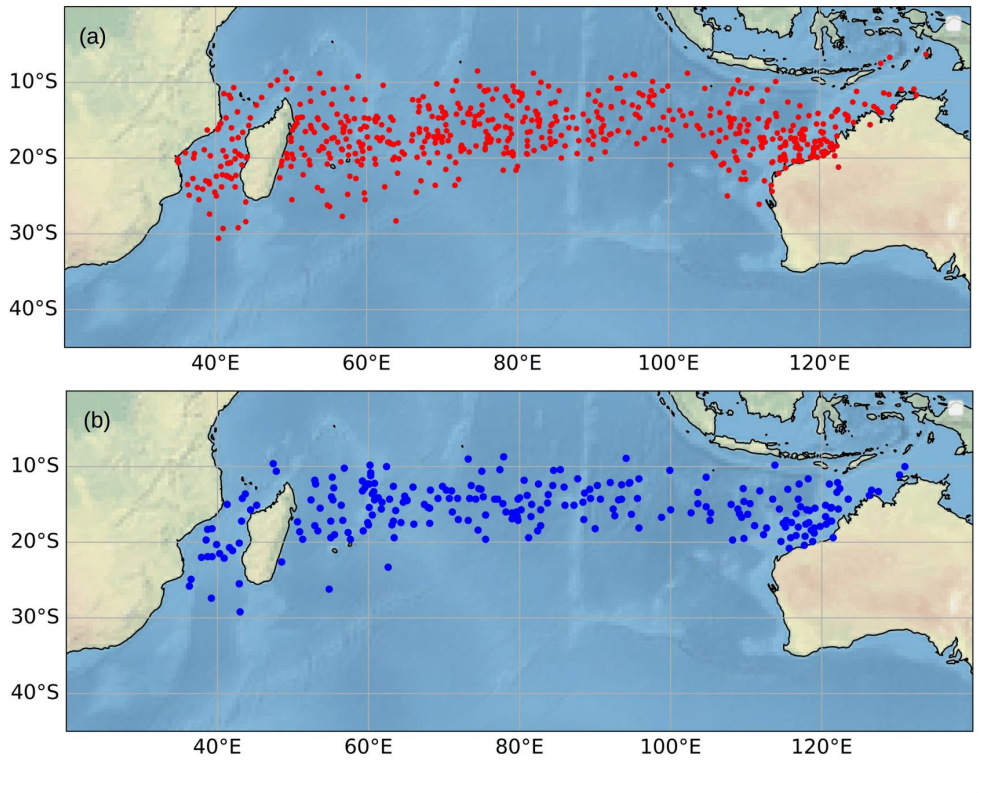

Figure 5.3. *(a) TC lifetime maximum intensity (LMI) location (b) TC rapid intensification location in the Southern Tropical Indian Ocean during November–April for the period 1983–2023.*

Further analysis shows that the latitude at which TCs attain their LMI generally lies between 10°S and 20°S during the season (Figure 5.2b, Figure 5.3a). However, west of 70°E and near the west coast of Australia, TCs are attaining LMI south of 20°S too (Figure 5.3a). Monthwise analysis shows that the most southward location of TC LMI occurs in February, when the mean latitude of LMI is around 18.96°S, whereas the most equatorward occurrence is in November, with a mean LMI latitude of 12.12°S (Figure 5.2b). This indicates a southward shift in the TC LMI location as the season progresses from November to February, followed by a gradual retreat thereafter. During the off-season months (May–October), the LMI tends to occur closer to the equator, reflecting the northward displacement of TC activity (Figure 5.2b).

5.2 Observed changes in TC frequency, intensity and rapid intensification in the basin

As in the North Indian Ocean, the Southern Tropical Indian Ocean has experienced a rapid rise in SSTs in recent decades, consistent with the global warming trend. Despite this

continuous warming, the total TC frequency during the season has shown a decreasing trend of 0.3 TCs per decade; however, this decline is not statistically significant (p = 0.44; Figure 5.4a). In contrast, the frequency of Category 1 or higher intensity TCs exhibits a marginal increasing trend of 0.1 TCs per decade, though this change is also statistically insignificant (p = 0.81; Figure 5.4b). Notably, the frequency of intense TCs (Category 3 or higher) shows a significant increasing trend of 0.4 TCs per decade (p = 0.15, Figure 5.4c). This contrasting behaviour—declining total TC frequency but increasing occurrence of intense TCs—suggests that although fewer TCs are forming, those that do develop tend to reach higher intensities.

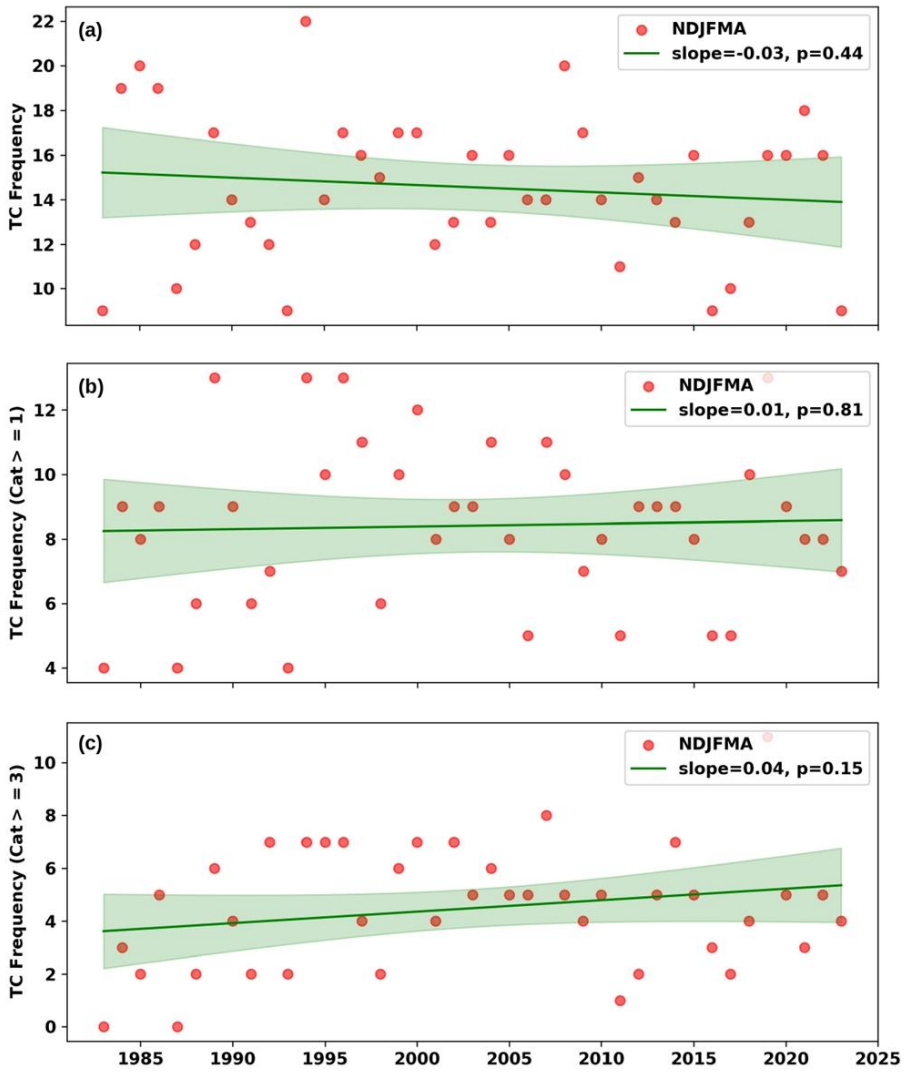

Figure 5.4.. *Observed trends in (a) TC frequency (b) TC frequency which has intensity ≥ Category 1 (c) TC frequency which has intensity ≥ Category 3 during the main TC season (November–April) of the Southern Tropical Indian Ocean for the period 1983–2023. The slope values indicate the trend/year and the p-value denotes its statistical significance using two tailed Student's t-test. The shading along the mean trend line denotes the 95th percentage confidence interval band.*

The increasing Category 3 or higher intensity TCs is further supported by the overall increase in the intensity (LMI) of TCs, which is increasing rapidly at the rate of 3.4 knots per year ($p < 0.01$; Figure 5.5a). Another unique feature that is observed is the interdecadal variability in the TC LMI, which needs detailed research in the future. Also, the upper limit of TC maximum intensity, denoted by the 90th percentile of LMI is increasing significantly at the rate of 6 knots per decade, highlighting that the upper limit of TC intensity that TC achieves in a season is increasing significantly ($p < 0.01$; Figure 5.5b).

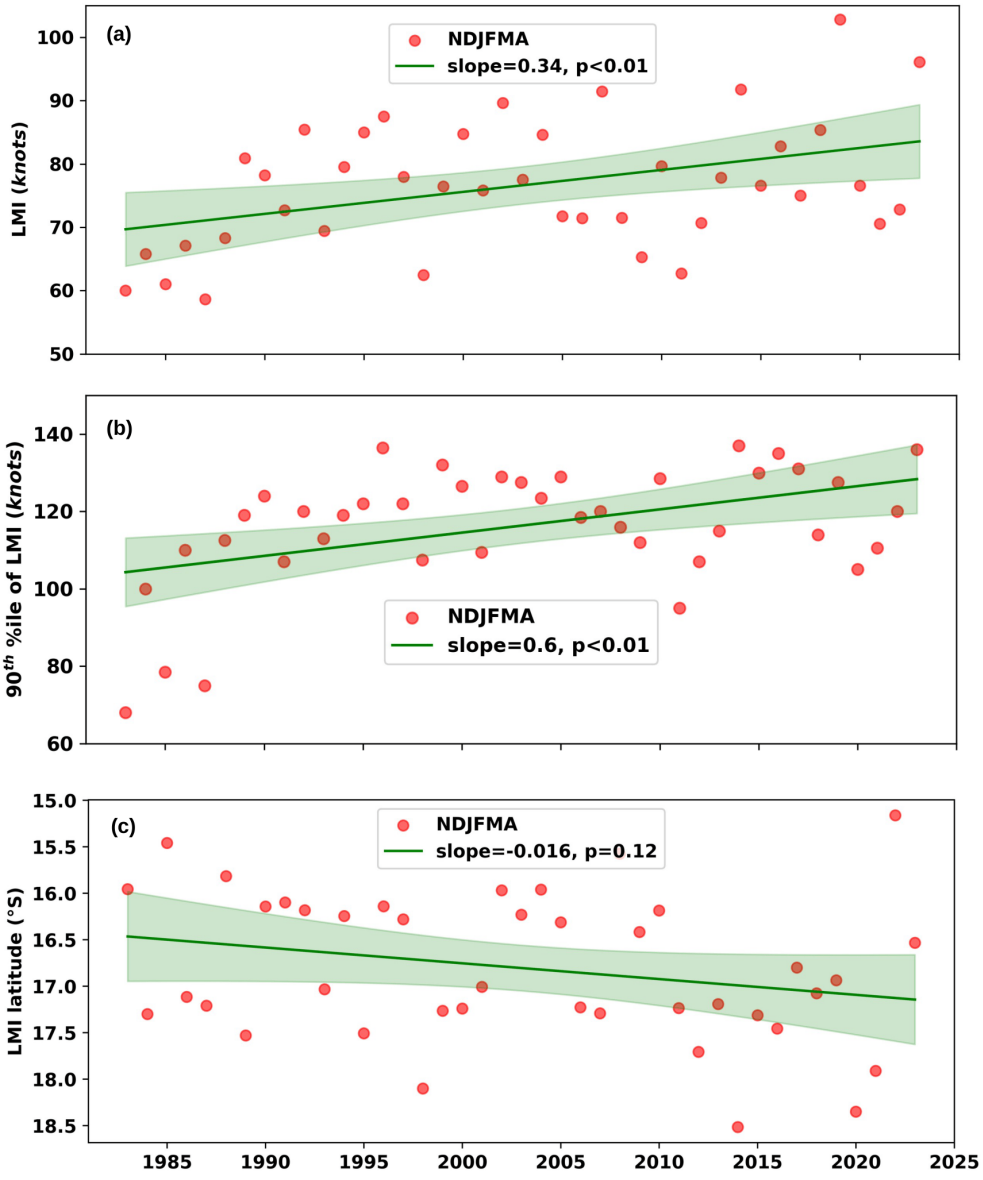

Figure 5.5*. Observed trends in (a) TC lifetime maximum intensity (LMI) (knots) (b) 90th percentile of LMI (c) TC LMI latitude (°S) during the main TC season (November–April) in the Southern Tropical Indian Ocean for the period 1983–2023. The slope values indicate the trend/year and the p-value denotes its statistical significance using two tailed Student's t-test. The shading along the mean trend line denotes the 95th percentage confidence interval band.*

Not only has the LMI of TCs increased, but the latitude at which TCs attain their LMI is also shifting poleward at a rate of 0.16° per decade (p = 0.12, Figure 5.5c). The observed poleward migration of TC LMI latitude indicates that the most intense phase of TCs is occurring progressively farther from the equator. This shift is consistent with the globally reported poleward migration of TC LMI locations (Daloz & Camargo, 2018), suggesting that large-scale climatic changes—such as the expansion of the tropics, poleward displacement of the subtropical jet, and changes in vertical wind shear and potential intensity may be influencing the spatial distribution of TC intensity and need in-depth research in the future. However, this poleward shift in TC LMI is in sharp contrast to the Bay of Bengal, where the overall TC LMI latitude is shifting equatorward.

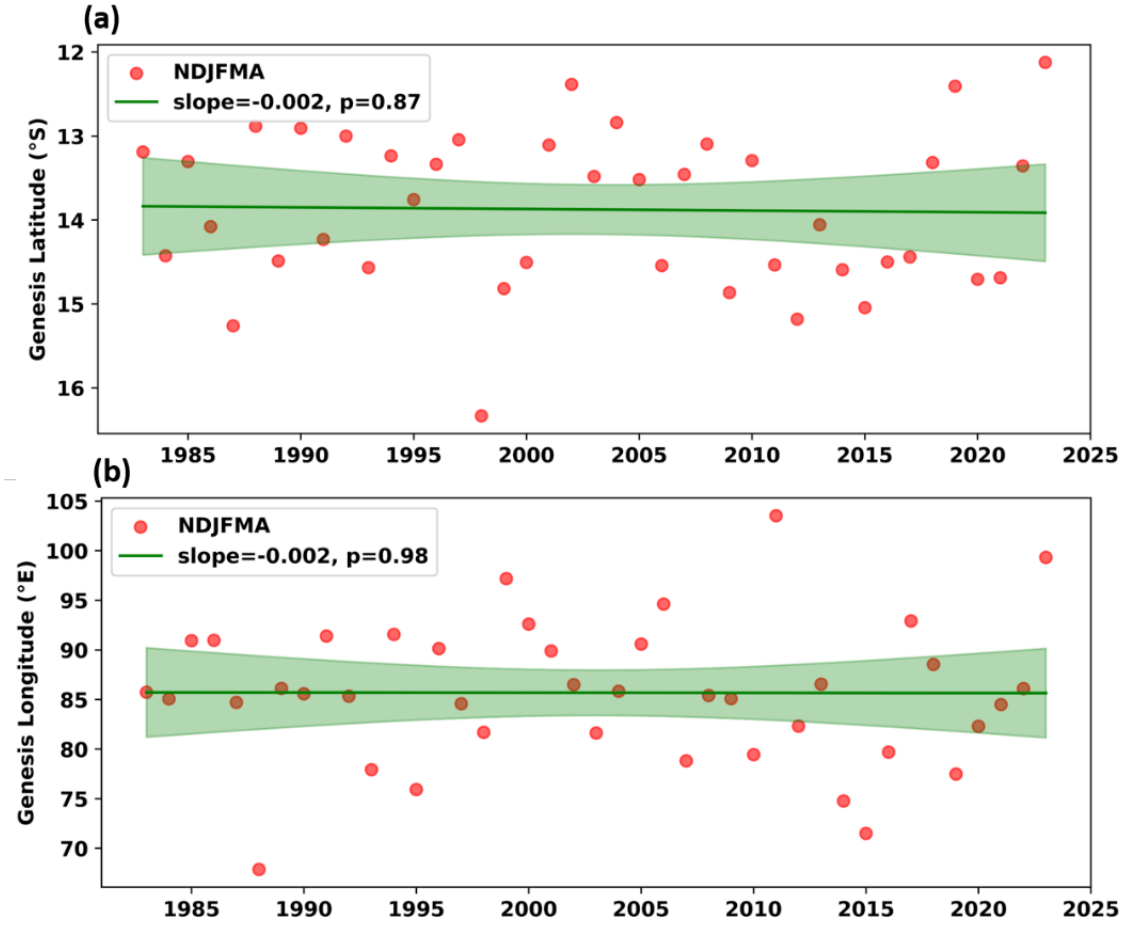

Figure 5.6. *Trend of (a) TC genesis latitude (°S) (b) TC genesis longitude (°E) during TC season (November–April) in the Southern Tropical Indian Ocean for the period 1983–2023. The shaded region around the trend line denotes the 95% confidence interval band. Slope value denotes the trend in latitude and longitude per year, whereas the p-value denotes the significance of the slope using the two-tailed Student's t-test.*

Although the LMI location is shifting poleward, there is no significant change in the TC genesis location, as indicated by the trends in genesis latitude and longitude (Figure 5.6). This suggests that the observed poleward shift in TC LMI location is likely driven by ocean–atmospheric factors, while changes in TC genesis play only a minimal role.

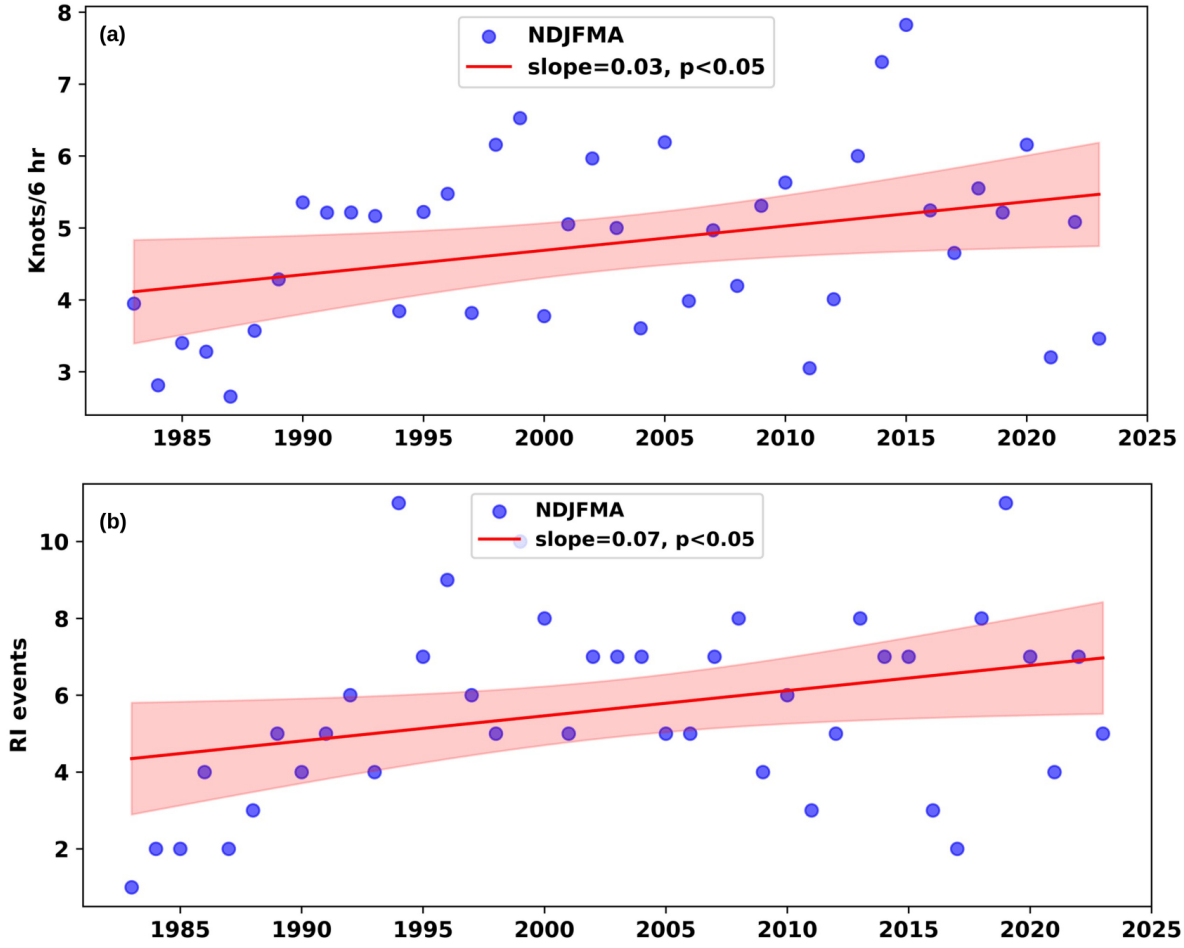

Figure 5.7. *Observed trends in (a) TC intensification rate (knots/6 hour) (b) Frequency of rapid intensification during the main TC season (November–April) for the period 1983–2023. The slope values indicate the trend/year and the p-value denotes its statistical significance using two tailed Student's t-test. The shading along the mean trend line denotes the 95th percentage confidence interval band.*

Further, in this basin during the season, on average 39.1% of TCs undergo rapid intensification, which means about one-third of TCs undergo rapid intensification. This rate of rapid intensification is even higher than the most active TC basin, i.e. western North Pacific, where this rate is 22.0% (Fudeyasu et al., 2018). We found that the frequency of TCs undergoing rapid intensification has increased significantly in the Southern Tropical Indian Ocean, at a rate of 0.7 TCs per decade ($p < 0.05$; Figure 5.7b). This rise in rapid intensification events is further supported by a statistically significant increase in the mean intensification rate

of TCs, which is increasing at the rate of 0.3 knots per 6 hours per decade ($p < 0.05$, Figure 5.7a). The increase in the rapid intensification of TCs in Southern Tropical Indian Ocean is linked to the rapid rise in SST and ocean heat content in the basin. In contrast, atmospheric parameters appear to play a relatively limited role in this increase (Vidya et al., 2021). These results suggest that TCs in this basin are not only becoming stronger but are also reaching their peak intensities over a much shorter period, indicating a growing tendency toward more explosive intensification events. Although the magnitude of this increase is smaller than that observed in the Arabian Sea, it exceeds the rate of intensification seen in the Bay of Bengal during the pre-monsoon season. This highlights the Southern Tropical Indian Ocean as an emerging hotspot for rapid TC intensification under a warming climate.

5.3 Observed changes in accumulated cyclone energy

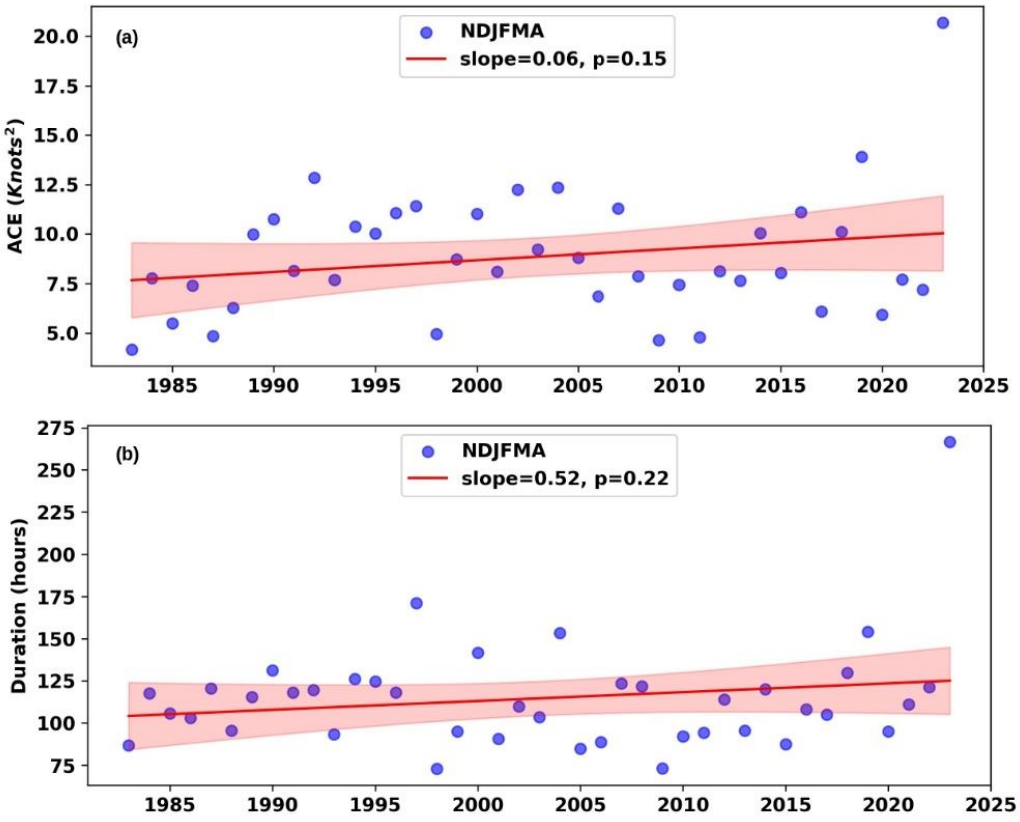

Figure 5.8. *Observed trends in (a) Accumulated Cyclone Energy/season (ACE, ×10^4 knots^2) (b) TC duration (hours) during the season (November–April) for the period 1983–2023. The slope values indicate the trend/year and the p-value denotes its statistical significance using two tailed Student's t-test. The shading along the mean trend line denotes the 95th percentage confidence interval band.*

As discussed earlier, the intensity of TCs in the Southern Tropical Indian Ocean has shown a significant increasing trend in recent decades. In addition to intensification, the duration of TCs during the season has also increased at a rate of 5.2 hours per decade ($p = 0.22$, Figure 5.8b). This implies that over the past four decades, the average TC lifetime in the basin has lengthened by approximately 1 day. The longer duration indicates that TCs are persisting over the ocean for extended periods, potentially allowing them to extract more heat energy from the ocean surface and thus sustain higher intensities.

However, despite the observed increases in both TC intensity and duration, the ACE shows little to no long-term trend (Figure 5.8a). This apparent contradiction can be explained by the concurrent decline in overall TC frequency in the basin, which offsets the contribution of stronger and longer-lived storms to total ACE. In essence, while individual TCs in the Southern Tropical Indian Ocean are becoming more intense and longer-lasting, their overall number is slightly decreasing. This compensating effect results in a near-neutral trend in basin-wide accumulated cyclone energy.

6. Future projection of tropical cyclone activity in the North Indian Ocean

6.1 Assessing the performance of CMIP6 HighResMIP historical models in simulating TC activity

In the previous section, we see that there are significant changes in the TC characteristics in the North Indian Ocean. With global warming, it is important to understand how the TCs will evolve in the near-future. As discussed in the methodology section, for the evaluation of the historical models, we have selected the observation period as 1979–2014 to match the model's historical period.

During the period 1979–2014, the observed climatological mean frequency of TCs over the North Indian Ocean is 1.1 TCs per year in the pre-monsoon season and 2.4 TCs per year in the post-monsoon season (Figure 6.1). This indicates that TC occurrence is nearly twice as frequent in the post-monsoon season compared to the pre-monsoon season, consistent with previous findings (Singh et al., 2000; Singh & Roxy, 2022). To evaluate the performance of CMIP6 HighResMIP models in realistically simulating TC characteristics over the North Indian Ocean during both seasons, the mean TC frequency from the historical simulations was

compared with observations derived from the IBTrACS dataset for the period 1979–2014 (Figure 6.1).

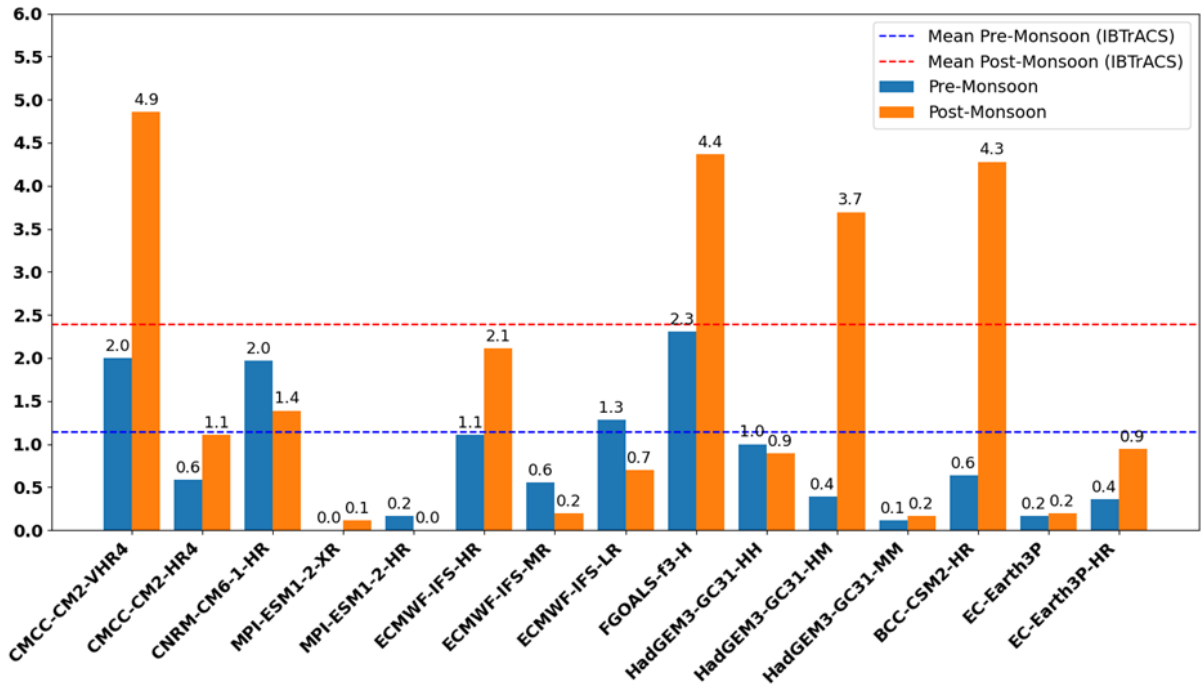

Figure 6.1. *Mean tropical cyclone frequency over the North Indian Ocean during 1979–2014 from 15 CMIP6 HighResMIP models (historical simulations) and observations from IBTrACS. Historical model data for the pre-monsoon (April–June) and post-monsoon (October–December) seasons are shown by blue and orange bars respectively, while IBTrACS mean TC frequency/year for the pre-monsoon and the post-monsoon season is represented by blue and red dotted lines.*

Among the 15 models analyzed, Two models (CMCC-CM2-VHR4 and FGOALS-f3-H) overestimate TC frequency in both seasons. Whereas BCC-CSM2-HR and HadGEM3-GC31-HM significantly overestimate the TC frequency during the post-monsoon season. In contrast, eight models (CMCC-CM2-HR4, MPI-ESM1-2-XR, MPI-ESM1-2-HR, ECMWF-IFS-MR, HadGEM3-GC31-HH, HadGEM3-GC31-MM, EC-Earth3P, and EC-Earth3P-HR) underestimate TC frequency in both the seasons. Notably, the MPI-ESM1-2-XR and MPI-ESM1-2-HR models fail to reproduce the observed TC frequency during the pre-monsoon and post-monsoon seasons, respectively (Figure 6.1). Previous studies have also reported that MPI models, irrespective of their resolution, exhibit poor skill in simulating TCs across the Northern Hemisphere (Pall et al., 2024; Roberts et al., 2020). The ECMWF-IFS-HR model shows the closest agreement with observations in both seasons.

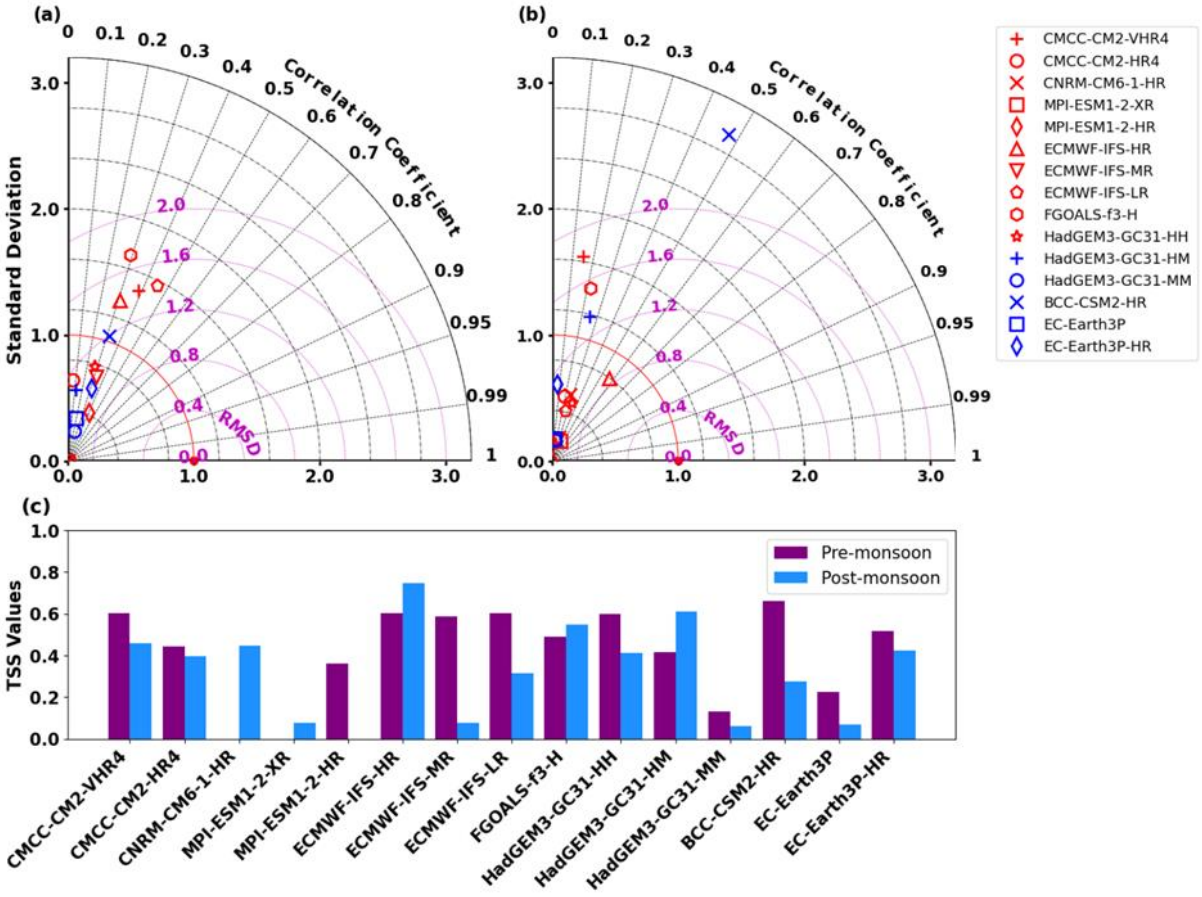

Figure 6.2. *Taylor analysis of cumulative genesis density of tropical cyclones (TC) from 15 CMIP6 HighResMIP models (historical simulations) over the North Indian Ocean during 1979–2014 for (a) pre-monsoon season (April–June), (b) post-monsoon season (October–December), and (c) Taylor skill scores of different models for TC genesis density during the pre-monsoon (purple) and post-monsoon (blue) seasons.*

To assess the performance of the 15 CMIP6 HighResMIP historical models, we performed a Taylor diagram analysis of the spatial distribution of TC genesis and TC track density and over the North Indian Ocean during the period 1979–2014, following the methodology outlined by Shan & Yu (2021). The analysis was conducted separately for the two TC seasons (Figures 6.2 and 6.3). Although Figure 6.1 presents results for all 15 models, it should be noted that future projections are not available for six models: BCC-CSM2-HR, CNRM-CM6-1-HR, ECMWF-IFS-HR, ECMWF-IFS-LR, ECMWF-IFS-MR and HadGEM3-GC31-HH, therefore these models are excluded from the detailed discussion.For the TC genesis, during the pre-monsoon season, BCC-ESM2-HR has the highest Taylor skill score of

~0.7, followed by CMCC-CM2-VHR4 (Figure 6.2c). This is because their standard deviation is reasonably closer to the observed value (Figure 6.2 a-b). FGOALS-f3-H, CMCC-CM2-HR4, HadGEM-GC31-HM and EC-Earth3P-HR also have a Taylor skill score in the range 0.4-0.5. During the post-monsoon season, HadGEM3-GC31-MM has the highest Taylor skill score, followed by FGOALS-f3-H. In this season, CMCC-CM2-VHR4, EC-Earth3P-HR and HadGEM3-GC31-HH have Taylor skill scores between 0.4-0.5.

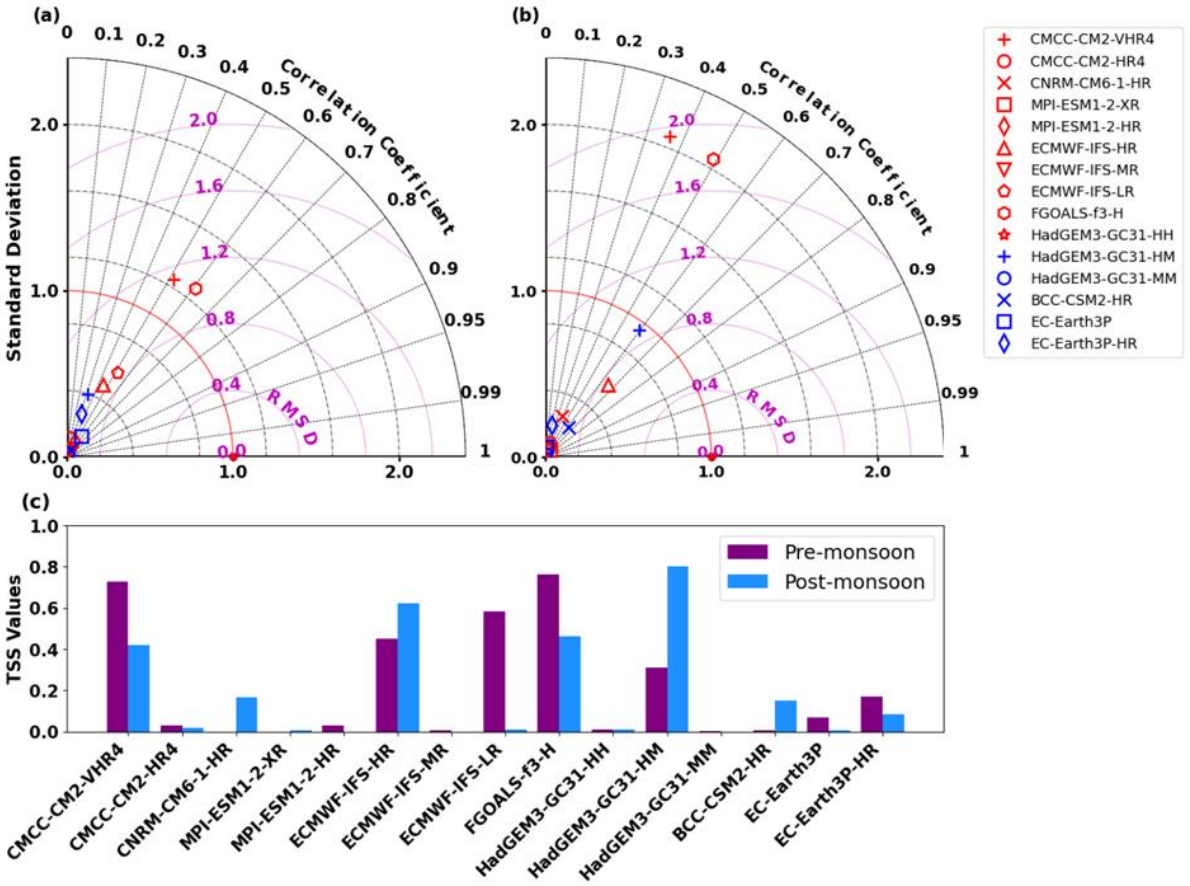

Figure 6.3. *Taylor analysis of cumulative track density of tropical cyclones from 15 CMIP6 HighResMIP models (historical simulations) over the North Indian Ocean during 1979–2014 for (a) pre-monsoon, (b) post-monsoon, and (c) Taylor skill scores of different models for track density during the pre-monsoon (purple) and post-monsoon (blue) seasons.*

The analysis of TC track density shows that during the pre-monsoon season, FGOALS-f3-H has the highest Taylor skill score, followed by CMCC-CM2-VHR4 and HadGEM3-GC31-HM. During the post-monsoon season, HadGEM3-GC31-HM has the highest Taylor skill score, followed by FGOALS-f3-H and CMCC-CM2-VHR4 (Figure 6.3). Whereas other models for which future projections are available show poor skill in capturing the TC track

density in both seasons. Therefore, out of the nine models, three—HadGEM3-GC31-HM, FGOALS-f3-H, and CMCC-CM2-VHR4 demonstrate better performance in simulating TC tracks during both the seasons over the North Indian Ocean. The CMCC-CM2-HR4 and EC-Earth3P-HR models perform well in simulating TC genesis (Figure 6.2c) but poorly in simulating TC tracks (Figure 6.3c). Overall, the HadGEM3-GC31-HM, FGOALS-f3-H, and CMCC-CM2-VHR4 models perform well in simulating both TC genesis and tracks during both the seasons. Therefore, we select the three best-performing models—HadGEM3-GC31-HM, FGOALS-f3-H, and CMCC-CM2-VHR4 for further analysis.

6.2 Projected changes in TC frequency over the North Indian Ocean

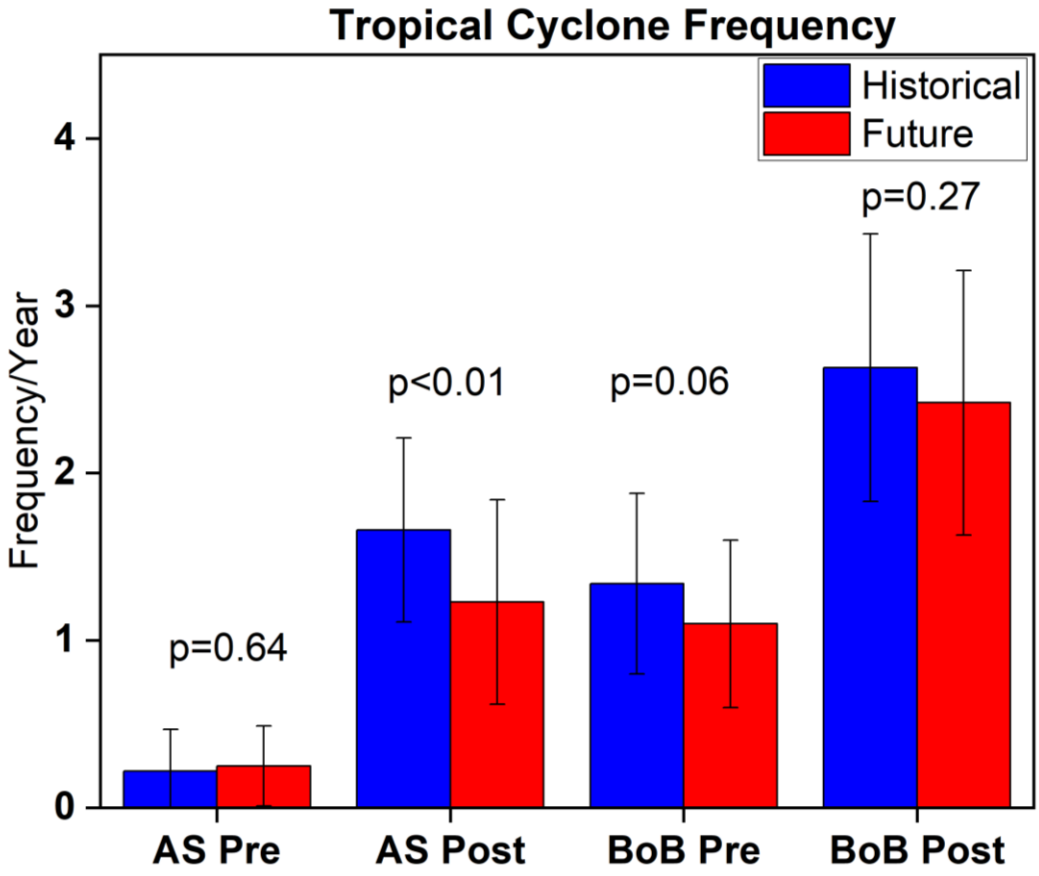

Figure 6.4. *Multi-model mean of historical simulations (1979–2014; blue bars) and future projections (2015–2050; red bars) of mean tropical cyclone frequency/year in the Arabian Sea and Bay of Bengal during the Pre-monsoon (April–June) and Post-monsoon (October–December) season. The vertical line denotes one standard deviation. The values above bars denote the statistical significance of the difference using p-value between the historical simulation and future projection for both the basins and seasons.*

Based on the multi-model mean of the three best-performing models, we examine the historical simulation (1979–2014) and future projection (2015–2050) of the TC frequency over the Bay of Bengal (Figure 6.4). TC frequency is calculated as the average number of TCs per year, based on the total number of TCs occurring during historical simulation and future projection. In the Bay of Bengal, the multi-model mean projects a decrease in TC frequency during both the seasons; however, the decline is statistically significant only in the pre-monsoon season ($p = 0.06$; 94% confidence level).On the other hand, in the Arabian Sea models are projecting a significant decrease in the TC frequency during the post-monsoon season ($p < 0.01$). However, no significant change is observed during the pre-monsoon season.

Table 6.1. *Multi-model mean of total TC frequency in different TC categories (Tropical storm, Category 1+2 and Category ≥ 3) in historical simulation (1979–2014) and future projection (2015–2050) for the Arabian Sea and Bay of Bengal during the pre-monsoon (April–June) and post-monsoon (October–December) season.*

	Tropical Storm (wind speed < 65 knots)		**Category 1-2 (wind speed > 64 knots ≤ 95 knots)**		**Category ≥ 3 (wind speed ≥ 100 knots)**	
	Historical	Future	Historical	Future	Historical	Future
Arabian Sea Pre-Monsoon	1	0.3	4.7	5.3	2.3	3.3
Arabian Sea Post-Monsoon	34.7	22	18.7	16.0	6.3	3.7
Bay of Bengal Pre-Monsoon	7.7	9.7	24.0	22.0	16.7	8.0
Bay of Bengal Post-Monsoon	54.0	49.0	34.3	30.0	6.3	8.0

6.3 Projected changes in TC intensity, duration and ACE over the north Indian Ocean

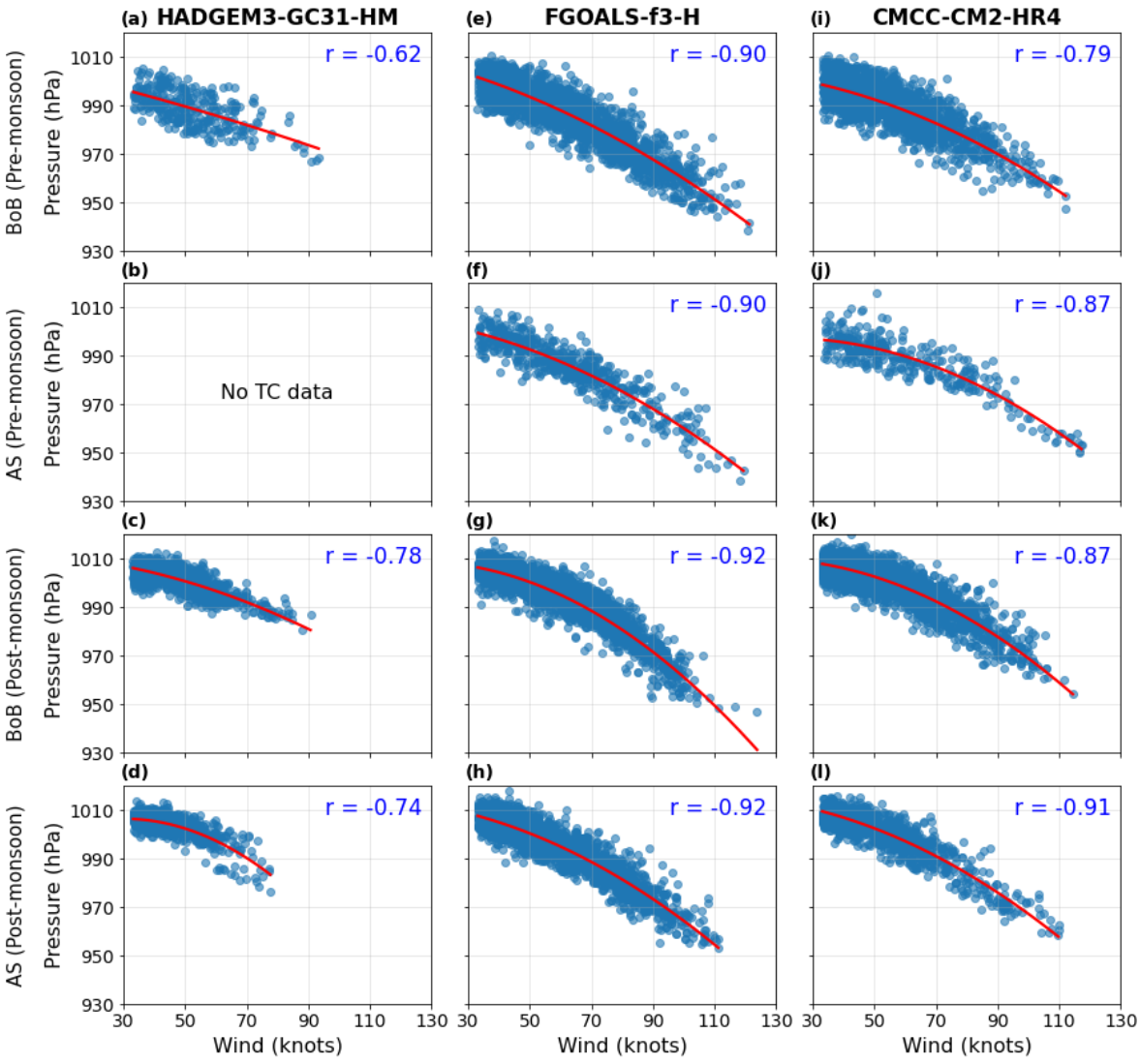

Figure 6.5. *TC wind speed (knots) and central pressure (hPa) relationship in the Bay of Bengal and Arabian Sea during the pre-monsoon (April–June) and post-monsoon (October–December) seasons for the historical period (1979–2014) as simulated by HadGEM3-GC31-HM (Left column), FGOALS-f3-H (Central column) and CMCC-CM2-HR4 (Right column) models. The r values in each sub-plot denote the correlation between TC wind and TC central pressure.*

We have computed TC intensity based on the minimum TC center pressure as well as based on TC maximum wind speed. From Figure 6.5, it can be seen that all three models can realistically capture the relationship between TC wind speed and central pressure and are in good agreement with the observations. In the Bay of Bengal during the pre-monsoon, not only the frequency but also the intensity of TC is projected to decrease. Based on the pressure, multi-

model mean is projecting an increase in the mean lowest pressure in TC center by 4 hPa (Figure 6.6a) indicating significant weakening of the TC ($p < 0.01$) as pressure is inversely proportional to TC intensity (Figure 6.5). Similarly, based on the wind speed criteria too, the multi-model mean is projecting weakening of TC by 4.6 %, which is statistically significant ($p = 0.08$) (Figure 6.6b). Also, in this season, the higher category TCs (Category ≥3; wind speed ≥ 100 knots) are projected to decline by nearly 52% which is statistically significant ($p < 0.01$; Table 6.1). During the post-monsoon season too multi-model is projecting slight weakening, however it is not significant (Figure 6.5). However, the intense TCs (Category ≥ 3) are projected to increase from one TC in every five years to one TC in every four year (Table 6.1). These findings align with previous studies by Roberts et al. (2020), who analyzed CMIP6 models, and Murakami et al. (2013), who used a high-resolution atmospheric general circulation model, both of which reported an overall reduction in annual TC frequency in the Bay of Bengal under a global warming scenario. In contrast, the projected decrease in high-intensity TCs in the Bay of Bengal differs from the western North Pacific, where CMIP6 HighResMIP multi-model projections indicate an increase in the occurrence of intense TCs (Tang et al., 2022).

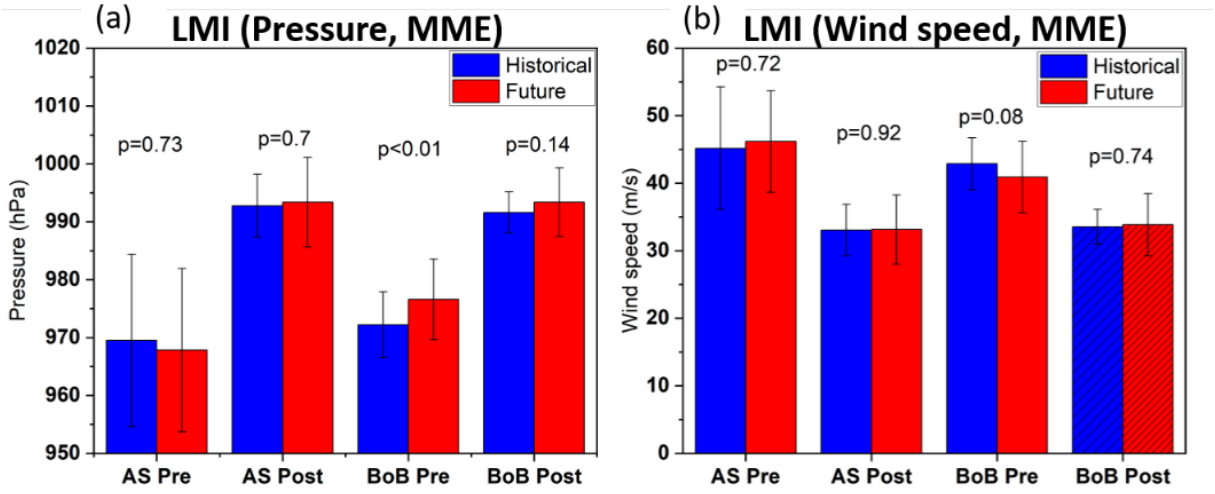

Figure 6.6. *Multi-model mean of historical simulations (1979–2014; blue bars) and future projections (2015–2050; red bars) of (a) Lifetime maximum intensity (LMI) of tropical cyclone (LMI based on pressure, hPa) (b) Lifetime maximum intensity (LMI) of tropical cyclone (LMI based on wind speed, m/s) in the Arabian Sea and Bay of Bengal during the Pre-monsoon (April–June) and Post-monsoon (October–December) season. The vertical line denotes one standard deviation. The values above bars denote the statistical significance of the difference using p-value between the historical simulation and future projection for both the basins and seasons.*

On the other hand, in the Arabian Sea, during the pre-monsoon season, the multi-model mean is projecting a slight increase in TC intensity (based on both wind and pressure criteria), though it is not statistically significant. This slight increase in TC intensity is consistent with the recent observed increasing trend in TC intensity in this basin. Whereas, during the post-monsoon season, an insignificant decline in TC intensity is projected by the multi-model mean (Figure 6.6). Earlier, we saw that during the post-monsoon season, with the increase in intensity of TC, more intense TCs are occurring in recent decades. However, the HighResMIP CMIP6 multi-model mean is projecting a decline from one intense TC (Category ≥3) in five years in historical simulation to one intense TC (Category ≥ 3) in every nine years (Table 6.1).

In the Arabian Sea, the CMIP6 HighResMIP multi-model mean projects a significant decline in TC duration during both seasons (Figure 6.7a). During the post-monsoon season, the projected decreases in both TC intensity and duration result in a reduction of ACE ($p = 0.17$). In contrast, during the pre-monsoon season, although TC duration is projected to decrease (Figure 6.7a), the slight, insignificant increase in TC intensity (Figure 6.6) leads to no significant change in ACE (Figure 6.7b). In the Bay of Bengal, during the pre-monsoon season, both TC intensity and duration are projected to decrease (Figures 6.6 and 6.7a), resulting in a corresponding decrease in ACE ($p = 0.26$). During the post-monsoon season, the projected decline in ACE ($p = 0.19$, Figure 6.7b) is primarily attributed to a significant reduction in TC duration (Figure 6.7a).

While these changes describe the overall TC activity in terms of intensity and duration, an examination of the TC intensification rate provides additional insight into potential risks. In the Arabian Sea, during the pre-monsoon season, the models project only an insignificant change in TC intensity; however, the TC intensification rate is projected to increase markedly, from 2 hPa per 6 hours to 2.5 hPa per 6 hours ($p = 0.14$, Figure 6.7c). This indicates that TCs in the region are likely to reach higher intensities more rapidly over shorter timespans. In contrast, during the post-monsoon season, no significant change in the TC intensification rate is projected for the Arabian Sea. In the Bay of Bengal, there is no significant change in the TC intensification rate in both seasons (Figure 6.7c). These results suggest that, while the Bay of Bengal TCs are expected to maintain their current intensification behavior, Arabian Sea TCs

may experience faster intensification especially during the pre-monsoon season, which could have implications for forecasting challenges in the region.

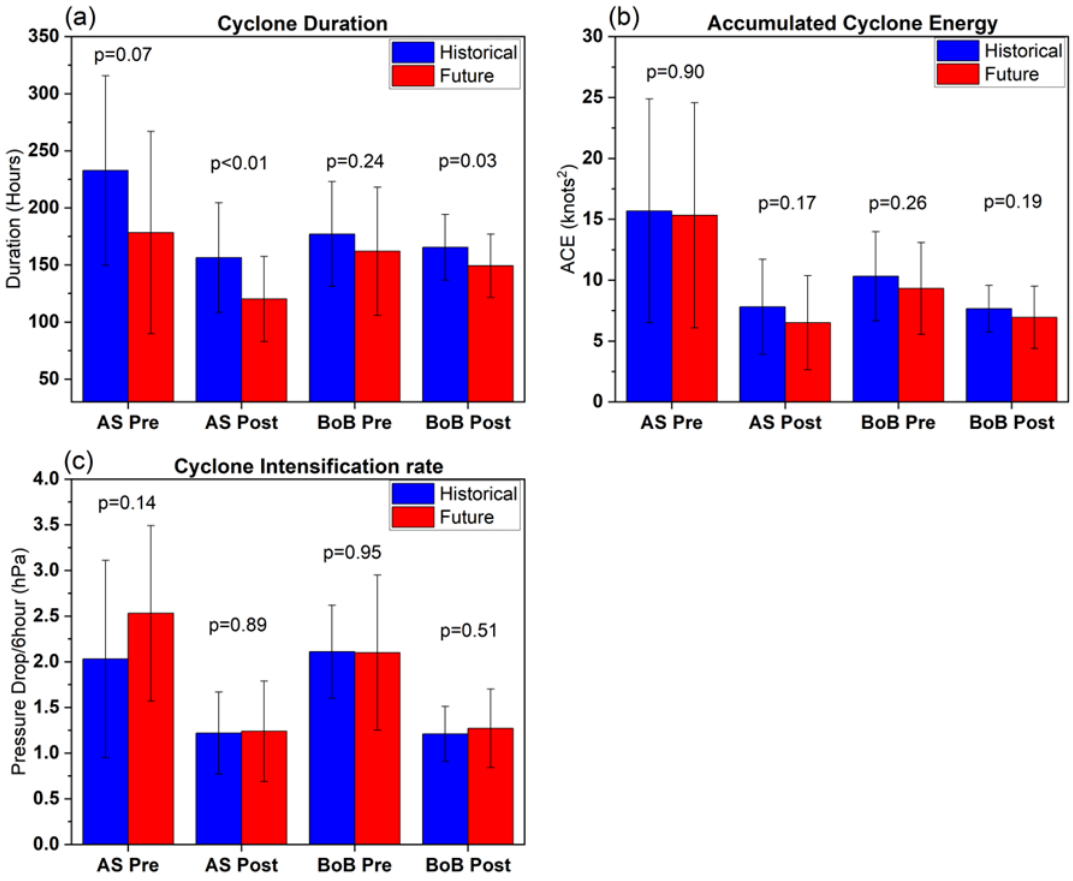

Figure 6.7. *Multi-model mean of historical simulations (1979–2014; blue bars) and future projections (2015–2050; red bars) of (a) TC Duration (hours) (b) Accumulated Cyclone Energy (ACE, ×10^4 knots^2) and (c) TC intensification rate (hPa/6 hours) in the Arabian Sea and Bay of Bengal during the Pre-monsoon (April–June) and Post-monsoon (October–December) season. The vertical line denotes one standard deviation. The values above bars denote the statistical significance of the difference using p-value between the historical simulation and future projection for both the basins and seasons.*

6.4 Projected changes in TC genesis, LMI location and TC tracks over the North Indian Ocean

Previous observations indicate an equatorward shift in the TC genesis location in recent years. To examine how TC genesis locations might evolve in the future, we computed genesis

positions using the 34-knot wind criterion. In the Bay of Bengal, the HighResMIP multi-model mean projects a negligible poleward shift in TC genesis for both seasons (Figure 6.8a). Also, a slight eastward shift in TC genesis location away from the east coast of India is projected in the near future. In the Arabian Sea, there is a negligible poleward shift during the post-monsoon season, while no change in TC genesis latitude is projected for the pre-monsoon season (Figure 6.8a). Overall, these results suggest that there is no significant shift in TC genesis location in either basin.

In addition to TC genesis locations, changes in the LMI location are crucial for understanding how close or far from the coast TCs attain their peak intensity, which directly impacts landfall intensity. In the Bay of Bengal, the CMIP6-HighResMIP multi-model mean projects no change in the LMI location during the pre-monsoon season in the near future (Figure 6.8b). During the post-monsoon season, a negligible eastward shift in LMI is projected, indicating a slight displacement away from the east coast of India. In the Arabian Sea, there is no significant change in LMI location during the pre-monsoon season and a minor westward shift during the post-monsoon season (Figure 6.8b). Overall, no significant changes in TC LMI location are projected for the Arabian Sea in the near future.

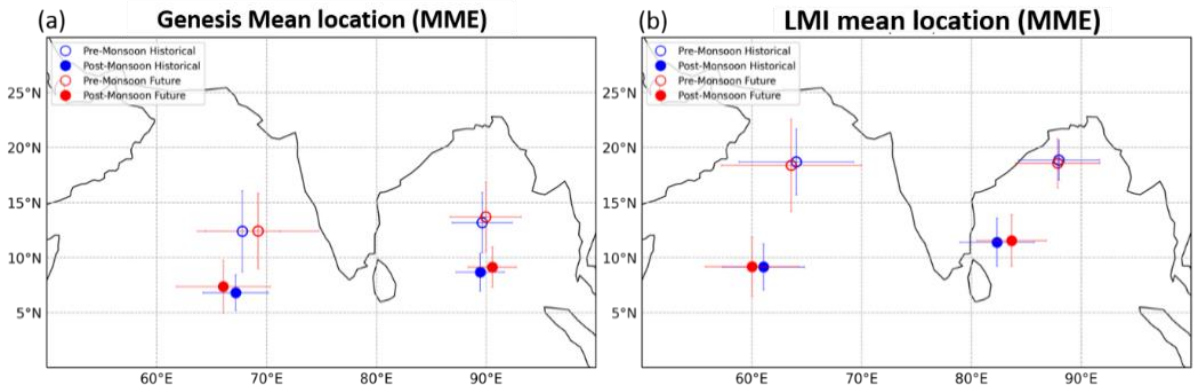

Figure 6.8. *Multi-model mean of historical simulation (1979–2014, blue) and future projection (2015-2050, red) of (a) TC genesis location (b) TC Lifetime maximum intensity location (based on pressure) in the Arabian Sea and the Bay of Bengal during the pre-monsoon season (hollow circle) and the post-monsoon season (filled circle). The lines around the mean TC genesis location and LMI location denote one standard deviation.*

We analyzed the historical simulations (1979–2014) and future projections (2015–2050) of TC track density from the CMIP6 HighResMIP multi-model mean during both the

seasons (Figure 6.9). The TC track points are binned into 2.5° × 2.5° grid boxes to obtain the spatial distribution of track density. To assess the projected changes in TC activity in the near future, we computed the difference in cumulative TC track density between the future and historical periods.

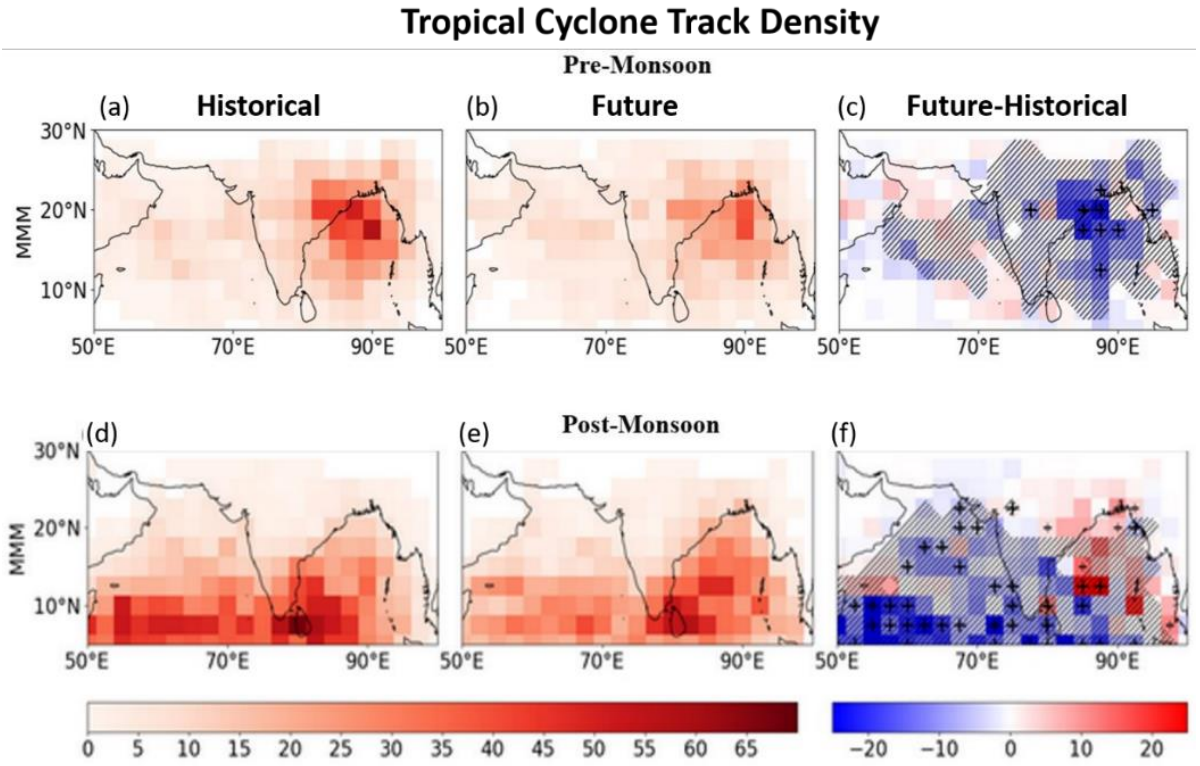

Figure 6.9. *Multi-model mean of (a, d) Historical simulation (1979–2014, left) and (b, e) Future projection (2015–2050, center) of TC cumulative track density during the pre-monsoon (first row) and post-monsoon season (2nd row). (c, f) Difference in the TC cumulative track density between the historical simulations and the future projections, where hatching represent that the difference between the two periods is statistically significant at 95% confidence interval and "+" in the multi model mean represents that all the three models agree with the changes in the TC track density in the near future projections.*

In the Arabian Sea, during the pre-monsoon season, the multi-model mean projects an insignificant increase in TC track density over the northern and northwestern parts of the basin (Figure 6.9a–c). In contrast, a significant reduction in TC tracks is projected along the Maharashtra and southern Gujarat coasts, as well as over the western and southwestern regions of the basin (west of 65°E). During the post-monsoon season, the multi-model mean projects a basin-wide significant decline in TC track density (Figure 6.9d–f), with the most pronounced

decrease occurring in the southern Arabian Sea (south of 15°N). This reduction in TC track density is due to the projected decrease in TC frequency over the basin (Figure 6.4).

In the Bay of Bengal, during the pre-monsoon season, the multi-model mean projects a significant decrease in TC track density across much of the basin, with the strongest reduction along the Odisha coast (Figure 6.9c). Conversely, during the post-monsoon season, the projections indicate a northward shift in TC tracks, characterized by an increase in track density along Odisha, West Bengal, and Bangladesh coasts, and a decrease along Tamil Nadu and Sri Lanka coasts (Figure 6.9d-f). The projection of poleward migration of TC track in this basin during the pre-monsoon season is consistent with the projection of poleward migration of TC tracks in the western North Pacific (Tang et al., 2022).

7. Summary

- We have reported the TC characteristics and their changes in the North Indian Ocean and Southern Tropical Indian Ocean in this manuscript. In the North Indian Ocean (including the Arabian Sea and the Bay of Bengal), on the average ~5 TCs form per year. In a calendar year, in the Bay of Bengal, the highest probability of TC occurrence is in November, whereas in the Arabian Sea, the highest probability of TC occurrence is in June.
- On the average, TCs in the Arabian Sea and the Bay of Bengal are 9.1% and 18.7% more intense during the pre-monsoon season as compared to the post-monsoon season.
- During the pre-monsoon season, most TC activity in the Arabian Sea occurs between 16 May and 15 June, whereas in the Bay of Bengal, it occurs earlier, mainly between 26 April and 21 May.
- During the post-monsoon season, the major TC threat is between 21 October-15 November in the Arabian Sea. Whereas in the Bay of Bengal TC threat is there throughout the season, with three distinct peaks in the TC activity.
- During the pre-monsoon season, about 41.4% of TCs in the Arabian Sea and 51.4% in the Bay of Bengal intensify to Category 1 or higher, compared to 36.8% and 35.6%, respectively, in the post-monsoon season. This suggests higher TC intensification efficiency in both the basins during the pre-monsoon season.
- Nearly one in three TCs in the Arabian Sea and one in four in the Bay of Bengal become major TCs (Category 3 or higher) in the pre-monsoon season, whereas the ratio decreases to one in six and one in seven, respectively, during the post-monsoon season.
- It is observed that during the pre-monsoon season, 34.5% of TCs in the Arabian Sea and 32.4% in the Bay of Bengal undergo rapid intensification. In contrast, during the post-monsoon season, 18.4% of TCs in the Arabian Sea and 16.1% in the Bay of Bengal experience rapid intensification. Thus, in both the basins, pre-monsoon TCs have a higher probability to intensify rapidly as compared to the post-monsoon season.
- In the Arabian Sea, approximately 38% and 31.5% of TCs make landfall with at least tropical storm strength (wind speed $\geq$ 34 knots) during the pre-monsoon and post-monsoon seasons respectively,. In contrast, in the Bay of Bengal, about 91.9% of TCs during the pre-monsoon season and 65.5% during the post-monsoon season make landfall with at least tropical storm intensity. Thus, the probability of TCs making

landfall with at least tropical storm intensity is significantly higher in the Bay of Bengal than in the Arabian Sea in both the TC seasons.

- The TC size in both the basins is larger during the pre-monsoon than the post-monsoon season.
- During the pre-monsoon season, TCs last longer at tropical storm or higher intensity, averaging 87.7 (78.7) hours in the Arabian Sea (Bay of Bengal) which is about 15 (13.5) hours longer than the post-monsoon season. However, when all TC stages (including depression and deep depression (wind speed ≥17 knots) are considered, Arabian Sea TCs persist slightly longer in the post-monsoon season (by 10.7 hours), suggesting their weaker stages dominate. In contrast, Bay of Bengal TCs remain longer-lived during the pre-monsoon season across both intensity thresholds, indicating greater overall persistence compared to post-monsoon systems.
- The land duration of TC (tropical storm strength) in the Arabian Sea is 16.2 (9.0) hours during the pre-monsoon (post-monsoon) seasons. In contrast, over the Bay of Bengal, the corresponding averages are 11.7 hours and 18.2 hours, respectively. Thus, during the pre-monsoon season, Arabian Sea TCs spend longer time over land at tropical storm or higher intensity than those in the Bay of Bengal, whereas during the post-monsoon season, Bay of Bengal TCs persist over land for longer durations than those in the Arabian Sea. However, when all intensity stages up to dissipation are considered, Arabian Sea TCs have longer durations over land compared to Bay of Bengal TCs in both seasons.
- Further, during the pre-monsoon season, the total track length over land is greater in the Arabian Sea than in the Bay of Bengal when all TC stages are included. However, when considering only tropical storm or higher intensity stages, Bay of Bengal TCs travel farther over land than Arabian Sea TCs in this season. Whereas, for the post-monsoon season, regardless of whether all TC stages or only tropical storm or higher intensity stages are considered, Bay of Bengal TCs consistently travel longer distances over land than the Arabian Sea TCs.
- In the Arabian Sea, pre-monsoon TCs move 0.68 m s^{-1} slower than those in the post-monsoon season, whereas in the Bay of Bengal, post-monsoon TCs move 0.14 m s^{-1} slower than pre-monsoon TCs. Slower translation speeds imply a longer duration of influence over a given region, thereby increasing the potential for prolonged impacts

from heavy rainfall, storm surges, and strong winds. Further, in both basins, TCs move faster over land compared to over the ocean.

Table 7.1. *Summary of climatology of various tropical cyclone (TC) characteristics in the Arabian Sea and the Bay of Bengal during the pre-monsoon (April–June) and post-monsoon (October–December) season for the period 1982–2023.*

	Arabian Sea		Bay of Bengal	
	Pre-monsoon	**Post-monsoon**	**Pre-monsoon**	**Post-monsoon**
Average TC Frequency	0.7	0.9	0.8	1.7
Average TC Lifetime maximum intensity (LMI, kmph)	126.8 ± 61.7	115.7 ± 54	139.6 ± 65.9	115.8 ± 50.5
Mean intensity (kmph)	107.8 ± 46.4	98.7 ± 43.3	108.3 ± 48.9	97.0 ± 40.1
TC duration when the system is at least tropical storm strength (wind speed >34 knots, hour)	87.7 ± 59.3	72.8 ± 50.5	78.7 ± 49.9	65.2 ± 50.8
TC duration including weaker intensity stage (wind speed ≥17 knots, hour)	138.8 ± 56.9	149.5 ± 75.6	125.2 ± 51.7	121.9 ± 58.4
TC track length (when the system is at least tropical storm strength (wind speed >34 knots, km)	978 ± 573	994.9 ± 666.7	1210.9 ± 729.1	927 ± 799.3
TC track length	1617.3 ± 690.0	2002.4 ± 948.8	1846.0 ± 736.4	1732.5 ± 954.9

including weaker intensity stage (wind speed ≥17 knots, km)				
Accumulated Cyclone Energy (ACE, $\times 10^4$ knots^2)	6.5	4.8	5.9	3.8
Translation speed (m s^{-1})	3.30 ± 0.92	3.98 ± 1.53	4.20 ± 1.0	4.06 ± 1.24
TC size (km)	148.3 ± 54.4	140.4 ± 52.1	157.0 ± 60.6	127.4 ± 45.7

- TC frequency in the Arabian Sea is increasing at the rate of ~0.2 TCs/decade during the post-monsoon season.
- The intensity (LMI) of TCs in the Arabian Sea during the pre-monsoon season has been increasing at a rate of 12.2 knots (22.6 km/hr) per decade. Similarly, during the post-monsoon season, TC intensity shows an increasing trend of 7.1 knots (13.1 km/hr) per decade. In the Bay of Bengal, there is no significant increasing trend in TC intensity.
- Not only the intensity of TC, but also the intensification rate of TCs in the Arabian Sea is increasing at the rate of 0.7 knots and 2.4 knots per 6 hour per decade during the pre-monsoon season and the post-monsoon season respectively. In line with it there is an increase in the frequency of TCs undergoing rapid intensification in both seasons.
- TC duration in the Arabian Sea is increasing at the rate of 14.4 hours per decade during the pre-monsoon season. During the post-monsoon season, TC duration shows only a marginal increase. Interestingly, in both seasons, TC land duration exhibits a decreasing trend. This indicates that although there is an overall increase in TC duration, the TC duration over land is declining.
- Due to the increase in intensity and duration of TCs in the Arabian Sea, there is a significant increase in the accumulated cyclone energy in the basin. It is increasing at the rate of 2.8 knots^2 and 2.9 knots^2 per decade during the pre-monsoon season and post-monsoon season respectively.
- The translation speed of TCs is declining in both basins during the post-monsoon season. However, over land, the rate of slowing down of TCs in less than that over the ocean.

- TC genesis latitude is shifting equatorward in both the basins and seasons, which is sharp contrast to the global basins.
- TC maximum intensity latitude in the Bay of Bengal is also shifting equatorward. This is again in contrast to the global basins. However, in the Arabian Sea, during the pre-monsoon season, it is shifting poleward, whereas during the post-monsoon season, it is shifting equatorward.
- TC size during the pre-monsoon season is increasing at the rate of 15.3 n mi (28.3 km) per decade and 29.4 n mi (54.4 km) per decade in the Arabian Sea and the Bay of Bengal respectively. On the contrary, during the post-monsoon season, TC size exhibits a non-significant declining trend.

Table 7.2. *Summary of the observed changes in TC characteristics in the Arabian Sea and the Bay of Bengal during the pre-monsoon and the post-monsoon season. Here, the increase/decrease values highlighted in bold and color indicate that the change in TC characteristics is statistically significant at a confidence level of at least 85% ($p \leq 0.15$).*

TC characteristics	Arabian Sea		Bay of Bengal	
	Pre-monsoon	**Post-monsoon**	**Pre-monsoon**	**Post-monsoon**
TC frequency	No change	Increase	No change	No change
Intensity (LMI)	**Increase**	**Increase**	Marginal increase	Marginal increase
Intensification rate	**Increase**	**Increase**	No change	No change
RI frequency	**Increase**	**Increase**	No change	Marginal increase
TC total duration	**Increase**	Marginal Increase	Marginal increase	Marginal increase
TC land duration	Decrease	Decrease	Marginal decrease	Marginal decrease
Accumulated Cyclone energy	**Increase**	**Increase**	Marginal increase	Marginal increase
Translation speed	No change	Decrease	Marginal increase	**Decrease**
TC size	**Increase**	Decrease	**Increase**	Marginal decrease

- In the Southern Tropical Indian Ocean, 71% of the annual TC frequency occurs between November to April. The most active TC month in this basin is February. Also, it is noted that the intensity of TCs is generally more in the later part of the active season i.e. from February-April, as compared to November-January.

- Similar to the Bay of Bengal, in the Southern Tropical Indian Ocean too, there is no significant change in the TC frequency in the basin during the season (November-April). However, the frequency of category ≥ 3 TCs is increasing at the rate of 0.4 TC per decade.
- This increase in the frequency of intense TCs is reflected by the changes in TC intensity which is increasing at the rate of 3.4 knots (6.3 km/hr) per decade. Also, the upper limit of TC intensity (i.e. the maximum intensity of TC in a given season) is increasing at the rate of 6 knots (11.1 km/hr) per decade. This indicates that in recent decades the TCs in the Southern Tropical Indian Ocean are becoming more and more intense.
- Similar to the Arabian Sea, TCs intensification rate in the Southern Tropical Indian Ocean is increasing rapidly. It is increasing at the rate of 0.3 knots per 6 hours per decade. Also, the frequency of TCs undergoing rapid intensification is increasing at the rate of 0.7 TC per decade. The number of TCs undergoing rapid intensification has increased from 4 TCs per season in the earlier part of the study period to ~6 TCs per season in recent years.
- Lastly, along with the increase in TC intensity in Southern Tropical Indian Ocean there is also a marginal increase in their duration, leading to an increase in the accumulated cyclone energy in the basin.
- To assess the impact of global warming on TC characteristics, we analyzed the multi-model mean from the best-performing CMIP6-HighResMIP models for the near-future period (2015–2050). The projections indicate a decrease in overall TC frequency in the Bay of Bengal during both the pre- and post-monsoon seasons. Furthermore, the frequency of intense TCs (Category ≥ 3) is projected to decline by approximately 53% during the pre-monsoon season. In contrast, during the post-monsoon season, the frequency of intense TCs is expected to marginally increase, from about one TC every six years in the historical period to one TC every 4.5 years in the near-future projections.
- In the Arabian Sea, multi-model mean is projecting a decrease in TC frequency during the post-monsoon season and no significant change during the pre-monsoon season.
- The multi-model mean projects a decrease in TC intensity in the Bay of Bengal during the pre-monsoon season and no significant change during the post-monsoon season. On the other hand, in the Arabian Sea, TC intensity is projected to increase marginally during the pre-monsoon season and no significant change during the post-monsoon season.

- The TC duration is projected to decrease in both basins and seasons.
- The TC intensification rate is projected to increase in the Arabian Sea during the pre-monsoon season. No significant change during the post-monsoon season. Whereas, in the Bay of Bengal, there is no significant change in the TC intensification rate in pre-monsoon season and marginal increase in the post-monsoon season.
- TC tracks are projected to shift poleward in the Bay of Bengal during the post-monsoon season. In the Arabian Sea, there is a slight northwest shift in TC tracks in pre-monsoon season. While, there is no concrete signal in the post-monsoon season.
- Observations indicate an equatorward shift in the latitude of TC genesis, whereas the multi-model mean projects a slight poleward shift in TC genesis latitude. In contrast, the multi-model mean shows almost no change in the latitude of TC maximum intensity.

Table 7.3. *Summary of the near-future projection (2015–2050) of TC characteristics in the Arabian Sea and the Bay of Bengal during the pre-monsoon and the post-monsoon season using CMIP6 HighResMIP multi-model mean. Here, the increase/decrease values highlighted in bold and color indicate that the change in TC characteristics is statistically significant at a confidence level of at least 85% ($p \leq 0.15$).*

TC characteristics	Arabian Sea		Bay of Bengal	
	Pre-monsoon	**Post-monsoon**	**Pre-monsoon**	**Post-monsoon**
TC frequency	No change	**Decrease**	**Decrease**	Marginal decrease
Average Intensity (LMI)	Marginal increase	No change	**Decrease**	Marginal decrease
Intensification rate	**Increase**	No change	No change	Marginal increase
Frequency of higher category TCs (Category ≥3)	No change	**Decrease**	**Decrease**	Marginal increase
TC total duration	**Decrease**	**Decrease**	Marginal decrease	**Decrease**
Accumulated Cyclone energy	No change	Marginal decrease	Marginal decrease	Marginal decrease

Acknowledgements

The authors express their sincere gratitude to the Director, Indian Institute of Tropical Meteorology (IITM), Pune, and the Ministry of Earth Sciences (MoES), Government of India, for their continued support. We acknowledge the Joint Typhoon Warning Center (JTWC) data as archived in the International Best Track Archive for Climate Stewardship (IBTrACS). We also acknowledge the World Climate Research Programme (WCRP), which, through its Working Group on Coupled Modelling (WGCM), coordinated and promoted CMIP6. We thank the climate modeling groups for producing and making available their model outputs, the Earth System Grid Federation (ESGF) for archiving the data and providing access, and the multiple funding agencies that support CMIP6 and ESGF. We also thank Dr. R.H. Kriplani, former scientist of IITM and Dr. Monica Sharma from IMD for reviewing the manuscript and for their suggestions and comments.

List of Acronyms

TCs – Tropical Cyclones

AS – Arabian Sea

BoB – Bay of Bengal

TS – Tropical Storm

Cat – Category

SST – Sea Surface Temperature

NOAA – National Oceanic and Atmospheric Administration

MJO – Madden–Julian Oscillation

ENSO – El–Niño Southern Oscillation

IOD – Indian Ocean Dipole

JTWC – Joint Typhoon Warning Centre

IBTrACS – International Best Track Archive for Climate Stewardship

HighResMIP – High Resolution Model Intercomparison Project

CMIP6 – Coupled Model Intercomparison Project Phase 6

ERA-20C – ECMWF Reanalysis of the 20th Century

SSP5–8.5 – Shared Socioeconomic Pathway 5, with an 8.5 Watt per meter squared (W/m2) radiative forcing scenario

LMI – Lifetime Maximum Intensity

ACE – Accumulated Cyclone Energy

CNRM – Centre National de Recherches Météorologiques

UZ – Université of Zaragoza

OWZ – Ōkubo-Weiss-Zeta

MSLP – Mean Sea Level Pressure

References

Adsul, R., Singh, V. K., Parekh, A., & Gnanaseelan, C. (2026a). Near future projections of tropical cyclone tracks over the Bay of Bengal using high resolution CMIP6 models. *Scientific Reports*, *16*(1), 5567. https://doi.org/10.1038/s41598-026-35482-w

Adsul, R., Singh, V. K., Parekh, A., & C. Gnanaseelan (2026b). Assessment of Tropical cyclone tracking algorithms for the north Indian Ocean, February 2026, IITM Technical Report No. TR-10, ISSN 0252-1075, ESSO/IITM/CVP/TR/01(2026)/205

Balaji, M., Chakraborty, A., & Mandal, M. (2018). Changes in tropical cyclone activity in north Indian Ocean during satellite era (1981–2014). *International Journal of Climatology*, *38*(6), 2819–2837. https://doi.org/10.1002/joc.5463

Beal, L. M., Vialard, J., Roxy, M. K., Li, J., Andres, M., Annamalai, H., et al. (2020). A roadmap to IndOOS-2: Better observations of the rapidly-warming Indian Ocean. *Bulletin of the American Meteorological Society*, 1–50. https://doi.org/10.1175/bams-d-19-0209.1

Bell, R., Strachan, J., Vidale, P. L., Hodges, K., & Roberts, M. (2013). Response of tropical cyclones to idealized climate change experiments in a global high-resolution coupled general circulation model. *Journal of Climate*, *26*(20), 7966–7980. https://doi.org/10.1175/JCLI-D-12-00749.1

Bell, S. S., Chand, S. S., Tory, K. J., & Turville, C. (2018). Statistical Assessment of the OWZ Tropical Cyclone Tracking Scheme in ERA-Interim. *Journal of Climate*, *31*(6), 2217–2232. https://doi.org/10.1175/JCLI-D-17-0548.1

Bhardwaj, P., & Singh, O. (2020). Climatological characteristics of Bay of Bengal tropical cyclones: 1972–2017. *Theoretical and Applied Climatology*, *139*(1–2), 615–629. https://doi.org/10.1007/s00704-019-02989-4

Bhardwaj, P., Pattanaik, D. R., & Singh, O. (2019). Tropical cyclone activity over Bay of Bengal in relation to El Niño-Southern Oscillation. *International Journal of Climatology*, *39*(14), 5452–5469. https://doi.org/10.1002/joc.6165

Bhatia, K., Baker, A., Yang, W., Vecchi, G., Knutson, T., Murakami, H., et al. (2022). A potential explanation for the global increase in tropical cyclone rapid intensification. *Nature Communications*, *13*(1), 6626. https://doi.org/10.1038/s41467-022-34321-6

Bhatia, K. T., Vecchi, G. A., Knutson, T. R., Murakami, H., Kossin, J., Dixon, K. W., &

Whitlock, C. E. (2019). Recent increases in tropical cyclone intensification rates. *Nature Communications*, *10*(1), 635. https://doi.org/10.1038/s41467-019-08471-z

Bourdin, S., Fromang, S., Dulac, W., Cattiaux, J., & Chauvin, F. (2022). Intercomparison of four algorithms for detecting tropical cyclones using ERA5. *Geoscientific Model Development*, *15*(17), 6759–6786. https://doi.org/10.5194/gmd-15-6759-2022

Brand S. (1972). Very large and very small typhoons of the western North Pacific Ocean. *Journal of the Meteorological Society of Japan. Ser. II*, *50*(4), 332–341. https://doi.org/10.2151/jmsj1965.50.4_332

Camargo, S. J. (2013). Global and Regional Aspects of Tropical Cyclone Activity in the CMIP5 Models. *Journal of Climate*, *26*(24), 9880–9902. https://doi.org/10.1175/JCLI-D-12-00549.1

Camargo, S. J., & Sobel, A. H. (2005). Western North Pacific tropical cyclone intensity and ENSO. *Journal of Climate*, *18*(15), 2996–3006. https://doi.org/10.1175/JCLI3457.1

Chan, K. T. F., & Chan, J. C. L. (2014). Impacts of initial vortex size and planetary vorticity on tropical cyclone size. *Quarterly Journal of the Royal Meteorological Society*, *140*(684), 2235–2248. https://doi.org/https://doi.org/10.1002/qj.2292

Chan, K. T. F., & Chan, J. C. L. (2015). Global climatology of tropical cyclone size as inferred from QuikSCAT data. *International Journal of Climatology*, *35*(15), 4843–4848. https://doi.org/https://doi.org/10.1002/joc.4307

Chand, S. S., Walsh, K. J. E., Camargo, S. J., Kossin, J. P., Tory, K. J., Wehner, M. F., et al. (2022). Declining tropical cyclone frequency under global warming. *Nature Climate Change*, *12*(7), 655–661. https://doi.org/10.1038/s41558-022-01388-4

Chauvin, F., Royer, J.-F., & Déqué, M. (2006). Response of hurricane-type vortices to global warming as simulated by ARPEGE-Climat at high resolution. *Climate Dynamics*, *27*(4), 377–399. https://doi.org/10.1007/s00382-006-0135-7

Chavas, D. R., Lin, N., Dong, W., & Lin, Y. (2016). Observed tropical cyclone size revisited. *Journal of Climate*, *29*(8), 2923–2939. https://doi.org/10.1175/JCLI-D-15-0731.1

Cocks, S. B., & Gray, W. M. (2002). Variability of the Outer Wind Profiles of Western North Pacific Typhoons: Classifications and Techniques for Analysis and Forecasting. *Monthly Weather Review*, *130*(8), 1989–2005. https://doi.org/10.1175/1520-

0493(2002)130<1989:VOTOWP>2.0.CO;2

Daloz, A. S., & Camargo, S. J. (2018). Is the poleward migration of tropical cyclone maximum intensity associated with a poleward migration of tropical cyclone genesis? *Climate Dynamics*, *50*(1–2), 705–715. https://doi.org/10.1007/s00382-017-3636-7

Deng, E., Xiang, Q., Chan, J. C. L., Dong, Y., Tu, S., Chan, P.-W., & Ni, Y.-Q. (2025). Increasing temporal stability of global tropical cyclone precipitation. *Npj Climate and Atmospheric Science*, *8*(1), 11. https://doi.org/10.1038/s41612-025-00896-2

Deshpande, M., Singh, V. K., Ganadhi, M. K., Roxy, M. K., Emmanuel, R., & Kumar, U. (2021). Changing status of tropical cyclones over the north Indian Ocean. *Climate Dynamics*, *57*(11–12), 3545–3567. https://doi.org/10.1007/S00382-021-05880-Z/FIGURES/13

Deshpande, M., Singh, V. K. V. K., Ganadhi, M. K., Roxy, M. K. K., Emmanuel, R., Kumar, U., et al. (2021). Changing Status of Tropical Cyclones over the North Indian Ocean. *Climate Dynamics*, *Accepted*(11–12), 3545–3567. https://doi.org/10.1007/S00382-021-05880-Z/FIGURES/13

Emanuel, K. (2005). Increasing destructiveness of tropical cyclones over the past 30 years. *Nature*, *436*(7051), 686–688. https://doi.org/10.1038/nature03906

Emanuel, K. (2017). Assessing the present and future probability of Hurricane Harvey's rainfall. *Proceedings of the National Academy of Sciences*, *114*(48), 12681–12684. https://doi.org/10.1073/pnas.1716222114

Emanuel, K. A. (1986). An Air-sea intercation theory for tropical cyclones. Part 1: Steady-State Maintenance. *Journal of Atmospheric Sciences*, *43*(6), 585–604.

Eyring, V., Bony, S., Meehl, G. A., Senior, C. A., Stevens, B., Stouffer, R. J., & Taylor, K. E. (2016). Overview of the Coupled Model Intercomparison Project Phase 6 (CMIP6) experimental design and organization. *Geoscientific Model Development*, *9*(5), 1937–1958. https://doi.org/10.5194/gmd-9-1937-2016

Felton, C. S., Subrahmanyam, B., & Murty, V. S. N. N. (2013). ENSO-modulated cyclogenesis over the Bay of Bengal. *Journal of Climate*, *26*(24), 9806–9818. https://doi.org/10.1175/JCLI-D-13-00134.1

Fudeyasu, H., Ito, K., & Miyamoto, Y. (2018). Characteristics of tropical cyclone rapid

intensification over the Western North Pacific. *Journal of Climate*, *31*(21), 8917–8930. https://doi.org/10.1175/JCLI-D-17-0653.1

Gao, S., & CHIU, L. S. (2010). Surface latent heat flux and rainfall associated with rapidly intensifying tropical cyclones over the western North Pacific. *International Journal of Remote Sensing*, *31*(17), 4699–4710. https://doi.org/10.1080/01431161.2010.485149

Gao, S., Zhai, S., Chiu, L. S., & Xia, D. (2016). Satellite air-sea enthalpy flux and intensity change of tropical cyclones over the western North Pacific. *Journal of Applied Meteorology and Climatology*, *55*(2), 425–444. https://doi.org/10.1175/JAMC-D-15-0171.1

Gao, S., Jia, S., Wan, Y., Li, T., Zhai, S., & Shen, X. (2019). The role of latent heat flux in tropical cyclogenesis over the Western North Pacific: Comparison of developing versus non-developing disturbances. *Journal of Marine Science and Engineering*, *7*(2), 28. https://doi.org/10.3390/jmse7020028

Girishkumar, M. S., Thanga Prakash, V. P., & Ravichandran, M. (2015). Influence of Pacific Decadal Oscillation on the relationship between ENSO and tropical cyclone activity in the Bay of Bengal during October–December. *Climate Dynamics*, *44*(11), 3469–3479. https://doi.org/10.1007/s00382-014-2282-6

Girishkumar, M. S., Suprit, K., Vishnu, S., Prakash, V. P. T. T., & Ravichandran, M. (2015). The role of ENSO and MJO on rapid intensification of tropical cyclones in the Bay of Bengal during October–December. *Theoretical and Applied Climatology*, *120*(3–4), 797–810. https://doi.org/10.1007/s00704-014-1214-z

Gori, A., Lin, N., & Smith, J. (2020). Assessing Compound Flooding From Landfalling Tropical Cyclones on the North Carolina Coast. *Water Resources Research*, *56*(4), e2019WR026788. https://doi.org/https://doi.org/10.1029/2019WR026788

Gray, W. M. (1968). Global view of the origin of tropical disturbances and storms. *Monthly Weather Review*, *96*(10), 669–700.

Grise, K. M., & Polvani, L. M. (2017). Understanding the Time Scales of the Tropospheric Circulation Response to Abrupt CO2 Forcing in the Southern Hemisphere: Seasonality and the Role of the Stratosphere. *Journal of Climate*, *30*(21), 8497–8515. https://doi.org/10.1175/JCLI-D-16-0849.1

Haarsma, R. J., Roberts, M. J., Vidale, P. L., Senior, C. A., Bellucci, A., Bao, Q., et al. (2016). High Resolution Model Intercomparison Project (HighResMIP~v1.0) for CMIP6. *Geoscientific Model Development*, *9*(11), 4185–4208. https://doi.org/10.5194/gmd-9-4185-2016

He, J., & Soden, B. J. (2015). Anthropogenic Weakening of the Tropical Circulation: The Relative Roles of Direct CO2 Forcing and Sea Surface Temperature Change. *Journal of Climate*, *28*(22), 8728–8742. https://doi.org/10.1175/JCLI-D-15-0205.1

Hill, K. A., & Lackmann, G. M. (2009). Influence of Environmental Humidity on Tropical Cyclone Size. *Monthly Weather Review*, *137*(10), 3294–3315. https://doi.org/10.1175/2009MWR2679.1

Jaimes, B., Shay, L. K., & Uhlhorn, E. W. (2015). Enthalpy and momentum fluxes during hurricane earl relative to underlying ocean features. *Monthly Weather Review*, *143*(1), 111–131. https://doi.org/10.1175/MWR-D-13-00277.1

Kaplan, J., & DeMaria, M. (2003). Large-scale characteristics of rapidly intensifying tropical cyclones in the North Atlantic basin. *Weather and Forecasting*, *18*(6), 1093–1108. https://doi.org/10.1175/1520-0434(2003)018<1093:LCORIT>2.0.CO;2

Kikuchi, K., Wang, B., & Fudeyasu, H. (2009). Genesis of tropical cyclone Nargis revealed by multiple satellite observations. *Geophysical Research Letters*, *36*(6), 1–5. https://doi.org/10.1029/2009GL037296

Kim, J.-S., Li, R. C.-Y., & Zhou, W. (2012). Effects of the Pacific-Japan teleconnection pattern on tropical cyclone activity and extreme precipitation events over the Korean peninsula. *Journal of Geophysical Research: Atmospheres*, *117*(D18). https://doi.org/https://doi.org/10.1029/2012JD017677

Knaff, J. A., & Sampson, C. R. (2015). After a Decade Are Atlantic Tropical Cyclone Gale Force Wind Radii Forecasts Now Skillful? *Weather and Forecasting*, *30*(3), 702–709. https://doi.org/10.1175/WAF-D-14-00149.1

Knaff, J. A., & Zehr, R. M. (2007). Reexamination of Tropical Cyclone Wind–Pressure Relationships. *Weather and Forecasting*, *22*(1), 71–88. https://doi.org/10.1175/WAF965.1

Knaff, J. A., Longmore, S. P., & Molenar, D. A. (2014). An Objective Satellite-Based Tropical

Cyclone Size Climatology. *Journal of Climate*, *27*(1), 455–476. https://doi.org/10.1175/JCLI-D-13-00096.1

Knaff, J. A., Sampson, C. R., & Chirokova, G. (2017). A Global Statistical–Dynamical Tropical Cyclone Wind Radii Forecast Scheme. *Weather and Forecasting*, *32*(2), 629–644. https://doi.org/10.1175/WAF-D-16-0168.1

Knapp, K. R., Kruk, M. C., Levinson, D. H., Diamond, H. J., Neumann, C. J., Kenneth R. Knapp, et al. (2010). The International Best Track Archive for Climate Stewardship (IBTrACS). *Bulletin of the American Meteorological Society*, *91*(3), 363–376. https://doi.org/10.1175/2009BAMS2755.1

Kossin, J. P. (2018). A global slowdown of tropical-cyclone translation speed. *Nature*, *558*(7708), 104–107. https://doi.org/10.1038/s41586-018-0158-3

Kossin, J. P., & Velden, C. S. (2004). A Pronounced Bias in Tropical Cyclone Minimum Sea Level Pressure Estimation Based on the Dvorak Technique. *Monthly Weather Review*, *132*(1), 165–173. https://doi.org/10.1175/1520-0493(2004)132<0165:APBITC>2.0.CO;2

Kranthi, G. M., Deshpande, M., Sunilkumar, K., Emmanuel, R., & Ingle, S. (2023). Climatology and characteristics of rapidly intensifying tropical cyclones over the North Indian Ocean. *International Journal of Climatology*, *43*(4), 1773–1795. https://doi.org/https://doi.org/10.1002/joc.7945

Krishnamohan, K. S., Mohanakumar, K., & Joseph, P. V. (2012). The influence of Madden-Julian Oscillation in the genesis of North Indian Ocean tropical cyclones. *Theoretical and Applied Climatology*, *109*(1–2), 271–282. https://doi.org/10.1007/s00704-011-0582-x

Kushwaha, V. K., Singh, V. K., Parekh, A., & Gnanaseelan, C. (2025). Revisiting the tropical cyclone genesis potential index for the Bay of Bengal post-monsoon season. *Journal of Earth System Science*, *134*(3), 153. https://doi.org/10.1007/s12040-025-02617-y

Landsea, C. W., & Franklin, J. L. (2013). Atlantic Hurricane Database Uncertainty and Presentation of a New Database Format. *Monthly Weather Review*, *141*(10), 3576–3592. https://doi.org/10.1175/MWR-D-12-00254.1

Li, R. C. Y., & Zhou, W. (2015). Interdecadal Changes in Summertime Tropical Cyclone Precipitation over Southeast China during 1960–2009. *Journal of Climate*, *28*(4), 1494–

1509. https://doi.org/10.1175/JCLI-D-14-00246.1

Li, Z., Yu, W., Li, T., Murty, V. S. N., Tangang, F., Centre, R., et al. (2013). Bimodal character of cyclone climatology in the bay of bengal modulated by monsoon seasonal cycle. *Journal of Climate*, *26*(3), 1033–1046. https://doi.org/10.1175/JCLI-D-11-00627.1

Li, Z., Li, T., Yu, W., Li, K., & Liu, Y. (2016). What controls the interannual variation of tropical cyclone genesis frequency over Bay of Bengal in the post-monsoon peak season? *Atmospheric Science Letters*, *17*(2), 148–154. https://doi.org/10.1002/asl.636

Lin, I. -I. I., Pun, I. F., & Lien, C. C. (2014). "category-6" supertyphoon Haiyan in global warming hiatus: Contribution from subsurface ocean warming. *Geophysical Research Letters*, *41*(23), 8547–8553. https://doi.org/10.1002/2014GL061281

Lin, J., Lee, C.-Y., Camargo, S. J., & Sobel, A. (2024). Poleward Migration of the Latitude of Maximum Tropical Cyclone Intensity—Forced or Natural? *Journal of Climate*, *37*(21), 5453–5463. https://doi.org/10.1175/JCLI-D-23-0705.1

Lin, S.-J., & Chou, K.-H. (2018). Characteristics of Size Change of Tropical Cyclones Traversing the Philippines. *Monthly Weather Review*, *146*(9), 2891–2911. https://doi.org/10.1175/MWR-D-18-0004.1

Liu, J., Yuan, C., & Luo, J.-J. (2023). Impacts of model resolution on responses of western North Pacific tropical cyclones to ENSO in the HighResMIP-PRIMAVERA ensemble. *Frontiers in Earth Science*, *11*. https://doi.org/10.3389/feart.2023.1169885

Liu, K. S., & Chan, J. C. L. (1999). Size of Tropical Cyclones as Inferred from ERS-1 and ERS-2 Data. *Monthly Weather Review*, *127*(12), 2992–3001. https://doi.org/10.1175/1520-0493(1999)127<2992:SOTCAI>2.0.CO;2

Lok, C. C. F., Chan, J. C. L., & Toumi, R. (2021). Tropical cyclones near landfall can induce their own intensification through feedbacks on radiative forcing. *Communications Earth & Environment*, *2*(1), 184. https://doi.org/10.1038/s43247-021-00259-8

Madsen, H., & Jakobsen, F. (2004). Cyclone induced storm surge and flood forecasting in the northern Bay of Bengal. *Coastal Engineering*, *51*(4), 277–296. https://doi.org/10.1016/j.coastaleng.2004.03.001

Mahala, B. K., Nayak, B. K., Mohanty, P. K., Kumar, B., Birendra, M. •, Nayak, K., et al. (2015). Impacts of ENSO and IOD on tropical cyclone activity in the Bay of Bengal.

Natural Hazards, *75*(2), 1105–1125. https://doi.org/10.1007/s11069-014-1360-8

Manikanta, N. D., Joseph, S., & Naidu, C. V. (2023). Recent global increase in multiple rapid intensification of tropical cyclones. *Scientific Reports*, *13*(1), 15949. https://doi.org/10.1038/s41598-023-43290-9

Mann, M. E., Rahmstorf, S., Kornhuber, K., Steinman, B. A., Miller, S. K., & Coumou, D. (2017). Influence of Anthropogenic Climate Change on Planetary Wave Resonance and Extreme Weather Events. *Scientific Reports*, *7*(1), 45242. https://doi.org/10.1038/srep45242

McPhaden, M. J., Foltz, G. R., Lee, T., Murty, V. S. N., Ravichandran, M., Vecchi, G. A., et al. (2009). Ocean-Atmosphere Interactions During Cyclone Nargis. *Eos, Transactions American Geophysical Union*, *90*(7), 53–54. https://doi.org/10.1029/2009EO070001

Mei, W., Pasquero, C., & Primeau, F. (2012). The effect of translation speed upon the intensity of tropical cyclones over the tropical ocean. *Geophysical Research Letters*, *39*(7), 1–6. https://doi.org/10.1029/2011GL050765

Merrill, R. T. (1984). A Comparison of Large and Small Tropical Cyclones. *Monthly Weather Review*, *112*(7), 1408–1418. https://doi.org/10.1175/1520-0493(1984)112<1408:ACOLAS>2.0.CO;2

Mohapatra, M., & Sharma, M. (2019). Cyclone warning services in India during recent years: A review. *Mausam*, *70*(4), 635–666.

Mohapatra, M., Bandyopadhyay, B. K., & Nayak, D. P. (2013). Evaluation of operational tropical cyclone intensity forecasts over north Indian Ocean issued by India Meteorological Department. *Natural Hazards*, *68*(2), 433–451. https://doi.org/10.1007/s11069-013-0624-z

Moon, I.-J., Kim, S.-H., Klotzbach, P., & Chan, J. C. L. (2015). Roles of interbasin frequency changes in the poleward shifts of the maximum intensity location of tropical cyclones. *Environmental Research Letters*, *10*(10), 104004. https://doi.org/10.1088/1748-9326/10/10/104004

Murakami, H., Sugi, M., & Kitoh, A. (2013). Future changes in tropical cyclone activity in the North Indian Ocean projected by high-resolution MRI-AGCMs. *Climate Dynamics*, *40*(7), 1949–1968. https://doi.org/10.1007/s00382-012-1407-z

Murakami, H., Vecchi, G. A., & Underwood, S. (2017). Increasing frequency of extremely severe cyclonic storms over the Arabian Sea. *Nature Climate Change*. https://doi.org/10.1038/s41558-017-0008-6

Nadimpalli, R., Mohanty, S., Pathak, N., Osuri, K. K., Mohanty, U. C., & Chatterjee, S. (2021). Understanding the characteristics of rapid intensity changes of Tropical Cyclones over North Indian Ocean. *SN Applied Sciences*, *3*(1), 68. https://doi.org/10.1007/s42452-020-03995-2

Neetu, S., Lengaigne, M., Vialard, J., Mangeas, M., Menkes, C. E., Suresh, I., et al. (2020). Quantifying the Benefits of Nonlinear Methods for Global Statistical Hindcasts of Tropical Cyclones Intensity. *Weather and Forecasting*, *35*(3), 807–820. https://doi.org/10.1175/WAF-D-19-0163.1

Ngoma, H., Wen, W., Ayugi, B., Babaousmail, H., Karim, R., & Ongoma, V. (2021). Evaluation of precipitation simulations in CMIP6 models over Uganda. *International Journal of Climatology*, *41*(9), 4743–4768. https://doi.org/https://doi.org/10.1002/joc.7098

O'Neill, B. C., Tebaldi, C., van Vuuren, D. P., Eyring, V., Friedlingstein, P., Hurtt, G., et al. (2016). The Scenario Model Intercomparison Project (ScenarioMIP) for CMIP6. *Geoscientific Model Development*, *9*(9), 3461–3482. https://doi.org/10.5194/gmd-9-3461-2016

Osuri, K. K., Nadimpalli, R., Mohanty, U. C., & Niyogi, D. (2017). Prediction of rapid intensification of tropical cyclone Phailin over the Bay of Bengal using the HWRF modelling system. *Quarterly Journal of the Royal Meteorological Society*, *143*(703), 678–690. https://doi.org/10.1002/qj.2956

Pall, P., Gagnon, A. S., Bollasina, M. A., Zarzycki, C. M., Huang, Y., Beckett, C. T. S., et al. (2024). Assessing South Indian Ocean tropical cyclone characteristics in HighResMIP simulations. *International Journal of Climatology*, *44*(13), 4792–4808. https://doi.org/https://doi.org/10.1002/joc.8609

Priya, P., Pattnaik, S., & Trivedi, D. (2022). Characteristics of the tropical cyclones over the North Indian Ocean Basins from the long-term datasets. *Meteorology and Atmospheric Physics*, *134*(4), 65. https://doi.org/10.1007/s00703-022-00904-7

Rajeevan, M., Srinivasan, J., Niranjan Kumar, K., Gnanaseelan, C., & Ali, M. M. (2013). On the epochal variation of intensity of tropical cyclones in the Arabian Sea. *Atmospheric Science Letters*, *14*(4), 249–255. https://doi.org/10.1002/asl2.447

Randriatsara, H. H.-R. H., Hu, Z., Xu, X., Ayugi, B., Sian, K. T. C. L. K., Mumo, R., et al. (2023). Performance evaluation of CMIP6 HighResMIP models in simulating precipitation over Madagascar. *International Journal of Climatology*, *43*(12), 5401–5421. https://doi.org/https://doi.org/10.1002/joc.8153

Roberts, M. J., Camp, J., Seddon, J., Vidale, P. L., Hodges, K., Vanniere, B., et al. (2020). Impact of Model Resolution on Tropical Cyclone Simulation Using the HighResMIP–PRIMAVERA Multimodel Ensemble. *Journal of Climate*, *33*(7), 2557–2583. https://doi.org/10.1175/JCLI-D-19-0639.1

Roberts, M. J., Camp, J., Seddon, J., Vidale, P. L., Hodges, K., Vannière, B., et al. (2020). Projected Future Changes in Tropical Cyclones Using the CMIP6 HighResMIP Multimodel Ensemble. *Geophysical Research Letters*, *47*(14), e2020GL088662. https://doi.org/https://doi.org/10.1029/2020GL088662

Roose, S., Ajayamohan, R. S., Ray, P., Xie, S.-P., Sabeerali, C. T., Mohapatra, M., et al. (2023). Pacific decadal oscillation causes fewer near-equatorial cyclones in the North Indian Ocean. *Nature Communications*, *14*(1), 5099. https://doi.org/10.1038/s41467-023-40642-x

Roxy, M. K., Dasgupta, P., McPhaden, M. J., Suematsu, T., Zhang, C., & Kim, D. (2019). Twofold expansion of the Indo-Pacific warm pool warps the MJO life cycle. *Nature*, *575*(7784), 647–651. https://doi.org/10.1038/s41586-019-1764-4

Saha, K., Sanders, F., & Shukla, J. (1981). Westward propagating predecessors of monsoon depressions (Bay of Bengal, South China Sea). *Monthly Weather Review*, *109*(2), 330–343. https://doi.org/10.1175/1520-0493(1981)109<0330:WPPOMD>2.0.CO;2

Sahoo, B., & Bhaskaran, P. K. (2016). Assessment on historical cyclone tracks in the Bay of Bengal, east coast of India. *International Journal of Climatology*, *36*(1), 95–109. https://doi.org/10.1002/joc.4331

Sahu, P. L., & Pattnaik, S. (2024). Investigation about the cause of the intense pre-monsoon cyclonic system over the Bay of Bengal. *Meteorology and Atmospheric Physics*, *136*(5),

34. https://doi.org/10.1007/s00703-024-01036-w

Schenkel, B. A., Lin, N., Chavas, D., Vecchi, G. A., Oppenheimer, M., & Brammer, A. (2018). Lifetime Evolution of Outer Tropical Cyclone Size and Structure as Diagnosed from Reanalysis and Climate Model Data. *Journal of Climate*, *31*(19), 7985–8004. https://doi.org/10.1175/JCLI-D-17-0630.1

Scoccimarro, E., Fogli, P. G., Reed, K. A., Gualdi, S., Masina, S., & Navarra, A. (2017). Tropical Cyclone Interaction with the Ocean: The Role of High-Frequency (Subdaily) Coupled Processes. *Journal of Climate*, *30*(1), 145–162. https://doi.org/10.1175/JCLI-D-16-0292.1

Shan, K., & Yu, X. (2020). Enhanced understanding of poleward migration of tropical cyclone genesis. *Environmental Research Letters*, *15*(10), 104062. https://doi.org/10.1088/1748-9326/abaf85

Shan, K., & Yu, X. (2021). Variability of Tropical Cyclone Landfalls in China. *Journal of Climate*, *34*(23), 9235–9247. https://doi.org/10.1175/JCLI-D-21-0031.1

Sharmila, S., & Walsh, K. J. E. (2018). Recent poleward shift of tropical cyclone formation linked to Hadley cell expansion. *Nature Climate Change*, *8*(8), 730–736. https://doi.org/10.1038/s41558-018-0227-5

Singh, O. P., Ali Khan, T. M., & Rahman, M. S. (2000). Changes in the frequency of tropical cyclones over the North Indian Ocean. *Meteorology and Atmospheric Physics*, *75*(1–2), 11–20. https://doi.org/10.1007/s007030070011

Singh, V.K., Roxy, M. K., Deshapnde, M., & Deshpande, M. (2020). The unusual long track and rapid intensification of very severe cyclone Ockhi. *Current Science*, *119*(5), 771–779.

Singh, Vineet Kumar, & Roxy, M. K. (2022). A review of ocean-atmosphere interactions during tropical cyclones in the north Indian Ocean. *Earth-Science Reviews*, *226*, 103967. https://doi.org/10.1016/j.earscirev.2022.103967

Singh, Vineet Kumar, Roxy, M. K., & Deshpande, M. (2022). Role of subtropical Rossby waves in governing the track of cyclones in the Bay of Bengal. *Quarterly Journal of the Royal Meteorological Society*, *148*(749), 3774–3787. https://doi.org/https://doi.org/10.1002/qj.4387

Singh, Vineet Kumar, Kim, H.-J., & Moon, I.-J. (2024). Seasonal differences in tropical

cyclone—induced sea surface cooling in the western North Pacific. *Quarterly Journal of the Royal Meteorological Society*, *150*(758), 447–461. https://doi.org/https://doi.org/10.1002/qj.4606

Singh, Vineet Kumar, Kim, H.-J., & Moon, I.-J. (2025). Mechanism driving stronger tropical cyclones in cooler autumn than the hottest summer. *Npj Climate and Atmospheric Science*, *8*(1), 132. https://doi.org/10.1038/s41612-025-01008-w

Sobel, A. H., Wing, A. A., Camargo, S. J., Patricola, C. M., Vecchi, G. A., Lee, C.-Y., & Tippett, M. K. (2021). Tropical Cyclone Frequency. *Earth's Future*, *9*(12), e2021EF002275. https://doi.org/https://doi.org/10.1029/2021EF002275

Song, J., & Klotzbach, P. J. (2018). What Has Controlled the Poleward Migration of Annual Averaged Location of Tropical Cyclone Lifetime Maximum Intensity Over the Western North Pacific Since 1961? *Geophysical Research Letters*, *45*(2), 1148–1156. https://doi.org/https://doi.org/10.1002/2017GL076883

Sreenivas, P., C. Gnanaseelan, K.V.S.R. Prasad (2012). Influence of El Niño and Indian Ocean Dipole on sea level variability in the Bay of Bengal Global and Planetary Change, 80-81, 215-225,

https://doi.org/10.1016/j.gloplacha.2011.11.001

Tang, Y., Huangfu, J., Huang, R., & Chen, W. (2022). Simulation and Projection of Tropical Cyclone Activities over the Western North Pacific by CMIP6 HighResMIP. *Journal of Climate*, *35*(23), 7771–7794. https://doi.org/10.1175/JCLI-D-21-0760.1

Taylor, K. E. (2001). Summarizing multiple aspects of model performance in a single diagram. *Journal of Geophysical Research: Atmospheres*, *106*(D7), 7183–7192. https://doi.org/https://doi.org/10.1029/2000JD900719

Teshiba, M., Fujita, H., Hashiguchi, H., Shibagaki, Y., Yamanaka, M. D., & Fukao, S. (2005). Detailed structure within a tropical cyclone "eye." *Geophysical Research Letters*, *32*(24). https://doi.org/https://doi.org/10.1029/2005GL023242

Tory, K. J., Dare, R. A., Davidson, N. E., McBride, J. L., & Chand, S. S. (2013). The importance of low-deformation vorticity in tropical cyclone formation. *Atmospheric Chemistry and Physics*, *13*(4), 2115–2132. https://doi.org/10.5194/acp-13-2115-2013

Trabing, B. C., & Bell, M. M. (2020). Understanding Error Distributions of Hurricane Intensity

Forecasts during Rapid Intensity Changes. *Weather and Forecasting*, *35*(6), 2219–2234. https://doi.org/10.1175/WAF-D-19-0253.1

Vidya, P. J., Ravichandran, M., Murtugudde, R., Subeesh, M. P., Chatterjee, S., Neetu, S., & Nuncio, M. (2020). Increased cyclone destruction potential in the Southern Indian Ocean. *Environmental Research Letters*, *16*(1). https://doi.org/10.1088/1748-9326/abceed

Vidya, P. J., Chatterjee, S., Ravichandran, M., Gautham, S., Nuncio, M., & Murtugudde, R. (2023). Intensification of Arabian Sea cyclone genesis potential and its association with Warm Arctic Cold Eurasia pattern. *Npj Climate and Atmospheric Science*, *6*(1), 146. https://doi.org/10.1038/s41612-023-00476-2

Vincent, E. M., Emanuel, K. A., Lengaigne, M., Vialard, J., & Madec, G. (2014). Influence of upper ocean stratification interannual variability on tropical cyclones. *J. Adv. Model. Earth Syst.*, *6*, 680–699.

Vinod, K. K., Soumya, M., Tkalich, P., & Vethamony, P. (2014). Ocean - Atmosphere interaction during thane cyclone: A numerical study using WRF. *Indian Journal of Geo-Marine Sciences*, *43*(7), 1230–1235.

Vinodhkumar, B., Busireddy, N. K. R., Ankur, K., Nadimpalli, R., & Osuri, K. K. (2021). On Occurrence of Rapid Intensification and Rainfall changes in Tropical Cyclones over the North Indian Ocean. *International Journal of Climatology*, *n/a*(June), 1–13. https://doi.org/10.1002/joc.7268

Wahiduzzaman, M., Cheung, K., Luo, J.-J., Bhaskaran, P. K., Tang, S., & Yuan, C. (2022). Impact assessment of Indian Ocean Dipole on the North Indian Ocean tropical cyclone prediction using a Statistical model. *Climate Dynamics*, *58*(3), 1275–1292. https://doi.org/10.1007/s00382-021-05960-0

Wang, Q., Guan, S., Luo, C., Zhao, W., Zhang, L., & Yang, S. (2025). Record-breaking lifespan, rapid intensification, and long-lasting coastal activity of tropical cyclone Freddy (2023) in the South Indian Ocean. *Environmental Research Letters*, *20*(6), 64038. https://doi.org/10.1088/1748-9326/add7ec

Wang, R., & Wu, L. (2019). Influence of Track Changes on the Poleward Shift of LMI Location of Western North Pacific Tropical Cyclones. *Journal of Climate*, *32*(23), 8437–8445. https://doi.org/10.1175/JCLI-D-18-0855.1

Webster, P. J., Holland, G. J., Curry, J. A., & Chang, H. R. (2005). Atmospheric science: Changes in tropical cyclone number, duration, and intensity in a warming environment. *Science*, *309*(5742), 1844–1846. https://doi.org/10.1126/science.1116448

Willoughby, H. E. (1998). Tropical Cyclone Eye Thermodynamics. *Monthly Weather Review*, *126*(12), 3053–3067. https://doi.org/10.1175/1520-0493(1998)126<3053:TCET>2.0.CO;2

Yuan, J. P., Jie, C., & Cao, J. (2013). North Indian Ocean tropical cyclone activities influenced by the Indian Ocean Dipole mode. *Science China Earth Sciences*, *56*(5), 855–865. https://doi.org/10.1007/s11430-012-4559-0

Zhan, R., & Wang, Y. (2017). Weak Tropical Cyclones Dominate the Poleward Migration of the Annual Mean Location of Lifetime Maximum Intensity of Northwest Pacific Tropical Cyclones since 1980. *Journal of Climate*, *30*(17), 6873–6882. https://doi.org/10.1175/JCLI-D-17-0019.1

Zhang, L., & Oey, L. (2019). Young Ocean Waves Favor the Rapid Intensification of Tropical Cyclones—A Global Observational Analysis. *Monthly Weather Review*, *147*(1), 311–328. https://doi.org/10.1175/MWR-D-18-0214.1